UNIVERSIDAD MICHOCANA DE SAN NICOLAS DE HIDALGO

INSTITUTO DE FÍSICA Y MATEMÁTICAS

TESIS

ASPECTS OF LOOP QUANTIZATION IN COSMOLOGICAL MODELS

PARA OBTENER EL GRADO DE

DOCTORA EN CIENCIAS DE AREA DE FÍSICA

QUE PRESENTA

ASIEH KARAMI MAJOOMERD

ASESOR:

DR. ALEJANDRO CORICHI RODRÍGUEZ GIL

MORELIA, MICHOACAN ENERO 2014.

Universidad Michoacana de San Nicolás de Hidalgo
Instituto de Física y Matemáticas

Aspects of Loop Quantization in Cosmological Models

Asieh Karami Majoomerd

Director de Tesis

Dr. Alejandro Corichi Rodríguez Gil

Tesis para Obtener el Grado de Doctor
en Ciencias en el Área de Física

Enero 2014

Abstract

As the first part, we consider the measure problem in standard slow-roll inflationary models from the perspective of loop quantum cosmology (LQC). We study the probability of having enough e-foldings and focus on its dependence on the quantum gravity scale, including the transition of the theory to the limit where general relativity is recovered. We show that the probability is highly dependent on initial conditions and different choices of initial surface in phase space yields different probabilities. While there is no preferable set of initial conditions in classical cosmology, the singularity-free scenario of loop quantum cosmology offers a natural choice of initial conditions, and suggests that enough inflation is generic.

In the second part, we consider the closed FLRW model within loop quantum cosmology. In spatially non-flat anisotropic models such as Bianchi II and IX, the standard method of defining the curvature through closed holonomies is not admissible. Instead, one has to implement the quantum constraints by approximating the connection via open holonomies. In the case of flat k=0 FLRW and Bianchi I models, these two quantization methods coincide, but in the case of the closed k=1 FLRW model they might yield different quantum theories. Since the quantization based on closed holonomies has been studied before, we derive the corresponding quantum constraint operators, and study in detail the issue of the self-adjointness of the quantum Hamiltonian constraint for the quantization based on open holonomies. Furthermore, we explore the different effective descriptions that these two different quantizations provide of the bouncing cyclic universe with and without adding the inverse corrections. In particular, as we show in detail, the most dramatic difference is that in the theory defined by the new quantization method, there is not one, but two different bounces through which the cyclic universe alternates. We show that for a large universe, these two bounces are very similar and, therefore, practically indistinguishable, approaching the dynamics of the quantum theory based on closed holonomies. Also, we show that the inclusion of the inverse corrections solves the unboundedness of the energy density and expansion near the bounce on the full (effective) phase space.

In the third part, we study the loop quantum cosmology of Bianchi IX model. In classical general relativity, the chaotic behavior of Bianchi IX model can display the generic local evolution near to a singularity. But it is expected that the Quantum effects can change it. We show that the modifications which come from Loop Quantum Gravity, imply a non-chaotic effective behavior in the vacuum Bianchi IX model.

To my parents and my dear grandmother

Acknowledgment

First and foremost, I would like to express my special appreciation and thanks to Dr. Alejandro Corichi who has been a great advisor, for his continues support, patient, guidance and his immense knowledge.

I would like to thank my committee members for reading my thesis and for their useful comments and suggestions.

I thank my officemates, Max Dohse, Edison Montoya and Irais Rubalcava with whom I had a memorable time during these years; especially thanks to Edison for his countless helps and for the discussions that we had about our works. I would also like to thank Saeed Rastgoo and Juan Daniel Reyes for many discussions about our works and answering my questions which helped me to understand things better.

My sincere appreciation and friendship goes to my closest friends especially Mona Arjang, Maryam Hassani, Elaheh Miezaei and Soghra Safaverdi who have always been great supports in all my struggles and frustrations in my new life.

Finally, I would like to express my deepest gratitude to my family; my parents, my grandmother, my brothers and sisters and my aunts and uncles for their unconditional love and support and for their encouragement all throughout my life to peruse my dreams.

This work was supported by CONACyT scholarship under number (CVU/ Becario) 334692/ 229125, by CONACyT 0177840 grant and by DGAPA-UNAM grants IN103610 and IN100212.

Table of Contents

List of Figures

Not only is the universe stranger than we think, it is stranger than we can think.

Werner Heisenberg

1 Introduction

In the beginning of the twentieth century general relativity and quantum mechanics as two revolutionary theories were introduced. They have changed our understanding of the world especially in large and small scales. Quantum effects are important in the microscopic world and general relativity is usually used for describing very large scale phenomena. However, in some cases the effects of both theories become important such as in very early universe or to study the interior of black holes which indicate that a theory of quantum gravity is required. Unfortunately, these two theories are inconsistent with each other. One of the main difference between them is the notion of time. Time in quantum mechanics is global and absolute, where in general relativity there is no global notion of time and proper time is measured by the metric tensor which its components are dynamical variables.

There have been many attempts to unify these two theories or find a theory which describes the observations of both theories. Despite of major efforts, currently non of them is complete. Some of these approaches are string theory, dynamical triangulization, casual sets and loop quantum gravity. In this thesis we consider loop quantum gravity.

1.1 Loop quantum gravity

Loop quantum gravity is a non-perturbative theory (see [1–3]) which is based on canonical quantization of general relativity in terms of the variables which are different from the standard metric variables. These variables are $SU(2)$ valued connections and their conjugates, densitiezed triads which are similar to the variables used in $SU(2)$ Yang-Mills theory. However, Hamiltonian and diffeomorphism constraints make the theory more complicated.

In the quantization process, on can take holonomies of connections and fluxes of densitized triads as elementary operators and obtain holonomy-flux Algebra [4]. The authors in [5, 6] have shown that under some certain physical inspired conditions, that algebra has unique representation with the property that the diffeomorphism group in this representation is unitarily implemented. In this representation the spectrum of geometrical operators such as area and volume are discrete which is the main prediction of loop quantum gravity. To find the physical Hilbert space, the Hamiltonian operator is required which is not very well understood generally. However, there are some studies in which some matter fields such as dust or a scalar field have been used as a clock to construct the Hamiltonian constraint operator [7, 8].

As has been mentioned, the main prediction of LQG is the underlying discreteness of quantum geometry. One of the results of this prediction is the resolution of classical big bang and big crunch in the quantization of the reduced phase space of cosmological models by using LQG methods known as loop quantum cosmology.

1.2 Loop quantum cosmology

In the past years, loop quantum cosmology (LQC) has become an interesting candidate for a quantum description of the early universe via homogeneous cosmological models (for a review see [9–13]). Based on the same quantization methods of loop quantum gravity, LQC has also become a testing ground for different conceptual and technical issues that arise in the full theory. Since in LQC one could start from a classical cosmological model (which is a symmetry reduced model due to the spatial homogeneity and sometimes isotropy) and then quantize it, it might not capture the true behavior of the full theory, however one could expect that it at least correctly displays the qualitative behavior of loop quantum gravity. In LQC, same as LQG, the elementary operators are fluxes of densitized triads and holonomies and since cosmological models are highly symmetric, the theory is no longer a quantum field theory and one needs just a finite number of specific paths and surfaces to define elementary operators. However, there are some

ambiguities to construct the holonomy operators. For example, in LQC the curvature is expressed by holonomies and the length of the curves using to calculate those holonomies can be chosen arbitrary. In earlier works on LQC, people chose that length to be a constant (μ_0 scheme) but after that some difficulties due to this choice discovered for example in [14] was shown that to have a correct semi-classical limit one should work with another choice which was called *improved dynamic* ($\bar{\mu}$ scheme).

It is perhaps not surprising that the model which was first fully understood is the spatially flat k=0 FLRW cosmological model coupled to the simplest kind of matter, namely a mass-less scalar field that serves as an internal time parameter [14–19]. It was shown numerically that the big bang singularity is replaced by a quantum bounce [14], that connects an early contraction phase of the universe with the current state of expansion. By means of an exact solvable model, this bounce was then understood to be generic and present for all states of the theory, and the energy density was shown to be absolutely bounded by a critical density $\rho_{\rm crit}$ of the order of the Planck density [18]. It was then shown that semi-classical states after the bounce have to come from states that were also semi-classically well before the bounce [19–22]. This results have also benefited from uniqueness results that warrants the physical consistency of the theory [23, 24]. Also, it was shown that for cosmological models studied by improved dynamic, in the presence of massless scalar field as a clock and with a proper choice of factor ordering of the constraint operator, the singular state[1] does not evolve to other states and vice versa which ensures the singularity resolution in quantum level.

Although as mentioned above, LQC is more simpler than the full theory, it is difficult to work with it in quantum level even numerically and as shown in [14] for some models, the behavior of the effective or semi-classical equations, which are classical equations with some quantum corrections, are good approximations to the numerical quantum evolutions even near the Planck scale, it would be useful to work with the effective equations.

1.2.1 Effective equations

The simplest isotropic cosmological models [14–17, 25–27] as well as the simplest anisotropic ones, namely Bianchi I, II and IX, has been studied via LQC[28–30]. The quantum theory in none of these cases has been solved, even numerically, except for flat and closed FLRW model. At the other hand, the solutions to the effective theory were shown in [14] to accurately describe the evolution of the expectation value of the observables in the quantum theory when they are

[1]The singular state is a state with support on zero volume and does not mean that the state is actually singular.

considered on semi-classical states. Those results were extended to open, closed and flat FLRW models with and without cosmological constant (see [31] for a review). Therefore, in order to study those homogeneous anisotropic models at the semi-classical level, one can generally assume that the effective theory reproduces the solutions to the quantum theory when semi-classical states are considered.

Let us now give a brief review of the effective formalism in LQC. To obtain the effective equations, one can work on the geometric quantum mechanics framework [32, 33]. The main idea is as follows: One can define the projection π from the Hilbert space $\mathcal{H}$ to the classical phase space Γ by taking the expectation values of the fundamental operators. Therefore, the Hilbert space $\mathcal{H}$ is a fiber bundle over the classical phase space Γ. To define the notion of horizontal vectors, we should recall that the horizontal subspace of the tangent space of a state in the Hilbert space is complementary to the vertical subspace of that state. Vertical tangent vectors are the vectors which in their directions, the fundamental quantum observables do not change. To define the horizontal subspace, one might use the symplectic form Ω on the Hilbert space. In this case, we define the horizontal subspace to be the Ω-orthogonal complement of the vertical subspace. Note that, by this, one can reconstruct the symplectic structure on the classical phase space by taking the horizontal part of the Ω as the symplectic form on Γ. Since one can show that the horizontal subspaces are integrable [32], there exist global horizontal sections of the Hilbert space over the classical phase space. Now, the goal is to find a horizontal section which is approximately preserved by the flow of the Hamiltonian constraint. If such section exists, the effective equations can simply be obtained by taking the expectation values in the generalized coherent states (which are semi-classical states). In [35] has been proven that for the flat FLRW model within loop quantum cosmology with a massless scalar field, this section does exist. In the rest of the thesis, we assume that this section can be found for the other cosmological models in loop quantum cosmology, too.

The fact that the effective theory provides an accurate description of the dynamics at the Planck scale is strongly using to explore the isotropic and anisotropic models, for example to find if classical singularity in the desired model is resolved or not, also to study inflationary scenario in the context of LQC (as an introduction see [34]). The effective theory is obtained from the quantum Hamiltonian operator by taking expectation values on appropriately defined states[35]. The thus obtained effective Hamiltonian then generates the dynamics on a classical phase space. It would be interesting to know whether the evolution of the semi-classical states reproduces the solutions which one gets from the effective theory. From this point of view, the study of the effective theory could be seen as the first step in this direction.

1.3 Motivation and Thesis Outline

To verify loop quantum gravity, it is helpful to apply loop quantum cosmology to the very early universe. The early universe provides us a natural arena to test different theories of quantum gravity. Inflation theory in the early universe is a successful solution for flatness, monopole and horizon problems in classical cosmology. However, there are some questions related to the inflation, for instance, what is the probability of occurring sufficient inflation in a model? If this probability is not large enough we encounter a problem with the fine tuning of initial parameters for inflation. For this reason it is interesting to study inflation in the effective description of LQC. In [36] it was shown that by using Liouville measure, the probability of having enough e-folding inflation in flat FLRW model in LQC context is near 1. We followed their work and studied the dependency of the probability on the quantum gravity scale, including the transition of the theory to the limit where general relativity (GR) is recovered. The results were seemingly in contrary to [37] which was a study on the probability in classical framework. In chapter 2, we offer an explanation and show that the conflicting results stem from different choices of initial conditions for the computation of the probability. This chapter is based on the work in [38].

As the second project, we wanted to extend these results to the closed FLRW model within LQC. However, there were some difficulties to find this probability such as unboundedness of energy density which gives an infinite volume when one integrates over the initial surface. In effective flat LQC, the matter density has a global maximum which is the density of matter field at the bounce for each solution. But in the effective closed model in which just holonomy corrections are included in, despite the fact that each solution has an upper bound, there is no global upper bound for all the solutions [25, 39, 40]. In addition for isotropic homogeneous models, quantization of the field strength is based on holonomies along closed loops but this method is not applicable for anistropic models with a nontrivial spatial curvature. For those models, one can use open holonomies to represent the Ashtekar connection and then find the curvature operator. Although for flat FLRW and Bianchi I models, these two ways of quantizing the field strength are equivalent, they lead to two different quantum theories for closed FLRW model. In [25, 26] the quantum theory for closed FLRW model by using closed holonomies was developed. Therefore it is interesting to study the model by other method and compare the results with the previous theory. In chapter 3, we quantize the model by using open holonomies and explore the effective dynamic of the theory and compare its results with the closed holonomy quantization. Furthermore, we add more quantum corrections to the effective theories to treat the infiniteness of some quantities such as matter density near the classical singularity. This chapter

is based on the papers [39] and [41].

In continuation, since Bianchi IX model is a more general model with anisotropy which classically contains the closed FLRW as its isotropic sector, we studied about the quantization of the Bianchi IX model and its effective description. Another reason for working with the Bianchi IX model is that in classical general relativity, a generic local solution near to a singularity can be described by a vacuum Bianchi IX solution which has chaotic behavior [42]. However, the quantum effects near the classical singularity might modify the chaotic behavior of the vacuum Bianchi IX solutions. The Bianchi IX model within LQC was studied in the past (e.g. [30, 43]) but we used different assumptions such as using different curve length to calculate the holonomies in quantization process or different choice of lapse (which gives us different quantum theories). In chapter 4, we show how the Hamiltonian constraint operator is obtained and then present the effective equations for the model which provide some corrections to the classical equations of motion. The correction terms include the holonomy correction effects and those which come from the inverse triad operators in the Hamiltonian constraint and could play an important role to avoid the classical chaotic behavior of the model and also resolve the singularity. This chapter is partly based on [44] and unpublished work.

For elegance and simplicity, throughout the thesis, we use the natural units i.e. $\hbar$=c=1.

We are an impossibility in an impossible universe.

Ray Bradbury

2 Inflation

The measure problem in cosmology has received some attention since it was suggested that one should weight, over the space of classical solutions to the equations of general relativity, those solutions that exhibit enough inflation to account for present observations [45, 46]. An early observation was that there exists a natural measure on the phase space of the theory with respect to which one should compute probabilities. Recently, Gibbons and Turok overcame some early difficulties in the total normalization and concluded that, for the simplest inflationary potentials in a FLRW universe, the probability of inflation was greatly suppressed [37]. One potential difficulty with such calculations pertains to the choice of initial conditions. Since all solutions to the equations of motion are singular in the past (for expanding universes), one needs a prescription for selecting initial conditions for those solutions. In [37] such a prescription was put forward in terms of a 'constant density surface', roughly speaking, at the end of inflation. Another possibility is given by defining a 'cut-off', in the form of a constant density surface at, say, the Planck scale, as was early suggested in [47].

Yet another possibility is that a quantum theory of gravity might be able to provide such Planck surface in a natural way. Such is indeed the case of loop quantum cosmology that has been able to achieve robust results regarding avoidance of big bang singularities [15, 18] (See, for instance, [11] for a recent survey). In LQC, all trajectories undergo a *bounce* that replaces the initial singularity, attain a maximum *critical density* [18], and preserve semiclassicality across the bounce [19], thanks to uniqueness results that warranty the consistency of the theory [23, 24].

Two key results in the measure problem have been obtained in LQC. First, it has been shown that one could account for the dynamics of the quantum universe by means of *effective* equations that capture the main quantum gravity effects and that reduce to the classical equations in the appropriate regime [35, 48]. This was used in [48] to show that, for several inflationary potentials, the characteristic 'attractor behavior' of inflationary dynamics [47, 49, 50] is recovered in the low energy regime. Furthermore, Ashtekar and Sloan showed recently that the natural measure of [37] can be finitely implemented in LQC, and proposed a natural Planck scale surface on which to compute probabilities [36]. Surprisingly, the probability for having enough e-foldings was shown to be close to one, in contrast to the result of Gibbons and Turok that was done for classical GR[1].

In loop quantum cosmology, the underlying discreteness of the quantum geometry manifests itself via a dimension-full parameter λ. In the LQC literature it is standard to choose the value of λ such that the minimum quantum of area corresponds to that found in LQG [1–3, 15]. But, if one considers this as a free *phenomenological* parameter of the theory, it is natural to ask whether in the limit $\lambda \to 0$, where the loop quantum geometric effects disappear, one can recover the standard Wheeler-DeWitt quantum cosmology. This has been answered with different levels of sophistication [15, 18, 51, 52]. The authors of [15] showed that the difference equation governing the LQC dynamics reduces to the differential WDW equation for the flat FLRW model in the large volume limit. Later, in [18] and [51, 52], the limit $\lambda \to 0$ was studied and it was shown that one does recover the standard WDW and the GR limit in some regime. In the case of *effective* classical equations, in this limit one recovers the equations of general relativity.

The purpose of this chapter is to explore the relation between loop quantum cosmology and general relativity, as we take the limit $\lambda \to 0$, regarding the measure problem in slow roll inflation. More precisely, we would like to understand the apparent tension between the results of Gibbons and Turok, with those of Ashtekar and Sloan. If one starts with the analysis of [36], that was done for a fixed value of λ (of the order of the Planck scale), and one takes the limit $\lambda \to 0$, one might expect to recover the results of Gibbons and Turok. As we shall show in detail this expectation is not realized. Indeed, quite the opposite occurs. As the value of the discreteness parameter is decreased, the probability of having enough inflation *increases* and approaches one in the limit. One would then be forced to conclude that in the general relativity limit of loop quantum cosmology, the probability of having enough inflation is (almost) one, in stark contrast with the analysis of

[1]There have been several previous attempts to study the issue of inflation within LQC. In [53] the natural measure of [37] was considered but the effects of the bounce and superinflation were ignored. In [54] the issue of the measure was not considered and only a small part of the parameter space was explored.

Gibbons and Turok.

What is then the source of this apparent tension? As we shall argue, the tension is resolved once one analyzes in detail the assumptions underlying both calculations. The difference turns out to be due to the initial conditions one imposes on the corresponding 'constant density surface'. In the Gibbons and Turok analysis this is taken near the end of inflation, well below the Planck scale, whereas in the LQC calculation one is taking it at the scale set by the parameter λ (which in the Ashtekar and Sloan analysis is close to the Planck scale). In the limit $\lambda \to 0$ the energy density at which the initial conditions are defined in LQC diverges, so one comes closer to the big bang singularity as one approaches the GR limit. It is this difference what accounts for the conflicting conclusions.

The structure of this chapter is as follows. In Sec. 2.1 and **??** we give a very brief review of the classical and quantum theory and effective description for loop quantum cosmology of a k=0 FLRW cosmology. In Sec. 2.3 we present the calculation of the probability for having $\mathcal{N}$ e-foldings or more in LQC. We put special attention to the discreteness parameter of LQC and the limit when it vanishes. Next, we give an argument based on global properties of the dynamics and the Liouville measure to understand the results of both [36] and [37]. We end in Sec. 2.4 with a discussion. Throughout the chapter we use Planck units, where G=$\hbar$=c=1, (rather than $8\pi G$ =1, a convention sometimes used in cosmology).

2.1 Classical and Quantum Theory of Flat FLRW Model

In flat FLRW model, the spatial manifold Σ is topologically $\mathbb{R}^3$ which is endowed with the action of Euclidean group. By using this action, one can introduce a fiducial, flat metric ${}^o q_{ab}$ and its compatible triad ${}^o e^a_i$ and co-triad ${}^o \omega^i_a$ on Σ. Because Σ is non-compact and the model is homogeneous, some of the integrals which appear in the Hamiltonian framework, diverge. To avoid this problem, since the spacetime is isotropic, one can fix a cell $\mathcal{V}$with volume V_o which is adapted to the fiducial triad and restrict the calculations on this cell.

The isotropic and homogeneous connections and densitized triads after fixing the gauge and spatial diffeomorphism freedom, can be written in terms of the fiducial quantities as follows,

$$A^i_a = \frac{c}{V_0^{1/3}}\, {}^o\omega^i_a \qquad ; \qquad E^a_i = \frac{p}{V_0^{2/3}} \sqrt{{}^o q}\, {}^o e^a_i \,. \tag{2.1}$$

Here, c is dimension-less and p has dimensions of length-squared. The Poisson

bracket for the phase space variables (c, p) is given by,

$$\{c, p\} = \frac{8\pi G\gamma}{3}\,, \tag{2.2}$$

with γ the Barbero-Immirzi parameter. Since the fiducial frames and co-frames are fixed and because of the way of parametrization of connections and triads, the only relevant constraint is the Hamiltonian constraint which in general, has the form,

$$\mathcal{C}_H = N\Big(\mathcal{H}_{\rm grav} + \mathcal{H}_{\rm matter}\Big), \tag{2.3}$$

where N is lapse function (which in this chapter we assume that it is 1), $\mathcal{H}_{\rm matter}$ is ρV (ρ is matter density) and

$$\mathcal{H}_{\rm grav} = \int_{\mathcal{V}} \frac{{\rm d}^3x}{8\pi G}\,\Big[\epsilon^{ij}{}_k\, e^{-1}\, E^a_i E^b_j\, F^k_{ab} - 2(1+\gamma^2) e^{-1}\, E^a_i E^b_j\, K^i_{[a} K^j_{b]}\Big] \tag{2.4}$$

where $e = \sqrt{|{\rm det}E|}$, F^kab is the curvature of Ashtekar connection and K^i_a is the extrinsic curvature. The curvature F^k_{ab} is,

$$F^k_{ab} = \frac{c^2}{V_0^{2/3}}\,\epsilon_{ij}{}^k\, {}^o\omega^i_a\, {}^o\omega^j_b \tag{2.5}$$

Therefore, for this model the gravitational part of the Hamiltonian constraint can be written as

$$\mathcal{H}_{\rm grav} = -\frac{1}{\gamma^2}\int_{\mathcal{V}} \frac{{\rm d}^3x}{8\pi G}\,\big[\epsilon^{ij}{}_k\, e^{-1}\, E^a_i E^b_j\, F^k_{ab}\big] = -\frac{\gamma^2}{6} c^2\sqrt{p}. \tag{2.6}$$

It is convenient to introduce new variables [18]: $\beta := c/|p|^{1/2}$ and $V = p^{3/2}$. The quantity V is just the volume of $\mathcal{V}$ and β is its canonically conjugate and their Poisson bracket is given by,

$$\{\beta, V\} = 4\pi G\gamma \tag{2.7}$$

To find the Friedman equation we need the volume's equation of motion and then using the constraint equation. The evolution equation of V is,

$$\dot{V} = \{V, \mathcal{H}_{\rm grav}\} = \frac{3}{\gamma}\beta V \tag{2.8}$$

and thus the standard Friedman equation,

$$H^2 := \left(\frac{\dot{V}}{3V}\right)^2 = \frac{8\pi G}{3}\,\rho. \tag{2.9}$$

To quantize the model, we take the gravitational part of the kinematical Hilbert space to be the square integrable functions on Bohr compactification on real line, $L^2(\mathbb{R}_{\rm Bohr}, d\mu_{\rm Bohr})$. We work with the basis $\{|v\rangle : v \in \mathbb{R}\}$ which diagonalizes the $\hat{V}$. These eigenstates satisfy

$$\langle v_i|v_j\rangle = \delta_{v_i,v_j}. \tag{2.10}$$

Also, we have to select a set of elementary observables which have unambiguous related operators to write the Hamiltonian constraint operator in terms of them. In loop quantum gravity these fundamental variables are the holonomies h_e defined by the connection A_a^i along edges e and the fluxes of the densitized triad E_i^a across surfaces. Since our model is isotropic and homogeneous, we choose V and $e^{i\alpha\lambda\beta/2}$ [2], where α is an arbitrary real number and λ is the square root of the smallest non-zero eigenvalue of the area operator in loop quantum gravity[3], to be the elementary variables. The action of their related operators on the basis are

$$\hat{V}|v\rangle = V_c|v||v\rangle, \qquad V_c = \left(\tfrac{4\pi\gamma}{3}\right)^{3/2}\tfrac{3\sqrt{3\sqrt{3}}}{2\sqrt{2}} \tag{2.11}$$

$$\widehat{e^{i\alpha\lambda\beta/2}}|v\rangle = |v-\alpha\rangle. \tag{2.12}$$

The first term in the gravitational part of the constraint is $\epsilon^{ij}{}_k E_i^a E_j^b/\sqrt{|q|}$. To find a well defined operator related to this term we can use Thiemann strategy[3]. We have the following classical identity from the full theory

$$\epsilon^{ij}{}_k \frac{E_i^a E_j^b}{\sqrt{|q|}} = \frac{\varepsilon}{2\pi G\gamma\mu}\ {}^o\epsilon^{abc}\ {}^o\omega_c^i \mathrm{Tr}\left(h_i^{(\mu)}\{h_i^{(\mu)-1}, V\}\tau_k\right) \tag{2.13}$$

where ε is 1 if the fiducial frames and physical ones have the same orientation otherwise is -1. Also the holonomy $h_i^{(\mu)}$ where $\mu V_o^{1/3}$ is the length of the curve along edge ${}^o e_i$ with respect to the fiducial metric is given by

$$\begin{aligned} h_i^{(\mu)} &= \cos(\frac{\mu c}{2})\mathbb{I} + 2\sin(\frac{\mu c}{2})\tau_i \\ &= \frac{1}{2}(e^{i\mu c/2} + e^{-i\mu c/2})\mathbb{I} - i(e^{i\mu c/2} - e^{-i\mu c/2})\tau_i, \end{aligned} \tag{2.14}$$

where $\mathbb{I}$ is unit 2×2 matrix and τ_i is a basis in Lie algebra su(2).[4] Note that here, μ is arbitrary. Therefore the related operator of this term is

$$\widehat{\epsilon^{ij}{}_k \frac{E_i^a E_j^b}{\sqrt{|q|}}} = \frac{\hat{\varepsilon}}{2i\hbar\pi G\gamma\mu}\ {}^o\epsilon^{abc}\ {}^o\omega_c^i \mathrm{Tr}\left(\hat{h}_i^{(\mu)}[\hat{h}_i^{(\mu)-1}, \hat{V}]\tau_k\right). \tag{2.15}$$

[2]Holonomy $h_i^{(\alpha)}$ along edge ${}^o e_i$ with the physical length $\alpha\lambda$ defined by connection A^i which appears in the Hamiltonian constraint operator, can be expressed by this operator.

[3]We will explain later in this section why λ appears in the theory.

[4]τ_i are equal to $\frac{\sigma_i}{2i}$ where σ_i are Pauli matrices and satisfying $\tau_i\tau_j = \frac{1}{2}\epsilon_{ijk}\tau_k - \frac{1}{4}\delta_{ij}$.

Note that for different choices of μ we will have different operators which are *not* equivalent.

To define related operator to the curvature F_{ab} we use the following strategy. Classically one can consider the square $\Box_{ij}$ which each of its sides has the length $\mu V_o^{1/3}$ with respect to the fiducial metric, in the $i-j$ plane spanned by a face of the elementary cell and then define the field strength as,

$$F_{ab}^k = -2 \lim_{Ar\Box \to 0} \mathrm{Tr}\left(\frac{h_{\Box_{ij}}^{(\mu)} - \mathbb{I}}{\mu^2 V_o^{2/3}} \right) \tau^k \ {}^o\omega_a^i \ {}^o\omega_b^j \tag{2.16}$$

To write down the curvature operator, we know that the limit $Ar\Box \to 0$ of the operator does not exist. However, in loop quantum gravity the eigenvalues of the area operator are discrete and there is a smallest non-zero eigenvalue, Δ, for the area operator which means that there is an area gap. Thus because of this area gap, it is more appropriate to take the limit of the $Ar\Box$ to go to this smallest non-zero eigenvalue than to let it to go to zero. Therefore the curvature operator F_{ab}^k is given by

$$\hat{F}_{ab}^k = \frac{\sin^2 \bar{\mu} c}{\bar{\mu}^2 V_o^{2/3}} \ {}^o\epsilon_{ij}^k \ {}^o\omega_a^i \ {}^o\omega_b^j = \frac{V^{2/3} \sin^2 \lambda\beta}{\lambda^2 V_o^{2/3}} \ {}^o\epsilon_{ij}^k \ {}^o\omega_a^i \ {}^o\omega_b^j \tag{2.17}$$

where $\bar{\mu} = \lambda/\sqrt{|p|}$ and $\lambda^2 = \Delta = 4\sqrt{3}\gamma\ell_{\mathrm{PL}}^2$ is equal to smallest non-zero eigenvalue of area operator.

We recall that in Eq.(2.15) the length of the edge which use for calculating the holonomies, is arbitrary but from now, for simplicity, we use the same length as the one for the curvature. Also in the rest we work in the natural unit that $\hbar$ is equal to 1. With these choices, the operator in Eq.(2.15) gets the form

$$\widehat{\epsilon_k^{ij} \frac{E_i^a E_j^b}{\sqrt{|q|}}} = \frac{\hat{\epsilon}\widehat{V^{2/3}}}{4\pi G\gamma\lambda} (\widehat{e^{i\lambda\beta/2}} \hat{V} \widehat{e^{-i\lambda\beta/2}} - \widehat{e^{-i\lambda\beta/2}} \hat{V} \widehat{e^{i\lambda\beta/2}}) \ {}^o\epsilon^{abc} \ {}^o\omega_c^k \tag{2.18}$$

where $\hat{\epsilon}$ is the operator related to ε. For simplicity we define operator $\hat{A}$ as follows

$$\hat{A} = \frac{\hat{\epsilon}}{4\pi G\gamma\lambda} (\widehat{e^{i\lambda\beta/2}} \hat{V} \widehat{e^{-i\lambda\beta/2}} - \widehat{e^{-i\lambda\beta/2}} \hat{V} \widehat{e^{i\lambda\beta/2}}) \tag{2.19}$$

The action of this operator on the basis of the gravitational part of the kinematical Hilbert space is

$$\hat{A}|v\rangle = A(v)|v\rangle, \tag{2.20}$$

where

$$A(v) = (|v+1| - |v-1|) = \begin{cases} |v| & |v| < 1 \\ 1 & |v| \geq 1 \end{cases} \tag{2.21}$$

Hence the Eq.(2.18) can be written as

$$\widehat{\epsilon^{ij}_{\ k}\frac{E^a_i E^b_j}{\sqrt{|q|}}} = \widehat{V^{2/3}}\hat{A}\ {}^o\epsilon^{abc}\ {}^o\omega^k_c \tag{2.22}$$

Finally the Hamiltonian constraint operator before factor ordering is given by

$$\hat{\mathcal{C}}_H = -\frac{3}{8\pi G\gamma^2\lambda^2}\left[\hat{V}\hat{A}\sin^2\lambda\beta\right] + \hat{\rho}\hat{V} \tag{2.23}$$

In the next chapter we will show that the gravitational part of the constraint operator with any choice of ordering, is essentially self adjoint.

2.2 Effective Equations of Flat FLRW Cosmology

The effective Hamiltonian that one obtained from loop quantum cosmology for a k=0 FRW model is [35]

$$\mathcal{H}_{\text{eff}} = -\frac{3}{8\pi\gamma^2\lambda^2}v\sin^2\lambda\beta + \rho v \tag{2.24}$$

where v is the volume and, on equations of motion, $\beta = \gamma H$, where H is the Hubble parameter. From the previous Hamiltonian the *effective* Friedman equation becomes,

$$\frac{\sin^2\lambda\beta}{\gamma^2\lambda^2} = \frac{8\pi}{3}\rho \tag{2.25}$$

or, equivalently

$$H^2 = \frac{8\pi}{3}\rho\left(1 - \frac{\rho}{\rho_{\text{crit}}}\right) \tag{2.26}$$

where the density is given by $\rho = \dot{\phi}^2/2 + V(\phi)$. Here $\rho_{\text{crit}} = 3/(8\pi\gamma^2\lambda^2)$, the *critical* density, is the density of the scalar field at the bounce. All trajectories undergo a bounce for which the density becomes exactly ρ_{crit}. In the low density regime, namely when $\lambda\beta \ll 1$ or $\rho \ll \rho_{\text{crit}}$ we approach classical general relativity. Note that the quantum geometry scale λ sets the scale for the critical density. With the standard value taken in the LQC literature $\lambda = \sqrt{4\sqrt{3}\pi\gamma}\,\ell_{Pl}$ and the Barbero-Immirzi parameter $\gamma \approx 0.237$ chosen to be compatible with the Hawking-Bekenstein entropy (for a recent summery of results see [55]), the critical density is $\rho_{\text{crit}} \approx 0.41\rho_{\text{Pl}}$ [18]. (Recall that is the Planck units we are using ℓ^2_{Pl}=$G\hbar$=1,

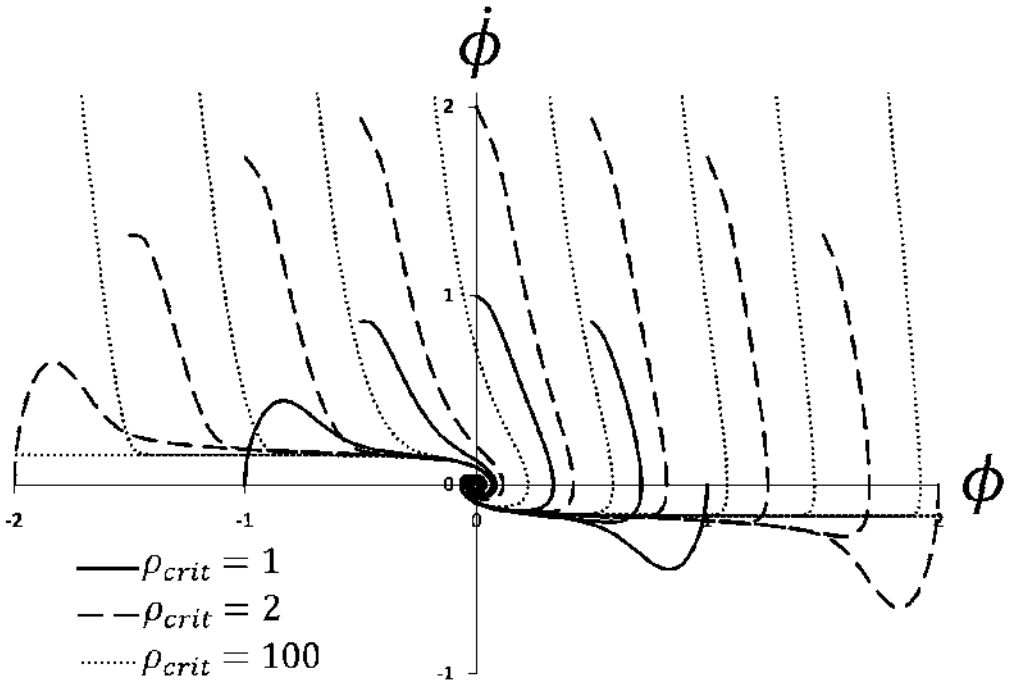

Figure 2.1: Three sets of trajectories are plotted for different values of the critical density. Note that near the origin, all trajectories approach the attractor.

and $\rho_{Pl} = 1$.) As we decrease the parameter λ, the critical density increases, so the 'classical limit' is attained in the limit when the critical density diverges.

The equation of motion for the scalar field ϕ yield the standard Klein Gordon equation is,

$$\ddot{\phi} + 3H\dot{\phi} + V_{,\phi} = 0 \tag{2.27}$$

For the simplest potential, namely $V = m^2\phi^2/2$, we have solved the equations of motion for various values of the critical density and for convenience, plotted them in Fig. 2.1. In the $(\phi, \dot{\phi})$ plane, the surfaces of constant density are ellipsoids defined by $\rho = \dot{\phi}^2/2 + m^2\phi^2/2$. All trajectories approach the 'critical density surface', the ellipse bounding the phase diagram where the bounce occurs and touch it tangentially. Something that one might expect and that was checked in [48], is that near the origin of the plane, where the density is small compared to the critical one, the LQC trajectories and the classical one should coincide. This can be seen in Fig. 2.1. As one decreases λ the critical density increases and the maximum ellipse defined by $\dot{\phi}_B^2/2 + m^2\phi_B^2/2 = \rho_{\rm crit}$ becomes larger. The classical limit (GR) can be approached as $\lambda \to 0$. One has to note however, that this limit is somewhat discontinuous [18, 51, 52], since all LQC trajectories bounce, for all

values of λ, while there is no bounce in GR. In this particular sense, the GR 'limit', and correspondingly the big bang, corresponds to an 'infinitely large ellipsoid', or the point at infinity in the $(\phi, \dot{\phi})$ plane (See Fig. 2.2).

2.3 Probability for Slow Roll Inflation in LQC

This section has two parts. In the first one, we calculate the probability for slow roll inflation in LQC and consider the limit when the discreteness parameter tends to zero. In the second part, we use qualitative aspects of the dynamics to gain a deeper understanding of the results.

2.3.1 Probability

Let us now evaluate the probability for inflation as done in [36], keeping track of the dependence on λ. Without loosing generality, we shall focus on the sector of the solution space for which $\dot{\phi}$ is nonnegative. Then, the Liouville measure $\mathrm{d}\mu$ when pulled back to the surface with constant β or equivalently with constant ρ, has the from [36],

$$\mathrm{d}\mu = \sqrt{8}\pi\gamma\, v(\rho - V(\phi))\, \mathrm{d}\phi\, \mathrm{d}v \tag{2.28}$$

We we further choose, as in [36], the surface of constant β (and ρ) at the bounce, we get

$$\mathrm{d}\mu = \frac{\sqrt{3\pi}}{\lambda}\, v_B \sqrt{1 - F_B}\, \mathrm{d}\phi_B \mathrm{d}v_B \tag{2.29}$$

where ϕ_B is the value of scalar field at the bounce, v_B is the volume of the universe at the bounce and $F_B = V(\phi_B)/\rho_{\mathrm{crit}}$. This is the measure that will be used for computing the probability of having $\mathcal{N}$ or more e-foldings.

The number of e-foldings during inflation, $\mathcal{N}$, can be written as

$$\mathcal{N} = \int_{t_o}^{t_{\mathrm{end}}} H\, \mathrm{d}t = \int_{\phi_o}^{\phi_{\mathrm{end}}} \frac{H}{\dot{\phi}}\, \mathrm{d}\phi \tag{2.30}$$

where t_o, ϕ_o, t_{end}, and ϕ_{end} are the time and value of the scalar field at the onset and at the end of inflation, respectively. We can use the slow roll conditions, $V(\phi) \gg \dot{\phi}/2$ and $V_{,\phi} \gg \ddot{\phi}$, together with Eq.(2.27) to approximate $\mathcal{N}$,

$$\mathcal{N} \approx -\int_{\phi_o}^{\phi_{\mathrm{end}}} \frac{3H^2}{V_{,\phi}}\, \mathrm{d}\phi = 2\pi \left(1 - \frac{\phi_o^2 + \phi_{\mathrm{end}}^2}{2\phi_{\mathrm{max}}^2}\right) (\phi_o^2 - \phi_{\mathrm{end}}^2) \tag{2.31}$$

where ϕ_{max} is the maximum value the scalar field can attain and is given by $\phi_{\mathrm{max}} = \sqrt{2\rho_{\mathrm{crit}}}/m$. For large values of $\mathcal{N}$, the value of the scalar field at the end

of inflation is much smaller than its value at the onset of inflation. Thus, for large (but finite) $\mathcal{N}$ we can neglect some terms and get,

$$\mathcal{N} \approx 2\pi \left(1 - \frac{\phi_o^2}{2\phi_{\max}^2}\right) \phi_o^2 \tag{2.32}$$

It should be noted that this is a slight overestimation of the value of $\mathcal{N}$ but this does not constitute a problem for our analysis. From this last equation, we can find the value $\phi_o^{\mathcal{N}}$ of the scalar field at the onset of inflation, for a given value of $\mathcal{N}$ as

$$\phi_{o\pm}^{\mathcal{N}} = \pm \frac{\sqrt{3(1 - \sqrt{1 - 8\mathcal{N}\gamma^2\lambda^2 m^2/3})}}{\sqrt{8\pi}\gamma\lambda m} \tag{2.33}$$

In the GR limit, that is, in the $\lambda \mapsto 0$ limit, we expect that $\phi_{o\pm}^{\mathcal{N}}$ be equal to $\pm\sqrt{\mathcal{N}/2\pi}$.

Let us now see how we can find ϕ_B^o which is the value of the scalar field at the bounce that evolves under the dynamics to $\phi_{o\pm}$ as the starting point of inflation. According to Eq.(2.27), if at the bounce $\phi_B^o > 0$ then $\ddot{\phi}_B < 0$ (and $\dot{\phi} > 0$). Similarly, if $\phi_B^o < 0$ then $\ddot{\phi}_B > 0$ (and $\dot{\phi}_B > 0$). In the second case, after some time, $\ddot{\phi}$ becomes zero and after that it will be negative, but near the onset of inflation it becomes zero again. Near the start of inflation at the time for which $\dot{\phi} = 0$, the value of the scalar field is larger than ϕ_B^o. After that, $\dot{\phi}$ becomes negative and the value of the scalar field starts to decrease but very soon after $\dot{\phi} = 0$, the inflationary era starts and the scalar field at the onset of inflation remains larger than the value of the scalar field at the bounce ($\phi_B^o < \phi_{o\pm}$).

Furthermore, because of the uniqueness of the solutions, ϕ_o is a monotonic function of ϕ_B and since ϕ_o is always greater than ϕ_B, then it is an increasing function of ϕ_B.

Given this, we can write the probability of having inflation with $\mathcal{N}$ e-folding or more as the quotient of the volume on the space of solutions occupied by solutions with $\mathcal{N}$ or more e-foldings divided by the total volume. Since the measure does not depend on volume v and the range of this coordinate is infinite, both terms are unbounded. However, we can very easily get rid of these spurious infinities by an appropriate renormalization (or gauge fixing [34, 56]). One possibility is to restrict the domain of the volume integral to the interval $v \in (1, 2)$ (in Planck units). With this choice, the volume integrals in the quotient cancel each other and we get,

$$
\begin{aligned}
P_{\mathcal{N}} &= \frac{\int_{-\phi_{\max}}^{\phi_a^{\mathcal{N}}} \sqrt{1-F_B}\,\mathrm{d}\phi_B + \int_{\phi_b^{\mathcal{N}}}^{\phi_{max}} \sqrt{1-F_B}\,\mathrm{d}\phi_B}{\int_{-\phi_{\max}}^{\phi_{\max}} \sqrt{1-F_B}\,\mathrm{d}\phi_B} \\
&= 1 - \frac{\int_{\phi_a^{\mathcal{N}}}^{\phi_b^{\mathcal{N}}} \sqrt{1-F_B}\,\mathrm{d}\phi_B}{\int_{-\phi_{\max}}^{\phi_{\max}} \sqrt{1-F_B}\,\mathrm{d}\phi_B}\,,
\end{aligned}
\tag{2.34}
$$

where $\phi_a^{\mathcal{N}}$ and $\phi_b^{\mathcal{N}}$ are the minimum and maximum value of ϕ at the bounce that cause inflation with $\mathcal{N}$ e-folding respectively and $\phi_{\max}$ is the maximum value of ϕ_B and is equal to $3/2\gamma\lambda m\sqrt{\pi}$. Then

$$
P_{\mathcal{N}} = 1 - \frac{\arcsin(2\gamma\lambda m\phi_b^{\mathcal{N}}\sqrt{\pi}/3) - \arcsin(2\gamma\lambda m\phi_a^{\mathcal{N}}\sqrt{\pi}/3) - 2\gamma\lambda m\sqrt{\pi}/3(\phi_b^{\mathcal{N}} - \phi_a^{\mathcal{N}})}{2(\pi/2-1)}
\tag{2.35}
$$

We have plotted in Fig. 2.1 the dynamical trajectories for three values of λ. As one can see, when λ becomes small, the trajectories (for finite values) are almost parallel. Then, in the limit $\lambda \to 0$ we can approximate $\phi_b^{\mathcal{N}} - \phi_a^{\mathcal{N}}$ by $\phi_{o+}^{\mathcal{N}} - \phi_{o-}^{\mathcal{N}}$ and since $\phi_{o\pm}^{\mathcal{N}}$ are finite, then the difference between $\phi_b^{\mathcal{N}}$ and $\phi_a^{\mathcal{N}}$ is finite. From the above discussion and Eq.(2.35), for a finite $\mathcal{N}$ we see that the probability is a decreasing function of λ ($2\gamma\lambda m\sqrt{\pi}\phi_b/3$ and $2\gamma\lambda m\sqrt{\pi}\phi_a/3 < 1$) and when λ goes to zero we have that $\arcsin(2\gamma\lambda m\phi_b^{\mathcal{N}}\sqrt{\pi}/3) \approx 2\gamma\lambda m\phi_b^{\mathcal{N}}\sqrt{\pi}/3$ (and equivalently for $\phi_a^{\mathcal{N}}$) and therefore the probability in Eq.(2.35) goes to 1. This is the first result of this chapter.

Let us now understand qualitatively why the probability increases as the LQC parameter decreases. As the analysis here presented and that of [36] shows, for a given value of ρ_{crit}, there is an interval $(\phi_a^{\mathcal{N}}, \phi_b^{\mathcal{N}})$, in the 'kinematically dominated regime' (where the energy density at the bounce is mainly due to the kinetic energy), where there are not enough e-foldings. This interval, as we have estimated before, depends on λ. In Fig. 2.2 we have plotted, for three values of ρ_{crit}, the 'critical trajectories' for which the transition occurs. That is, these trajectories have an almost identical behavior at small densities, so they inflate in the same fashion, and touch the bounce surface at the points $\phi_a^{\mathcal{N}}$ and $\phi_b^{\mathcal{N}}$. If we now follow them to higher densities 'back in time', what one sees from the graph is that as λ decreases, and ρ_{crit} increases, the intersection points tend to the $\dot{\phi}$ axis. The relative size of the interval $(\phi_a^{\mathcal{N}}, \phi_b^{\mathcal{N}})$ in the total allowed interval $(-\phi_{\max}, \phi_{\max})$ also goes to zero as $\rho_{\mathrm{crit}} \to \infty$[5]. Since the integrand does not diverge, this already implies that the quotient vanishes and the probability goes to 1.

[5]Recall that $\phi_{\max}$ is obtained from the value of the potential at the bounce $\rho_{\mathrm{crit}} = V(\phi_{\max})$. In our case $\phi_{\max} = \sqrt{2\,\rho_{\mathrm{crit}}}/m$, so the interval in which the scalar field can take values also diverges as $\rho_{\mathrm{crit}} \to \infty$.

Note also that this result is independent of the precise value of $\mathcal{N}$ (as long as it is large enough for our approximation to be valid). Does this mean that we can take the limit $\mathcal{N} \to \infty$ and also have probability one? In order to answer this one should exercise some care. For any finite value of $\mathcal{N}$, the probability will tend to one as we make λ smaller for two reasons. The first one is that the dynamics of the effective equations is such that those trajectories that do not have enough inflation get 'funneled', for large enough values of the critical density, into the interval $(\phi_a^{\mathcal{N}}, \phi_b^{\mathcal{N}})$ that remains bounded, while the total interval for ϕ grows with $\rho_{\rm crit}$. This only happens because we are taking the bounce surface as the reference surface where the probability is computed. Furthermore, the measure is such that relative volume we associate to those trajectories is very small and becomes zero in the $\lambda \to 0$ limit. This does not mean that we can fix λ and, say, take the limit $\mathcal{N} \to \infty$.

A final remark is in order. In our analysis, as plotted in Fig. 2.2, the criteria for how much inflation there is coincides with that of [36]. That is, we start with the critical density of LQC (of the order of the Planck density), which gives an initial condition from which to measure e-foldings, and find those trajectories –in theories with a different λ– for which the dynamics at low densities coincide, where inflation actually occurs. This is also in the spirit of [47], which suggested to take initial conditions at the Planck scale. Our strategy has to be contrasted with a possible alternative that involves going closer to the big bang, as we decrease λ, and use that as initial condition in the e-folding counting. The problem with this choice is that, as one approaches the big bang that has zero volume, the number of e-foldings diverges for all trajectories, so even the question of which trajectories have enough inflation becomes meaningless, since every trajectory would have an infinite number of e-foldings.

2.3.2 Comparison

Let us now come to the question of how we can reconcile the results of Gibbons and Turok [37] on the one side and those of Ashtekar and Sloan [36] on the other. The first possible objection is: How can we compare two results that are taken on two different theories, GR on one side and LQC on the other? As we have seen before, one can in fact approximate very well the low density GR trajectories by (low density) LQC effective trajectories. Thus, the region of interest in the Gibbons and Turok analysis, $\rho_{\rm GT}/\rho_{\rm crit} \ll 1$, which is for trajectories near the end of inflation (and therefore, around the constant density surface in our Figure 2.2), one can take the LQC effective trajectories without any problems as a very good approximation to the GR dynamics. This allows us to 'embed' the low density GR dynamics in the effective LQC description with very good accuracy.

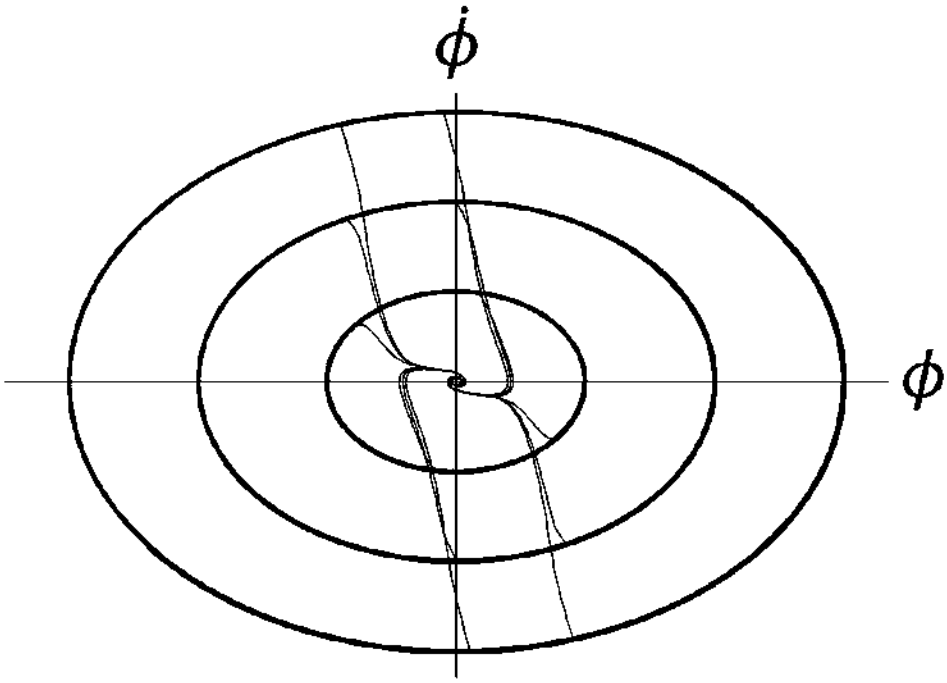

Figure 2.2: Here we are plotting trajectories for three different values of the critical density $\rho_{\rm crit}$. In each case, we have a boundary of the trajectories in the $(\dot{\phi}, \phi)$ plane, corresponding to the bounce, that are depicted as ellipsoids. The smallest ellipsoid can be taken as the LQC one, and the larger ones are closer to the GR limit. The 'critical' curves that separate the region of enough e-foldings, as determined by the LQC scale, are then plotted for the three different values of the critical density $\rho_{\rm crit}$. One can see that, as the critical density increases, the intersection with the ellipsoid of critical density comes closer to the $\dot{\phi}$ axis.

With this assumption, we can now compare the two result within the effective LQC description. We have two constant density surfaces, as depicted in Fig. 2.3. The external ellipsoid corresponds of course to the critical density $\rho_{\rm crit}$ at scale λ, while the small one corresponds to the density $\rho_{\rm GT}$ as chosen by Gibbons and Turok[6]. One puzzling fact about the huge discrepancy in results is that both analysis use the natural Liouville measure (properly normalized) to compute the probability on constant density surfaces. One important property of the Liouville measure is that it is invariant under the dynamical evolution. So, how come we arrive to two very different conclusions?

[6]The figure is not to scale, since we are asking that $\rho_{\rm GT} \ll \rho_{\rm crit}$. The relative densities in the figure were taken to illustrate our point.

There are two key observations to understand this apparent tension. The first one pertains to the question of whether the time evolution invariance of the Liouville measure implies that the probability is also invariant. On a first view, one might imagine that the probability has to be invariant since one is just measuring the relative phase space volume of those trajectories with $\mathcal{N}$ e-foldings or more, relative to the total volume in phase space. Now, the technical step that allowed to normalize the phase space volume (the total phase space volume is infinite) in [37] and [36] was to realize that there is an invariance in the space of classical solutions by rescaling the physical volume. This invariance has its origin in the fact that, instead of describing the whole universe, one has to restrict attention to a fiducial region R in space (the spatial volume of the whole universe in k=0 FRW is infinite, so one needs to consider a region with a finite volume). Since this choice is arbitrary, one can in principle chose a smaller/larger region for which we assign a smaller/larger volume, but the physics should be unchanged. When one takes care of this ambiguity, either by taking an appropriately chosen 'interval in v' as we done in the previous part, or by an appropriate gauge fixing [34, 36], one still has to be careful about the possible change in physical volume during the dynamical evolution that would also induce a change in relative volume in phase space.

Let us see how this comes about. Invariance of the Liouville measure means that the volume in phase space is preserved. Let focus our attention in the quadrant in the space of solutions, with coordinates (v_B, ϕ_B), defined by $1 \leq v_B \leq 2$ and $-\phi_{\rm max} \leq \phi_B \leq \phi_{\rm max}$, and follow it through its dynamical evolution. If we now take another 'gauge fixing' at a lower energy density, say ρ_1 (See Fig. 2.3), we immediately notice that the range in ϕ is much smaller. Since the total volume of the quadrant we are following has to be the same (due to the dynamical invariance of the Liouville measure), the range in v has to increase, as it indeed does, since most solutions inflate. The crucial point here is to realize that the change in volume $\Delta v = v_1 - v_B$ from the bounce to the ρ_1 surface depends on the value of ϕ. Thus, the lines, say, $v_B(\phi_B) = 1$ at the bounce gets mapped, in general to a curve $v_1(\phi_1)$ that is no longer constant as a function of ϕ_1. That is, each solution has a different change in physical volume depending on the value of the scalar field at the bounce. But, if one is only keeping track of the change in the 'phase space coordinate' ϕ when computing the probability, then the *relative volume in phase space*, as measured by only ϕ, can indeed change. Since this is precisely what one means by probability in the analysis of [36,37] and here, we are led to conclude that the probability indeed depends on the surface on which it is computed. Since this argument did not use any particular detail of the LQC dynamics, this ambiguity in the probability depending on the choice of constant density surface is also present in general relativity. Let us now see what further assumption are made in both

calculations.

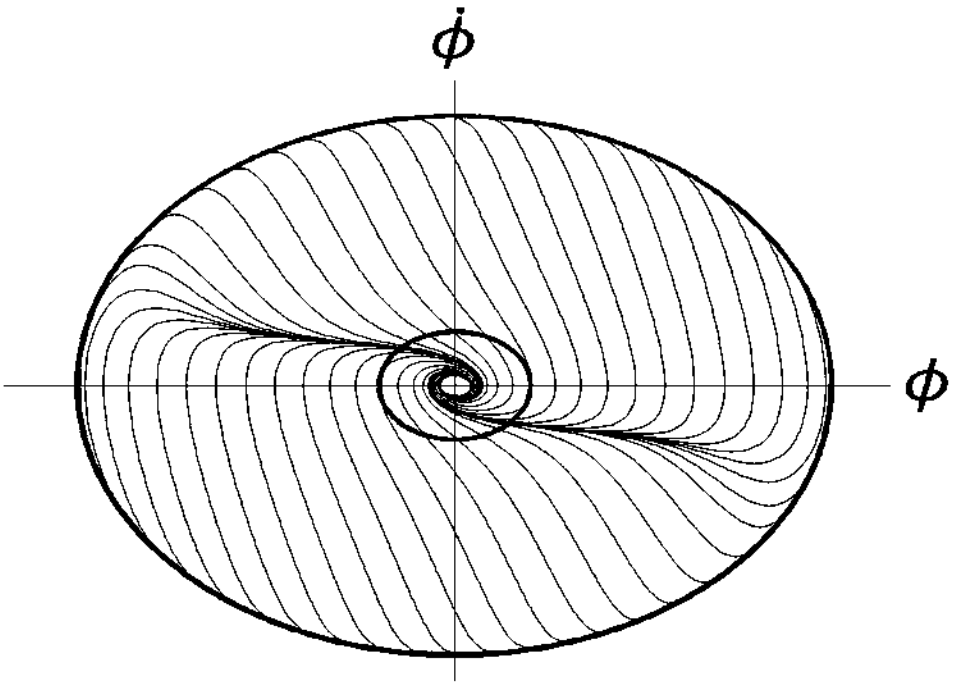

Figure 2.3: For a fixed value of $\rho_{\rm crit}$, we plot the exterior, critical density surface and a surface of constant density $\rho_{\rm GT} \ll \rho_{\rm crit}$ (not drawn to scale, of course) on the $(\dot{\phi}, \phi)$ plane. Trajectories with a uniform distribution at the LQC bounce ellipsoid are plotted. Note that trajectories for which there is enough inflation get funneled into a small region in the smaller $\rho_{\rm GT}$ ellipse. Near this surface, the GR and LQC dynamics almost coincide

The second observation is the following. When computing the probability of having $\mathcal{N}$ e-foldings, one has to assume an a-priory probability distribution $\mathbf{P}(\phi, v)$ of the classical trajectories, and then integrate this probability distribution with respect to the corresponding measure. In [36], the authors consider the most natural choices, namely, the probability is computed on the critical density surface (i.e., the bounce) using, as the integration measure, the Liouville measure. By invoking Laplace's 'principle of indifference' as in [37], they consider a *uniform* distribution on the space of trajectories (labeled by (ϕ, v)) and performed an appropriate gauge fixing with respect to the volume rescaling freedom available, in the same spirit we have done here. We have illustrated this scenario in Fig. 2.3, where we plotted trajectories uniformly distributed in ϕ along the critical density surface. If we now follow these trajectories along the dynamical evolution we notice that, when they

intersect the $\rho = \rho_{\rm GT}$ surface, they are no longer uniformly distributed. Quite the opposite. Due to the global properties of the dynamics, the trajectories are funneled into the 'attractor' on the plane $(\phi, \dot{\phi})$ and, therefore, effectively acquire a new 'probability distribution' $\tilde{\mathbf{P}}(\phi)$ on the $\rho = \rho_{\rm GT}$ surface[7].

If we were to compute the probability of inflation on the Gibbons and Turok surface, but *weighted with the induced distribution* $\tilde{\mathbf{P}}(\phi)$, we would of course get the same result of Ashtekar and Sloan, given our previous discussion. What Gibbons and Turok did instead was to assume a uniform distribution $\mathbf{P}(\phi)$ on the $\rho = \rho_{\rm GT}$ surface. With respect to the uniform distribution, the phase space volume of inflating solutions is very small and the probability is therefore, very close to zero. Had we chosen to compute the probability on a surface with even lower density, the result would even be smaller. This constitutes the main difference between both calculations[8].

Furthermore, we can now understand why the probability found by Gibbons and Turok is so small. If we look at the region of Fig. 2.2 for which there is not enough inflation (in between the critical curves) on the LQC critical density surface, and follow those trajectories as in Fig. 2.3, we see that those trajectories occupy now a much larger region on the $\rho = \rho_{\rm GT}$ ellipsoid. In other words, the trajectories for which there is enough inflation get funneled into a small region in the $\rho = \rho_{\rm GT}$ surface that, when integrated with respect to the uniform distribution $\mathbf{P}(\phi)$ of [37], give a very small contribution to the probability. One could also consider the opposite situation in which one starts with an uniform distribution on the GT surface and 'evolve back' in time to the bounce surface. In that case, the dynamics will 'expel' the trajectories in such a way that the probability distribution $\mathbf{P}'(\phi)$ induced on the bounce surface is concentrated on the region where there is not enough inflation. If one integrates that probability distribution with respect to the Liouville measure the resulting probability is very close to zero, as found by Gibbons and Turok in [37].[9]

[7] We can view this induced probability distribution as a way of keeping track of the relative change in phase space volume do to the dynamics that induces a differentiated change in physical volume v for different trajectories. Namely, the distribution is given by $\tilde{\mathbf{P}}(\phi) = v_{\rm GT}(\phi)$, in terms of the volume $v_{\rm GT}$, as a function of ϕ on the Gibbons-Turok constant density surface.

[8] Note that Linde had pointed out that the assumption of Gibbons and Turok to take uniform initial conditions at the end of inflation might be the source of their negative result [50], but the mechanism he outlined is different from ours, since he was not taking the Liouville measure into account.

[9] One should note that, as previously discussed, in order to make the distinction of which trajectories have enough e-foldings, one has to introduce a cut-off for the initial condition. Here we have adopted the LQC scale as a natural unambiguous choice.

2.4 Discussion

Let us summarize our results. We have reanalyzed the treatment of the simplest inflationary model from the perspective of loop quantum cosmology. By using effective equation we studied the structure of the space of classical solutions with the aim of answering the question: How probable is it to achieve enough e-foldings? In particular we have considered this question keeping the discreteness parameter of loop quantum cosmology as a free parameter. When the parameter vanishes, one expects the dynamics to reduce to the standard, general relativity behavior. The first result is that, as previously shown in [36], the probability for enough inflation is very close to one when the discreteness parameter λ is of the order of the Planck scale. We then considered the dependence of the probability as one decreases the parameter and it approaches the general relativity limit. As we have shown, the probability increases and approaches one as one reaches the limit. Next, we studied the global properties of the system to understand the underlying reason for the discrepancy of these results and those of [37] in which the probability of enough inflation was computed to be close to zero, within general relativity. What we found is that this discrepancy is due to the differences in the underlying assumptions in both calculations. As it turns out the probability as computed in both [37] and [36] depends very strongly on the *constant density surface* where it is calculated. While Ashtekar and Sloan assume a uniform distribution of classical trajectories at the naturally defined surface available due to the universal existence of the bounce, Gibbons and Turok take it at an arbitrarily defined surface at the end of inflation. Given the large difference in scales involved and due to the global properties of the dynamics and the probability measure, these two assumptions have strikingly different consequences. During the evolution from the bounce to the Gibbons-Turok scale, most of the trajectories that undergo enough inflation –contributing significantly to the probability– get funneled into a small region at the later scale, that has a correspondingly small contribution to the probability. This is the origin of the apparent tension.

We have thus found two very different results even for GR. On the one hand the Gibbons-Turok result involves several, somewhat ad-hoc, assumptions given that there is no preferred choice of scale on GR. On the other hand, there is the limit of LQC when the discreteness parameter vanishes. In this later case we have, for each scale, calculations based on unambiguous and natural choices that provide a well defined result, even when the GR limit of LQC is non-smooth. Thus even when in the $\lambda \to 0$ limit one is approaching arbitrarily close to the singularity, the probability of having $\mathcal{N}$ e-foldings –as measured from the Planck scale down– can be given some meaning. As we have seen, the result that in the GR, $\lambda \to 0$ limit, the probability goes to one for any finite value of $\mathcal{N}$, seems to be generic.

Whether this result is physically meaningful is, however, a completely different issue. In the situation in which λ is taken well below the Planck scale, we are implicitly assuming that the classical equations are still valid. This is perhaps, too strong an assumption. One generically expects quantum effects to dominate near and below the Planck scale. This is precisely what LQC provides for us via its effective equations.

Let us end with a series of remarks.

1. Given that these two results are based on assumptions that yield completely opposite predictions, one might then ask what is the physically reasonable assumption to make? How can we justify one choice over the other? Is there a 'canonical' choice of initial condition? In loop quantum cosmology we know that the bounce is generic for inflationary potentials [57], and the effective equations are a very good approximation to the dynamics of semiclassical states [35]. Since every such effective trajectory goes through a bounce, selecting the surface of constant density, at the bounce, seems a rather natural choice. One should emphasize then that there does not exist a similar surface that is preferred in the classical GR case. As we have seen, the probability does depend in a rather dramatic way on the choice of such surface. Without any extra input, the LQC choice seems to be the most natural.

2. Even if one does not regard loop quantum cosmology as a fundamental theory, one can still view its effective dynamics and choice of surface as in [36] as a procedure to *regulate* the classical calculation. The bounce provides then the preferred 'cut-off' surface envisioned by the authors of [47], but in an unambiguous fashion. From this perspective, what is amazing is that one can *remove the regulator* and obtain a finite answer. Furthermore, this 'canonical answer' indicates that inflation with enough e-foldings is generic even in this particular way of approaching the GR limit.

3. As we have seen from our analysis here, the reason for the LQC result stems from the choice of surface where to compute the probability and *not* directly from any effect from the quantum geometry underlying LQC. In fact, as we remove the parameter encoding the quantum geometric effects, the probability of inflation increases[10].

4. In our analysis we have used qualitative aspects of the global dynamics of the system. Therefore, our arguments and conclusions are insensitive to changes in the free parameters of the model. That is, our result are rather robust.

[10]This is consistent with early calculations on LQC where the integration was performed at low densities [53].

5. One should keep in mind that these results are purely classical. It is to be expected that quantum effects might provide a more realistic *distribution* on the space of classical trajectories. Some proposals have been put forward, but in the context of particular states and only for those trajectories satisfying WKB conditions [58, 59]. One could imagine that semiclassical states in LQC might provide an improved distribution from which one might get a 'quantum corrected' estimation of the probability for enough inflation. This matter should certainly be studied in detail.

Two things are infinite: the universe and human stupidity; and I'm not sure about the universe.

Albert Einstein

3
Closed FLRW Model

The spatially flat k=0 FRW cosmological model coupled to a mass-less scalar field that serves as an internal time parameter [14–19] was the first fully understood model in LQC. After that, the same quantization methods were applied to other isotropic models with and without a cosmological constant. Thus, a closed k=1 was extensively studied in [25] and [26], while the open k=-1 was considered in [27]. A detailed study of singularity resolution for these models was recently completed in [60], extending previous results for the flat case [61]. For the flat model, a cosmological constant was included in [62] and a massive scalar field in [57], where singularity resolution was also shown to emerge as a feature of the theory.

An extension of this consistent quantization method was successfully implemented for the simples anisotropic cosmology, namely a Bianchi I spacetime in [28]. It was soon realized that, for anisotropic models with a nontrivial spatial curvature, this quantization method based on considering holonomies along closed loops was no longer applicable. The operator associated to the field strength was no longer well defined on the kinematical Hilbert space of the theory used so far. The proposal put forward in [29] was to consider *open* holonomies to represent the connection, and then define the curvature out of the resulting operator. As it turns out, this quantization method has some resemblance to the quantization procedure known as 'polymerization' [51]. For the quantization of Bianchi IX cosmological models, it was also noted that this 'connection quantization' could be successfully implemented [30], and the singularity could also be resolved.

A natural issue that one would like to investigate are the physical consequences

of this 'new' loop quantization. Do we have the same qualitative behavior as in the holonomy based quantization? This question has been satisfactorily (but trivially) answered in some cases where both quantizations are available. When the spatial curvature vanishes, as is the case of the k=0 FRW and Bianchi I models, both quantization methods coincide [29, 63] (once one appropriately fixes a free parameter). It is then quite natural to ask whether the same feature is present in other models where the intrinsic spatial curvature in non-trivial. Is there an important effect that the spatial curvature carries? In this respect, the k=1 FRW model is unique to answer this question since, (to our knowledge) it is the only such model for which both loop quantizations exist.

In this chapter, the *connection based* quantum theory for a k=1 FRW model shall be developed and explored its more important features by using an effective description of the dynamics. We shall then compare this description with that from the standard –holonomy based– loop quantization explored in [25, 26], where the effective description has been shown to correctly capture the dynamics of semiclassical states [25]. Perhaps somewhat surprisingly, what we find is that in the new –connection based– quantum theory, the corresponding cyclic universe undergoes a series of bounces and recollapses, but now *there are two different kind of bounces*. In the cosmic evolution, the universe alternates between these two bounces where both the density and minimum volume differ. Interestingly, for universes that grow to become 'large' before the expansion stops, the two bounces become more similar to each other, so that for a large universe like ours, they become almost indistinguishable.

We shall also study the effective equations with more quantum corrections. Thought those effective equations might not capture the correct behavior of semi-classical states quantitatively, one can use them to describe the behavior of the system qualitatively. [1]

3.1 Preliminaries: The k=1 Cosmology

The spacetime under consideration are of the form $M = \Sigma \times \mathbb{R}$, where Σ is a topological three-sphere $\mathbb{S}^3$ which can be identified by symmetry group SU(2). It is standard to endow Σ with a fiducial basis of one-forms ${}^o\omega_a^i$ and vectors ${}^oe_i^a$. We

[1] There has been some controversy regarding the necessity or 'utility' of including such effects. We know, on the one hand, that such corrections are meaningless for the open flat FLRW model (see for instance [14, 18, 31] for discussions), since in that case the invariance of the classical theory under constant rescalings is incompatible with the appearance of a new length scale, as introduced by such correction terms. In the case of closed universes, on the other hand, one should expect that those terms not only are allowed, but might play an important role in the theory.

can naturally define co-frames on Σ via

$$g^{-1}\mathrm{d}g := {}^o\omega = {}^o\omega^i \tau_i \tag{3.1}$$

where g is an element of SU(2). We denote ${}^oe^a_i$ as dual frames such that ${}^oe^a_i {}^o\omega^j_a = \delta^j_i$ and ${}^oe^a_i {}^o\omega^i_b = \delta^a_b$. The above definition for natural left-invariant 1-form ${}^o\omega$ follows that the frames ${}^oe^a_i$ and the co-frames ${}^o\omega^i_a$ satisfy the Maurer-Cartan equations

$$\mathrm{d}{}^o\omega^i + \frac{1}{2}{}^o\epsilon^i{}_{jk}\, {}^o\omega^j \wedge {}^o\omega^k = 0 \quad \text{and} \quad [{}^oe_i, {}^oe_j] = {}^o\epsilon_{ij}{}^k {}^oe_k \tag{3.2}$$

Where ${}^o\epsilon_{ijk}$ is completely antisymmetric tensor and defined such that ${}^o\epsilon_{123} = 1$. We will use ${}^o\omega^i$ and ${}^oe_i$ as our fiducial frames and co-frames.

The fiducial metric on Σ is then ${}^oq_{ab} := {}^o\omega^i_a\, {}^o\omega^j_b\, k_{ij}$, with k_{ij} the Killing-Cartan metric on su(2). Here, the fiducial metric ${}^oq_{ab}$ is the metric of a three sphere of radius a_0. The volume of Σ with respect to ${}^oq_{ab}$ will be denoted by $V_0 = 2\pi^2\, a_0^3$. We also define the quantity $\ell_0 := V_0^{1/3}$. It can be written as $\ell_0 =: \vartheta\, a_0$, where the quantity $\vartheta := (2\pi^2)^{1/3}$ will appear in many expressions.[2] If we put ϑ equal to 0, the equations for k=1 model will reduce to those ones for k=0 model.

The isotropic and homogeneous connections and triads can be written in terms of the fiducial quantities as follows,

$$A^i_a = \frac{c}{\ell_0}\, {}^o\omega^i_a \qquad ; \qquad E^a_i = \frac{p}{\ell_0^2}\sqrt{{}^oq}\, {}^oe^a_i \,. \tag{3.3}$$

Here, c is dimension-less and p has dimensions of length-squared. The metric and extrinsic curvature can be recovered from the pair (c, p) as follows,

$$q_{ab} = \frac{|p|}{\ell_0^2}\, {}^oq_{ab} \qquad \text{and} \qquad \gamma K_{ab} = \left(c - \frac{\ell_0}{2}\right) \frac{|p|}{\ell_0^2}\, {}^oq_{ab} \tag{3.4}$$

Note that the total volume V of the hypersurface Σ is given by $V = |p|^{3/2}$. The Poisson bracket for the phase space variables (c, p) is given, as in the k=0 case by,

$$\{c, p\} = \frac{8\pi G\gamma}{3}\,, \tag{3.5}$$

with γ the Barbero-Immirzi parameter. From here, one can calculate the curvature F^k_{ab} of the connection A^i_a on Σ as,

$$F^k_{ab} = \frac{c^2 - 2\vartheta c}{\ell_0^2}\, \epsilon_{ij}{}^k\, {}^o\omega^i_a\, {}^o\omega^j_b \tag{3.6}$$

[2]Note that these conventions follow those of [25] (compare to [60]). In spite of this, several of our equations will be different.

Since the fiducial frames and co-frames are fixed and because of the way of parametrization of connections and triads, the only relevant constraint is the Hamiltonian constraint that has the form,

$$\mathcal{C}_H = N\Big(\mathcal{H}_{\rm grav} + \mathcal{H}_{\rm matter}\Big), \tag{3.7}$$

where N is lapse function (which in this chapter we assume that it is 1), $\mathcal{H}_{\rm matter}$ is ρV (ρ is matter density) and

$$\mathcal{H}_{\rm grav} = \int_\Sigma \frac{{\rm d}^3x}{8\pi G}\,\Big[\epsilon^{ij}{}_k\, e^{-1}\, E^a_i E^b_j\, F^k_{ab} - 2(1+\gamma^2) e^{-1}\, E^a_i E^b_j\, K^i_{[a} K^j_{b]}\Big] \tag{3.8}$$

where $e = \sqrt{|{\rm det}E|}$, and K^i_a is the extrinsic curvature. By means of the relation $A^i_a = \Gamma^i_a + \gamma K^i_a$, with Γ^i_a the spin-connection compatible with the triad, we can re-express the second term of the Hamiltonian constraint as,

$$E^a_i E^b_j\, K^i_{[a} K^j_{b]} = \frac{1}{2\gamma^2}\epsilon^{ij}{}_k\, E^a_i E^b_j (F^k_{ab} - \Omega^k_{ab})\,. \tag{3.9}$$

Here Ω^k_{ab} is the curvature of the spin-connection Γ^i_a. The advantage of this substitution is that for this model, this expression has a simple form,

$$\Omega^k_{ab} = -\frac{1}{a_0^2}\,\epsilon_{ij}{}^k\, {}^o\omega^i_a\, {}^o\omega^j_b \tag{3.10}$$

With this, the gravitational constraint can be reduced to,

$$\mathcal{H}_{\rm grav} = -\frac{3}{8\pi G\gamma^2}\,\sqrt{|p|}\,\left[(c-\vartheta)^2 + \gamma^2\vartheta^2\right] \tag{3.11}$$

It is convenient to introduce new variables [18]: $\beta := c/|p|^{1/2}$ and $V = p^{3/2}$. The quantity V is just the volume of Σ and β is its canonically conjugate,

$$\{\beta, V\} = 4\pi G\gamma \tag{3.12}$$

We can then compute the evolution equations of V and β in order to find interesting geometrical scalars. Then,

$$\dot{V} = \{V, \mathcal{H}_{\rm grav}\} = \frac{3}{\gamma}\left(\beta V - \vartheta V^{2/3}\right) \tag{3.13}$$

from which we can find the standard Friedman equation using the constraint equation $\mathcal{H} = \mathcal{H}_{\rm grav} + \mathcal{H}_{\rm matt} \approx 0$ and $\mathcal{H}_{\rm matt} = V\rho$,

$$H^2 := \left(\frac{\dot{V}}{3V}\right)^2 = \frac{8\pi G}{3}\,\rho - \frac{\vartheta^2}{V^{2/3}}\,. \tag{3.14}$$

We can now compute $\dot{\beta} = \{\beta, \mathcal{H}\}$,

$$\dot{\beta} := -\frac{3}{2\gamma}\left[\beta^2 - \frac{4}{3}\vartheta\beta V^{-1/3} + \frac{1}{3}(1+\gamma^2)\vartheta^2 V^{-2/3}\right] + 4\pi G\gamma P \tag{3.15}$$

where we have used the standard definition of pressure as $P := \frac{\partial \mathcal{H}_{\rm matt}}{\partial V}$. We can readily find the time evolution of the expansion parameter $\theta = 3H$ as,

$$\dot{\theta} = 4\pi G(\rho - 3P) - \frac{3\,\vartheta^2}{V^{2/3}} \tag{3.16}$$

From Eq. (3.14) we can see that the condition for a turnaround point, namely when $H = 0$ is that the density satisfies $\rho_{\rm turn} := \frac{3}{8\pi G}\,\frac{\vartheta^2}{V^{2/3}}$. This is the point where the Hubble parameter vanishes. From (3.15) we see that, if $P > -\rho/3$ then $\dot{\theta} < 0$ at the turnaround point, which means that there is a transition from an expanding phase (where $\theta > 0$) to a contracting phase (where $\theta < 0$), so it corresponds to a point of *re-collapse*.

3.2 Loop quantization I: The holonomy way

This section has two parts. In the first one, we recall the effective equations for the quantization of the k=1 model as developed in Ref.[25], and explore some of its consequences for arbitrary matter content. As an example, we restrict our attention to the case of a mass-less scalar field. In the second part we study the effective equations with more quantum corrections.

3.2.1 Effective equations for holonomy-based quantization

The basic strategy of loop quantization is that the effects of quantum geometry are manifested by means of holonomies around closed loops that carry the information about the field strength of the connection.

For a 3-sphere with radius equal to a_o, the line element can be written as

$$\mathrm{d}s^2 = a_o^2(\mathrm{d}\alpha'^2 + \mathrm{d}\beta'^2 + \mathrm{d}\gamma'^2 + 2\cos\beta\mathrm{d}\alpha'\mathrm{d}\gamma')$$

where $0 \leq \alpha' \leq \pi$, $0 \leq \beta' \leq \pi/2$ and $0 \leq \gamma' \leq 2\pi$. With a simple redefinition of coordinates, $\alpha = 2\alpha'$, $\beta = 2\beta'$ and $\gamma = 2\gamma'$, it can be written as

$$\mathrm{d}s^2 = \frac{a_o^2}{4}(\mathrm{d}\alpha^2 + \mathrm{d}\beta^2 + \mathrm{d}\gamma^2 + 2\cos\beta\mathrm{d}\alpha\mathrm{d}\gamma) \tag{3.17}$$

where $0 \leq \alpha \leq 2\pi$, $0 \leq \beta \leq \pi$ and $0 \leq \gamma \leq 4\pi$. For this metric, the volume of Σ is $V_0 = 2\phi^2\, a_0$. Recall that we have defined $\ell_o = V_o^{1/3}$, and $\vartheta = \ell_o/a_o = (2\pi^2)^{1/3}$.

Let us now compute the holonomy along the edge e with length ℓ', parameterized by ℓ, tangential to vector $t^a = (\partial/\partial\ell)^a$. It is given by

$$h^{(\mu)} = \exp(\int_e A \cdot \mathrm{d}e(\ell)) = \exp(\int_0^{\ell'} t^a A_a^j \tau_j \mathrm{d}\ell)\,. \tag{3.18}$$

If we want to use some angular parameters like θ instead of ℓ we will have, for a general integral,

$$\int_0^{\ell'} \mathrm{d}\ell\ t(F) = \int_0^{\ell'/a} \mathrm{d}\theta\ t'(F) \tag{3.19}$$

with $t' = \frac{\partial}{\partial\theta}$ and a playing the role of a 'radius', since $\ell = a\,\theta$. For our problem, we can define

$$t' = \pm\frac{a_o}{2}\,{}^o e_3 = \pm\frac{\ell_o}{2\vartheta}\,{}^o e_3 \quad \text{or} \quad \pm\frac{a_o}{2}\xi_3 = \pm\frac{\ell_o}{2\vartheta}\,\xi_3\,.$$

Therefore, to calculate a component of F_{ab}^k of the curvature, we can construct a closed loop as follows. In coordinates (α, β, γ)
i) Move from $(0, \pi/2, 0)$ to $(0, \pi/2, 2\vartheta\mu)$ following ${}^o e_3 = \partial/\partial\gamma$,
ii) Then move from $(0, \pi/2, 2\vartheta\mu)$ to $(2\vartheta\mu, \pi/2, 2\vartheta\mu)$ following $-\xi_3 = \partial/\partial\alpha$,
iii) Next, move from $(2\vartheta\mu, \pi/2, 2\vartheta\mu)$ to $(2\vartheta\mu, \pi/2, 0)$ following $-{}^o e_3$, and finally
iv) Move from $(2\vartheta\mu, \pi/2, 0)$ to $(0, \pi/2, 0)$ following ξ_3.

The open holonomy along one edge, with parameter μ is given by

$$h^{(\mu)} = \exp(\int_0^{2\mu\ell_o/a_o} t'^a A_a^j \tau_j \mathrm{d}\theta) \tag{3.20}$$

where $\theta = \alpha$ or γ depending on the edge, and the effective radius of the 3-sphere used to translate from lengths to angles is $a_0/2$ (compatible with the fiducial metric (3.17)). Thus, we will have for the closed loop defined above,

$$h_{\square_{31}} = h_4 h_3 h_2 h_1 = e^{\tau_1 \mu c} e^{-\tau_3 \mu c} e^{-(\sin(2\vartheta\mu)\tau_2 + \cos(2\vartheta\mu)\tau_1)\mu c} e^{\tau_3 \mu c} \tag{3.21}$$

then we have

$${}^o e_3^a {}^o e_1^b F_{ab}^k = \lim_{\mu\to 0} \frac{2}{\mu^2 \ell_o^2} \mathrm{Tr}(h_{\square_{31}} \tau^k) = -\frac{1}{\ell_o^2}(c^2 - 2\vartheta c) \tag{3.22}$$

recovering thus the classical expression for curvature. If we do not take the limit $\mu \to 0$ but instead take the area as the smallest eigenvalue of the area operator, or equivalently $\bar{\mu}^2|p| = \lambda^2$ then the curvature can be approximated, at scale λ, as

$${}^\lambda F_{ab}^k = \frac{\sin^2 \bar{\mu}(c - \vartheta) - \sin^2(\bar{\mu}\vartheta)}{\bar{\mu}^2 \ell_o^2}\ \epsilon_{ij}{}^k\, {}^o\omega_a^i\, {}^o\omega_b^j \tag{3.23}$$

where $\bar{\mu} = \sqrt{\lambda^2/|p|}$. In terms of the new variables $\beta = c|p|^{-1/2}$ and $V = |p|^{3/2}$, it can be written as,

$$ {}^{\lambda}F^k_{ab} = \frac{V^{2/3}}{\lambda^2 \ell_0^2} \left[\sin^2(\lambda\beta - D) - \sin^2 D\right] \; \epsilon_{ij}{}^k \, {}^{o}\omega^i_a \, {}^{o}\omega^j_b \tag{3.24} $$

where we have defined $D := \lambda\vartheta/V^{1/3}$. With this form of the curvature as defined by closed holonomies, and neglecting the so called inverse triad corrections, one can arrive at the form of the effective Hamiltonian,

$$ \mathcal{H}_{\text{eff}} = -\frac{3}{8\pi G\gamma^2\lambda^2} V \left[\sin^2(\lambda\beta - D) - \sin^2 D + (1+\gamma^2)D^2\right] + \rho V \tag{3.25} $$

We can now compute the equations of motion from the effective Hamiltonian as,

$$ \dot{V} = \{V, \mathcal{H}_{\text{eff}}\} = \{V, \beta\} \frac{\partial \mathcal{H}_{\text{eff}}}{\partial \beta} = \frac{3}{\lambda\gamma} V \sin(\lambda\beta - D)\cos(\lambda\beta - D)\,. $$

From here, we can find the expansion as,

$$ \theta = \frac{\dot{V}}{V} = \frac{3}{\lambda\gamma}\sin(\lambda\beta - D)\cos(\lambda\beta - D) = \frac{3}{2\lambda\gamma}\sin 2(\lambda\beta - D)\,. \tag{3.26} $$

From the above equation we can see that the absolute value of expansion has an absolute upper limit equal to $|\theta| \leq 3/2\lambda\gamma$. We can now compute the modified, *effective Friedman equation*, by computing $H^2 = \frac{\theta^2}{9}$,

$$ \begin{aligned} H^2 &= \frac{1}{\lambda^2\gamma^2}\left(\frac{8\pi G\gamma^2\lambda^2}{3}\rho + \sin^2 D - (1+\gamma^2)D^2\right)\left(1 - \frac{8\pi G\gamma^2\lambda^2}{3}\rho - \sin^2 D + (1+\gamma^2)D^2\right) \\ &= \frac{8\pi G}{3}(\rho - \rho_1)\left(1 - \frac{\rho - \rho_1}{\rho_{crit}}\right) \end{aligned} \tag{3.27} $$

where $\rho_1 = \rho_{\text{crit}}[(1+\gamma^2)D^2 - \sin^2 D]$ and $\rho_{\text{crit}} = 3/(8\pi G\gamma^2\lambda^2)$ is the *critical density* of the $k = 0$ FRW model. We can immediately note from Eq. (3.27) that there are two points where the Hubble parameter H vanishes and the Universe has a turnaround. The first one corresponds to the point $\rho = \rho_1$. Note that ρ_1, in the limit $\lambda \to 0$, tends to $\rho_1 \mapsto \frac{3}{8\pi G}\frac{\vartheta^2}{V^{2/3}}$, which is the classical value for re-collapse as given by Eq. (3.14). Thus, in the limit of large volumes one expects ρ_1 to represent the density at re-collapse. The second value for density where the Hubble parameter vanishes is given by $\rho = \rho_{\text{crit}} + \rho_1$. Note that these densities, where there is a turnaround, is not an universal constant for all trajectories as was

the case for the k=0 model (for the bounce at $\rho = \rho_{\rm crit}$). Instead, the quantity ρ_1 is a function of volume and depends on each individual trajectory. The second density for turnaround is bounded below by $\rho_{\rm crit}$.[3] There is an alternate way of analyzing the two turnaround points. From the expression of the expansion (3.26) we can see that the Hubble parameter vanishes when

$$\sin 2(\lambda\beta - D) = \sin(\lambda\beta - D)\cos(\lambda\beta - D) = 0 \tag{3.28}$$

There are two possibilities for this.

i) When $\lambda\beta - D = \frac{(2n+1)}{2}\,\pi\,,$

for n integer, which corresponds to $\rho = \rho_{\rm crit} + \rho_1$. The other possibility is,

ii) $\lambda\beta - D = m\,\pi$

where m is an integer number. This corresponds to $\rho = \rho_1$.

In fact, these considerations suggest that we could define a new variable $\tilde{\beta} := \beta - D/\lambda = (c - \vartheta)/\sqrt{p}$, that would also be 'conjugate' to V ($\{\tilde{\beta}, V\} = 4\pi G\gamma$). In terms of $\tilde{\beta}$ many expressions would simplify, and it would reduce to β in the k=0 case.

In order to determine which of the turnaround points corresponds to a bounce and which one to a re-collapse, we need to consider the rest of the effective equations of motion,

$$\begin{aligned}\dot{\beta} &= 4\pi G\gamma P \\ &- \frac{1}{2\gamma\lambda^2}\left[3\sin^2(\lambda\beta - D) - 3\sin^2 D + D\sin 2(\lambda\beta - D) + D\sin 2D + (1+\gamma^2)D^2\right] \\ &= -4\pi G\gamma\left[\rho - \rho_2 + P\right]\end{aligned} \tag{3.29}$$

where

$$\rho_2 = \frac{\rho_{crit} D}{3}\left[2(1+\gamma^2)D - \sin 2(\lambda\beta - D) - \sin 2D\right] \tag{3.30}$$

The Ricci scalar is given by,

$$\begin{aligned} R &= 2\dot{\theta} + \frac{4\theta^2}{3} + \frac{6\vartheta^2}{V^{2/3}} \\ &= 8\pi G\rho\left(1 + 2\frac{\rho - \rho_1}{\rho_{\rm crit}}\right) + 32\pi G\rho_1\left(1 - \frac{\rho - \rho_1}{\rho_{\rm crit}}\right) \\ &\quad -24\pi G(P - \rho_3)\left(1 - 2\frac{\rho - \rho_1}{\rho_{\rm crit}}\right) + \frac{6\vartheta^2}{V^{2/3}} \end{aligned} \tag{3.31}$$

[3]Also note that since ρ_1 depends explicitly on the volume, the values it takes at the bounce and classical turnaround point are different, so it could happen that $\rho = \rho_1$ is actually larger than in the other root, and it corresponds to the bounce while $\rho = \rho_{\rm crit} + \rho_1$ corresponds to a re-collapse [44].

The time derivative of the expansion is given by,

$$\begin{aligned}\dot{\theta} &= \cos 2(\lambda\beta - D)\left(\frac{3}{\gamma}\dot{\beta} + \frac{\theta D}{\gamma\lambda}\right) = \left(\frac{3}{\gamma}\dot{\beta} + \frac{\theta D}{\gamma\lambda}\right)\left[1 - 2\frac{\rho - \rho_1}{\rho_{\rm crit}}\right] \\ &= -12\pi G\left(\rho - \rho_3 + P\right)\left[1 - 2\frac{\rho - \rho_1}{\rho_{\rm crit}}\right] \end{aligned} \tag{3.32}$$

with

$$\rho_3 = \rho_2 + \frac{\rho_{crit} D}{3}\sin 2(\lambda\beta - D) = \frac{\rho_{crit} D}{3}\left[2(1+\gamma^2)D - \sin 2D\right]$$

Finally, the contracted Ricci curvature appearing in Raychaudhuri equation is given by,

$$\begin{aligned} R_{ab}\xi^a\xi^b &= -\dot{\theta} - \frac{1}{3}\theta^2 \\ &= 4\pi G\rho\left(1 - 4\frac{\rho - \rho_1}{\rho_{crit}}\right) + 8\pi G\rho_1\left(1 - \frac{\rho - \rho_1}{\rho_{crit}}\right) \\ &\quad +12\pi G(P - \rho_3)\left(1 - 2\frac{\rho - \rho_1}{\rho_{crit}}\right) \end{aligned} \tag{3.33}$$

It is straightforward to show that the continuity equation $\dot{\rho} + 3H(\rho + P) = 0$ is also satisfied in this case [60].

Let us now determine the nature of the turnaround points. From Eq. (3.32) we can see that in case i) above, where $\theta = 0$ and $\rho = \rho_{\rm crit} + \rho_1$, we have then,

$$\dot{\theta} = -\frac{1}{\gamma}\dot{\beta} \tag{3.34}$$

Therefore, the nature of the turnaround is determined by the sign of $\dot{\beta}$. If $\dot{\beta} < 0$ then $\dot{\theta} > 0$ and the point corresponds to a *bounce*. However, if $\dot{\beta} > 0$ then $\dot{\theta} < 0$ and the point corresponds to a *re-collapse*.

For case ii), again from Eq. (3.32), and using $\theta = 0$ and $\rho = \rho_1$ we can see that,

$$\dot{\theta} = \frac{1}{\gamma}\dot{\beta} \tag{3.35}$$

Therefore, if $\dot{\beta} < 0$ then $\dot{\theta} < 0$ and the point corresponds to a *re-collapse*. In the other case, when $\dot{\beta} > 0$ then $\dot{\theta} < 0$ and the point corresponds to a *bounce*. From this discussion, we can see that the nature of the turnaround points can change if, during the dynamical evolution, $\dot{\beta}$ changes sign. This phenomena has indeed been observed in certain cases [44].

3.2.1.1 Concrete example: A massless scalar

Up until now, we have considered arbitrary matter sources. Let us now restrict our attention to the simplest case of a massless scalar field ϕ, where the density is given by $\rho = \dot{\phi}^2/2$ [25]. In this case, $\dot{\beta} < 0$ and does not change during the dynamical evolution. This means that the case i) above corresponds to the bounce and case ii) to the re-collapse. In order to find the minimum and maximum volume we can put the maximum or minimum density in one side of the expression of density to have,

$$\frac{p_\phi^2}{2V_{\mathrm{max}^2}} = \rho_{\mathrm{crit}} \left[(1+\gamma^2) \frac{\lambda^2 \vartheta^2}{V_{\mathrm{max}}^{2/3}} - \sin^2 \frac{\lambda\vartheta}{V_{\mathrm{max}}^{1/3}} \right] \tag{3.36}$$

and

$$\frac{p_\phi^2}{2V_{\mathrm{min}}^2} = \rho_{\mathrm{crit}} \left[1 + (1+\gamma^2) \frac{\lambda^2 \vartheta^2}{V_{\mathrm{min}}^{2/3}} - \sin^2 \frac{\lambda\vartheta}{V_{\mathrm{min}}^{1/3}} \right] \tag{3.37}$$

From numerical simulations performed in Ref. [25] and analytical considerations for the k=0 model [21,22], we know that the constant of the motion p_ϕ determines how *semiclassical* the state is. To be precise, as one increases the value of p_ϕ, in natural Planck units, it becomes easier to construct semiclassical states peaked on that value of the field momenta. It is then natural to expect that p_ϕ measures in a way, how *large* the Universe can grow before the re-collapse phase starts. That is certainly true for the classical equations of motion. Since we expect that the classical equations are a good approximation to the effective equations of motion in the low density regime, the volume at with the expansion stops should coincide when this transition happens at low densities in Planck units. Therefore, let us assume that $V_{\mathrm{max}}^{1/3} \gg \vartheta\lambda$, which means,

$$p_\phi^2 = 2V_{\mathrm{max}}^2 \rho_{\mathrm{crit}} \left[(1+\gamma^2) \frac{\lambda^2\vartheta^2}{V_{\mathrm{max}}^{2/3}} - \sin^2 \left(\frac{\lambda\vartheta}{V_{\mathrm{max}}^{1/3}} \right) \right] \approx 2V_{\mathrm{max}}^2 \rho_{\mathrm{crit}} \frac{\gamma^2\lambda^2\vartheta^2}{V_{\mathrm{max}}^{2/3}} \tag{3.38}$$

from which we can see that the maximum value of volume approaches the classical value

$$V_{\mathrm{max}} = \left(\frac{64\pi G}{3\vartheta^2} \right)^{3/4} p_\phi^{3/2} \tag{3.39}$$

from above. Let us now estimate the value of the bounce in the same regime, where the value of p_ϕ is large.

$$p_\phi^2 = 2V_{\mathrm{min}}^2 \rho_{\mathrm{crit}} \left[1 + (1+\gamma^2) \frac{\lambda^2\vartheta^2}{V_{\mathrm{min}}^{2/3}} - \sin^2 \left(\frac{\lambda\vartheta}{V_{\mathrm{min}}^{1/3}} \right) \right] \approx 2V_{\mathrm{min}}^2 \rho_{\mathrm{crit}} \tag{3.40}$$

Therefore, the volume at the bounce also approaches the k=0 value

$$V_{\rm min} = \frac{1}{\sqrt{2\rho_{\rm crit}}}\, p_\phi \tag{3.41}$$

from above.

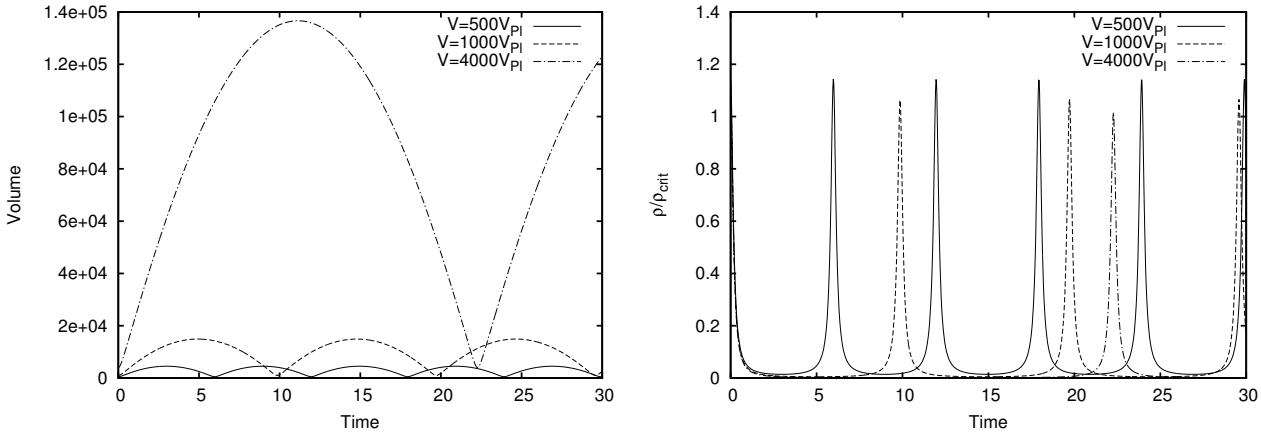

Figure 3.1: Time evolution of the volume V (left) and the density ρ (right) for three values of the volume at the bounce $V_{\rm b}$. $V_{\rm b} = 500\ell_{\rm Pl}$ (—- line), $V_{\rm b} = 1000\ell_{\rm Pl}$ ($-\,-\,-\,-\,-$ line), and $V_{\rm b} = 4000\ell_{\rm Pl}$ ($-\cdot-\cdot-\cdot-$ line).

In Fig. 3.1 we have plotted the time evolution of three universes for three different values of volume $V_{\rm b}$ at the bounce. From our previous expressions we see that the higher the value of the volume at the bounce, the higher the field momentum p_ϕ and the more semiclassical the trajectory. Note that this can be seen from the fact that the universe grows to larger values as one increases p_ϕ, and the density at the bounce *decreases* and tends to the value $\rho_{\rm crit}$.

3.2.2 Effective Equations with Inverse Triad Corrections

If we want to find some effective equations which give us a possibility to study about small volumes, we have to add the effects of those operators which come from the inverse power of triads because their eigenvalues in small volumes have different behavior than their classical quantities. The constraint operator without operator ordering is [25]

$$\hat{\mathcal{C}_H} = -\frac{3}{8\pi G\gamma^2\lambda^2}\hat{A}(\hat{|p|^{3/2}}\sin^2\bar{\mu}(c-\vartheta) - \hat{|p|^{3/2}}\sin^2\bar{\mu}\vartheta + (1+\gamma^2)\lambda^2\vartheta^2\hat{|p|^{1/2}}) + \hat{\rho}\hat{|p|}^{3/2} \tag{3.42}$$

where the operator $\hat{A}$ has eigenvalues

$$A(V) = \frac{1}{2V_c}(V + V_c - |V - V_c|) = \begin{cases} V/V_c & V < V_c \\ 1 & V \geq V_c \end{cases} \tag{3.43}$$

and $V_c = 2\pi\gamma\lambda\ell_{\rm Pl}^2$. This operator is part of $\epsilon_k^{ij} E_i^q E_j^b/\sqrt{|q|}$. We will talk about it in more details in the next section.

Therefore the modified effective equation can be written as

$$\begin{aligned}\mathcal{H}_{eff} = &-\frac{3}{8\pi G\gamma^2\lambda^5} A(V)\left[|p|^{3/2}\sin^2\bar{\mu}(c-\vartheta) - |p|^{3/2}\sin^2\bar{\mu}\vartheta + (1+\gamma^2)\lambda^2\vartheta^2\sqrt{|p|}\right] \\ &+ \rho|p|^{3/2}\end{aligned} \tag{3.44}$$

We can rewrite the above equation with variables β and V

$$\begin{aligned}\mathcal{H}_{eff} = &-\frac{3}{8\pi G\gamma^2\lambda^5} A(V)\left[V\sin^2(\lambda\beta - D) - V\sin^2 D + (1+\gamma^2)\lambda^2\vartheta^2 V^{1/3}\right] \\ &+ \rho V\end{aligned} \tag{3.45}$$

Therefore, the equation of motions are

$$\dot{V} = -\{\beta, V\}\frac{\partial\mathcal{H}_{eff}}{\partial\beta} = \frac{3}{\gamma\lambda}A(V)V\sin(\lambda\beta - D)\cos(\lambda\beta - D) \tag{3.46}$$

$$\begin{aligned}\dot{\beta} = \{\beta, V\}\frac{\partial\mathcal{H}_{eff}}{\partial V} = &-\frac{3}{2\gamma\lambda^2}\Bigg[\Big(VA_{,V} + A(V)\Big)\Big(\sin^2(\lambda\beta - D) - \sin^2 D\Big) \\ &+(1+\gamma^2)\lambda^2\vartheta^2 A_{,V}V^{1/3} + \frac{\lambda\vartheta}{3}A(V)V^{-1/3}\Big(\sin 2(\lambda\beta - D) + \sin 2D\Big) \\ &+\frac{1+\gamma^2}{3}\lambda^2\vartheta^2 A(V)V^{-2/3}\Bigg] + 4\pi G\gamma\Big(V\frac{\partial\rho}{\partial V} + \rho\Big)\end{aligned} \tag{3.47}$$

where the derivative of $A(V)$ is

$$A_{,V} = \frac{1}{2V_c}\left(1 - \frac{|V - V_c|}{V - V_c}\right) = \begin{cases} 1/V_c & V < V_c \\ 0 & V > V_c \end{cases} \tag{3.48}$$

The expansion is

$$\theta = \frac{\dot{V}}{V} = \frac{3}{\gamma\lambda}A(V)\sin(\lambda\beta - D)\cos(\lambda\beta - D) \tag{3.49}$$

and since $|\sin 2(\lambda\beta - D)| \leq 1$ the expansion is bounded. Expansion has some zeros which are referred to turnaround points and can be bounces or recollapses. With using the time derivative of expansion we can identify the nature of turnaround points. The expression for $\dot{\theta}$ is

$$\dot{\theta} = A(V)\cos 2(\lambda\beta - D)\left(\frac{3}{\gamma}\dot{\beta} + \frac{\theta D}{\gamma\lambda}\right) + \frac{3}{2\lambda\gamma}\dot{V}A_{,V}\sin 2(\lambda\beta - D) \tag{3.50}$$

which has the same relation with $\dot{\beta}$ in turnaround points as the previous section.

It is also useful to study about matter density. The density is

$$\rho = \frac{3}{8\pi G\gamma^2\lambda^5}A(V)\left[\sin^2(\lambda\beta - D) - \sin^2 D + (1+\gamma^2)\lambda^2\vartheta^2 V^{-2/3}\right] \tag{3.51}$$

From the Eqs.(3.43),(3.51), it is easy to show that

$$\rho \leq \frac{3}{8\pi G\gamma^2\lambda^5}\left[1 + (1+\gamma^2)\lambda^2\vartheta^2 V_c^{-2/3}\right] \tag{3.52}$$

which means that density has a global upper limit. In previous section without inverse triad correction, every trajectory had its own maximum density but there was no global maximum density for all trajectories.

To summarize this section, we have seen that the effective dynamics of the holonomy based quantization, as defined in [25], yields a cyclic universe with a bounce at a matter densities that are larger than in the flat k=0 case. In the 'large volume regime', the volume at which the expansion of the universe stops approaches the value given by general relativity. Through-out the evolution, a key geometrical scalar such as the expansion of cosmological observers remains absolutely bounded, and is saturated by all trajectories at the end of the superinflation regime that follows the bounce. These results complement those of [60] where it was shown that, within this quantization, singularity resolution in generic for a large class of matter. Also, we have shown that by adding inverse triad corrections, density has a global upper bound.

3.3 Loop quantization II: The connection way

For Bianchi II and IX cosmological models, where the spatial geometry has non trivial curvature, it was realized that the standard method of loop quantization based on holonomies for closed loops, was not implementable in the Hilbert space of loop quantum cosmology. A new quantization prescription was put forward in [29] and also employed in [30]. The basic idea is to define an operator for the

connection, by means of open holonomies, from which one can define the curvature. In this section we shall employ this quantization procedure to the closed k=1 FRW model.

To be precise, we define the connection by an open holonomy, from which we arrive at the expression for the connection

$$A_a^i = \frac{\sin \bar{\mu} c}{\bar{\mu}} \, {}^o\omega_a^i \tag{3.53}$$

where $\bar{\mu}$ is the length of the curve which we use to calculate the holonomy along it and here we take $\bar{\mu} = \sqrt{\lambda^2/|p|}$. Just as the previous section, we shall use the variables β and V instead of c and p.

This section has four parts. In the first one we derive the loop quantization for this prescription, writing in detail the quantum equations that define the theory when the matter is given by a massless scalar field. This resulting formalism can then be directly compared to that of [25]. In the second part, We prove that the gravitational part of the Hamiltonian operator is essentially self adjoint. We also prove some other properties for that operator which is similar to the results of [26]. In the third part, we consider the effective Hamiltonian and equations of motion derived from the quantum theory and analyze some of their general properties. At the end of this part, we specialize in the massless scalar case where we can find explicit formulae for some of the relevant parameters of the solutions. In the last part we study the effective Hamiltonian and equations of motion with inverse triad corrections.

3.3.1 Quantum Kinematics

Let us start by recalling the classical Hamiltonian constraint,

$$\mathcal{C}_H = \int_{\mathcal{V}} N \left[-\frac{E_i^a E_j^b}{16\pi G\gamma^2 \sqrt{|q|}} \epsilon^{ij}{}_k \left(F_{ab}^k - (1+\gamma^2)\Omega_{ab}^k \right) + \mathcal{H}_{matter} \right] \mathrm{d}^3x \tag{3.54}$$

where N is lapse function which we take it 1[4], $\mathcal{H}_{matter} = \rho V$ (here we take $\rho = p_\phi^2/2V^2$) and Ω_{ab} is the curvature of spin connection Γ_a^i which is compatible with the triads (Eq.(3.10)).

As is standard in loop quantum cosmology, the gravitational part of the kinematical Hilbert space where the constraints are to be implemented, is given by the

[4]To quantize the constraint with lapse function which differs from 1, we can quantize the constraint with lapse equals to one and find a well defined operator for lapse function and order them.

so called *polymer Hilbert space* [51]. It is equal to the square integrable functions on Bohr compactification on real line, $L^2(\mathbb{R}_{Bohr}, d\mu_{Bohr})$.

To quantize the constraint, we should introduce well defined operators related to each term of it. Since in loop quantum gravity they are the holonomies h_e defined by the connection A_a^i along edges e and the fluxes of the densitized triad E_i^a across surfaces, for this model we choose holonomies $h_i^{(\mu)}$ along edge $\mu\ell_o{}^o e_i$ defined by connection A^i and p_i. Therefore, we need to express the constraint in terms of these functions and their Poisson brackets and after that replace them by the operator $\hat{h_i^{(\mu)}}$ and $\hat{p}$ and their commutators divided by $i\hbar$. The holonomy $h_i^{(\mu)}$ is given by

$$\begin{aligned} h_i^{(\mu)} &= \cos(\frac{\mu c}{2})\mathbb{I} + 2\sin(\frac{\mu c}{2})\tau_i \\ &= \frac{1}{2}(e^{i\mu c/2} + e^{-i\mu c/2})\mathbb{I} - i(e^{i\mu c/2} - e^{-i\mu c/2})\tau_i \end{aligned} \tag{3.55}$$

Therefore, it is more convenient to take $\widehat{e^{i\alpha c}}$ as an elementary operator instead of its related holonomy.

To find a well defined operator related to the term $\epsilon^{ij}{}_k E_i^a E_j^b/\sqrt{|q|}$ we can use Thiemann strategy[3] as previous chapter. Recall that there is the following classical identity from the full theory

$$\epsilon^{ij}{}_k \frac{E_i^a E_j^b}{\sqrt{|q|}} = \frac{\varepsilon}{2\pi G\gamma\mu}\ {}^o\epsilon^{abc}\ {}^o\omega_c^i \mathrm{Tr}\left(h_i^{(\mu)}\{h_i^{(\mu)-1}, V\}\tau_k\right) \tag{3.56}$$

where ε is 1 if the fiducial frames and physical ones have the same orientation otherwise is -1. Note that here, μ is arbitrary. Therefore the related operator of this term is

$$\widehat{\epsilon^{ij}{}_k \frac{E_i^a E_j^b}{\sqrt{|q|}}} = \frac{\varepsilon}{2i\hbar\pi G\gamma\mu}\ {}^o\epsilon^{abc}\ {}^o\omega_c^i \mathrm{Tr}\left(\hat{h}_i^{(\mu)}[\hat{h}_i^{(\mu)-1}, \hat{V}]\tau_k\right) \tag{3.57}$$

where $\hat{V} = |\hat{p}|^{3/2}$ is volume operator. One should note that for different choices of μ we will have different operators which are *not* equivalent.

By choosing the matter field as a massless scalar field, we have V^{-2} in the density operator and to introduce a well defined operator for it, we use the same strategy as above. Classically there is following identity [10]

$$V^{-1} = \left(\frac{3}{8\pi G\gamma\mu\ell j(j+1)(2j+1)}\mathrm{Tr}(h_i^{(\mu)}\{h_i^{(\mu)-1}, V^{2\ell/3}\}\tau_i)\right)^{3/(2-2\ell)} \tag{3.58}$$

where ℓ is a number between 0 and 1 and $j \in \frac{1}{2}\mathbb{N}$ is for representation. Therefore the related operator will be

$$\widehat{V^{-1}} = \left(\frac{3}{8i\hbar\pi G\gamma\mu\ell j(j+1)(2j+1)}\mathrm{Tr}(\hat{h}_i^{(\mu)}[\hat{h}_i^{(\mu)-1}, \hat{V}^{2\ell/3}]\tau_i)\right)^{3/(2-2\ell)} \tag{3.59}$$

We should note that with different ℓ, j and μ we will have different inequivalent operators but they approach to each other when V goes to infinity. For simplicity we will take $j = 1/2$, $\ell = 1/2$ or $1/4$.

To define related operator to the curvature F_{ab} we use Eq.(3.53).

$$\hat{F}^k_{ab} = \frac{1}{\ell_o^2}(\frac{\varepsilon}{\bar{\mu}^2}\sin^2\bar{\mu}c - \frac{2\vartheta}{\bar{\mu}}\sin\bar{\mu}c)\ {}^o\epsilon^k{}_{ij}\ {}^o\omega^i_a\ {}^o\omega^j_b \tag{3.60}$$

We recall that $\bar{\mu} = \lambda/\sqrt{|p|}$ where λ^2 is equal to smallest non-zero eigenvalue of area operator.

Since the length of each path for calculating holonomies to find the curvature F_{ab} in fiducial cell is $\bar{\mu}\ell_o$, we will use this length to compute operators in Eqs.(3.57) and (3.59). Also in the rest we work in the natural unit that $\hbar$ is equal to 1. With these choices, the operator in Eq.(3.57) gets the form

$$\widehat{\epsilon^{ij}{}_k\frac{E^a_iE^b_j}{\sqrt{|q|}}} = \frac{\hat{\epsilon}\widehat{\sqrt{|p|}}}{4\pi G\gamma\lambda}(\widehat{e^{i\bar{\mu}c/2}}\hat{V}\widehat{e^{-i\bar{\mu}c/2}} - \widehat{e^{-i\bar{\mu}c/2}}\hat{V}\widehat{e^{i\bar{\mu}c/2}})\ {}^o\epsilon^{abc}\ {}^o\omega^k_c \tag{3.61}$$

where $\hat{\epsilon}$ is the operator related to ε. Same as the previous chapter, for simplicity we define operator $\hat{A}$ as follows

$$\hat{A} = \frac{\hat{\epsilon}}{4\pi G\gamma\lambda}(\widehat{e^{i\bar{\mu}c/2}}\hat{V}\widehat{e^{-i\bar{\mu}c/2}} - \widehat{e^{-i\bar{\mu}c/2}}\hat{V}\widehat{e^{i\bar{\mu}c/2}}) \tag{3.62}$$

Hence the Eq.(3.61) can be written as

$$\widehat{\epsilon^{ij}{}_k\frac{E^a_iE^b_j}{\sqrt{|q|}}} = \widehat{\sqrt{|p|}}\hat{A}\ {}^o\epsilon^{abc}\ {}^o\omega^k_c \tag{3.63}$$

To find $\widehat{V^{-1}}$, if we choose $\ell = 1/2$ then we can write $\widehat{V^{-1}} = \hat{f}^3$ where $\hat{f}$ is

$$\hat{f} = \frac{3}{4\pi G\gamma\lambda}\hat{V}^{1/3}(\widehat{e^{i\bar{\mu}c/2}}\hat{V}^{1/3}\widehat{e^{-i\bar{\mu}c/2}} - \widehat{e^{-i\bar{\mu}c/2}}\hat{V}^{1/3}\widehat{e^{i\bar{\mu}c/2}}) \tag{3.64}$$

But if we choose $\ell = 1/4$ then $\widehat{V^{-1}} = \hat{g}^6$ where $\hat{g}$ is

$$\hat{g} = \frac{1}{2\pi G\gamma\lambda}\hat{V}^{1/3}(\widehat{e^{i\bar{\mu}c/2}}\hat{V}^{1/2}\widehat{e^{-i\bar{\mu}c/2}} - \widehat{e^{-i\bar{\mu}c/2}}\hat{V}^{1/2}\widehat{e^{i\bar{\mu}c/2}}) \tag{3.65}$$

We will use this choice in the rest. Because as we will shown in next chapter, it is compatible with the definition of inverse triads operators in Bianchi IX.

Because of the form of the operators contained in the constraint operator, it is simpler to work with variables β and V and take $\hat{V}$ and $\widehat{e^{i\lambda\beta/2}}$ as elementary operators.

In the Hilbert space, we can choose a basis of eigenstates,

$$\hat{v}|v\rangle = v|v\rangle \tag{3.66}$$

which is related to the volume $\hat{V}$ as follows: $\hat{V}|v\rangle = \left(\frac{8\pi\gamma}{6}\right)^{3/2}\frac{|v|}{K}|v\rangle = V_c|v||v\rangle$ with $K = 2\sqrt{2}/(3\sqrt{3\sqrt{3}})$ and $V_c = 2\pi\gamma\lambda\ell_{\rm Pl}^2$. This space is endowed with the hermitian scalar product defined by

$$\langle v_i|v_j\rangle = \delta_{v_i,v_j}. \tag{3.67}$$

In this basis, $\widehat{\exp i\alpha\lambda}\beta$ ($\alpha \in \mathbb{R}$) becomes a translation operator.

$$\widehat{e^{i\alpha\lambda\beta/2}}|v\rangle = |v-\alpha\rangle \tag{3.68}$$

then

$$\widehat{\sin\lambda\beta}|v\rangle = \frac{1}{2i}(|v-2\rangle - |v+2\rangle) \tag{3.69}$$

Also, it is easy to show that the eigenvalues of $\hat{f}$ and $\hat{g}$ are

$$f(v) = \frac{3}{2}V_c^{1/3}|v|^{1/3}\left[|v+1|^{1/3} - |v-1|^{1/3}\right], \tag{3.70}$$

$$g(v) = V_c^{1/6}|v|^{1/3}\left[\sqrt{|v+1|} - \sqrt{|v-1|}\right], \tag{3.71}$$

The eigenvalues for operator $\hat{A}$ are the same as Eq.(2.21) in previous chapter.

Finally after defining well behaved operators, the Hamiltonian constraint operator before factor ordering is

$$\hat{\mathcal{C}}_H = -\frac{3}{8\pi G\gamma^2\lambda^2}\left[\hat{V}\hat{A}\sin^2\lambda\beta - 2\lambda\vartheta\hat{V}^{2/3}\hat{A}\sin\lambda\beta\hat{+}\lambda^2\vartheta^2(1+\gamma^2)\hat{V}^{1/3}\hat{A}\right] + \frac{\hat{p}_\phi^2}{2}\widehat{V^{-2}}\hat{V} \tag{3.72}$$

Several operator orderings can be chosen, however each one will leads to a different constraint operator and thus different quantum theory. To show this difference we will work with two constraint operators which have different orderings.[5]

[5]However, one might expect that their qualitative behavior be similar.

The first one is

$$\begin{aligned}\hat{\mathcal{C}}_H^{(1)} &= \hat{\mathcal{C}}_{\rm grav}^{(1)} + \hat{\mathcal{C}}_{\rm matt}^{(1)} \\ &\quad -\frac{3}{8\pi G\gamma^2\lambda^2}\Big[\sin\lambda\beta\hat{V}\hat{A}\sin\lambda\beta - \lambda\vartheta\hat{\epsilon}\hat{V}^{2/3}\hat{A}\sin\lambda\beta - \lambda\vartheta\sin\lambda\beta\hat{\epsilon}\hat{V}^{2/3}\hat{A} \\ &\quad +\lambda^2\vartheta^2(1+\gamma^2)\hat{V}^{1/3}\hat{A}\Big] + \frac{\hat{p}_\phi^2}{2}\widehat{V^{-2}}\hat{V} \end{aligned} \tag{3.73}$$

For this one, we order operators same as in previous works on k=1 model with curvature based quantization in $\bar{\mu}$ scheme [25, 26]. The action of this Hamiltonian constraint operator on a state is given by

$$-g(v)^{12}V(v)\partial_\phi^2\Psi(v;\phi) = \hat{\mathcal{C}}_{\rm grav}^{(1)}\Psi(v;\phi) \tag{3.74}$$

where

$$\begin{aligned}\hat{\mathcal{C}}_{\rm grav}^{(1)}\Psi(v;\phi) &= \frac{3}{4\pi G\gamma^2\lambda^2}\Bigg[\Bigg(V(v+2)A(v+2) + V(v-2)A(v-2) \\ &\quad +\lambda^2\vartheta^2(1+\gamma^2)V^{1/3}(v)\Bigg)\Psi(v;\phi) \\ &\quad +\frac{\lambda\vartheta}{2i}\Bigg(V^{2/3}(v)A(v) + V^{2/3}(v-2)A(v-2)\Bigg)\Psi(v-2;\phi) \\ &\quad -\frac{\lambda\vartheta}{2i}\Bigg(V^{2/3}(v)A(v) + V^{2/3}(v+2)A(v+2)\Bigg)\Psi(v+2;\phi) \\ &\quad -V(v-2)A(v-2)\Psi(v-4;\phi) - V(v+2)A(v+2)\Psi(v+4;\phi)\Bigg] \end{aligned} \tag{3.75}$$

The final quantum theory has a structure very similar to that of [25]. An interesting state for consideration is the one which has support on zero volume namely $\Psi(0;\phi)$. Left side of Eq.(3.74) annihilates this state but the right side has a non trivial action on this state.

The second constrain operator is

$$\begin{aligned}\hat{\mathcal{C}}_H^{(2)} &= \hat{\mathcal{C}}_{\rm grav}^{(2)} + \hat{\mathcal{C}}_{\rm matt}^{(2)} \\ &\quad -\frac{3}{8\pi G\gamma^2\lambda^2}\Big[\hat{V}^{1/3}\sin\lambda\beta\hat{V}^{1/3}\hat{A}\sin\lambda\beta\hat{V}^{1/3} - \lambda\vartheta\hat{V}^{1/3}(\hat{\epsilon}\hat{A}\sin\lambda\beta \\ &\quad +\sin\lambda\beta\hat{\epsilon}\hat{A})V^{1/3} + \lambda^2\vartheta^2(1+\gamma^2)\hat{V}^{1/3}\hat{A}\Big] + \frac{\hat{p}_\phi^2}{2}\widehat{V^{-2}}\hat{V} \end{aligned} \tag{3.76}$$

The action of this Hamiltonian operator on a state is

$$-g(v)^{12}V(v)\partial_\phi^2\Psi(v;\phi) = \hat{\mathcal{C}}^{(2)}_{\rm grav}\Psi(v;\phi) \tag{3.77}$$

where

$$\begin{aligned}\hat{\mathcal{C}}^{(2)}_{\rm grav}\Psi(v;\phi) &= -\frac{3}{8\pi G\gamma^2\lambda^2}\Big[-V^{1/3}(v)V^{1/3}(v+2)V^{1/3}(v+4)A(v+2)\Psi(v+4;\phi)\\
&+\frac{i\lambda\vartheta}{2}[\mathrm{sgn}(v)A(v)+\mathrm{sgn}(v+2)A(v+2)]\Psi(v+2;\phi)\\
&+V^{2/3}(v)[V^{1/3}(v-2)A(v-2)+V^{1/3}(v+2)A(v+2)\\
&+\lambda^2\vartheta^2(1+\gamma^2)V^{1/3}(v)A(v)]\Psi(v;\phi)\\
&-\frac{i\lambda\vartheta}{2}[\mathrm{sgn}(v)A(v)+\mathrm{sgn}(v-2)A(v-2)]\Psi(v-2;\phi)\\
&-V^{1/3}(v)V^{1/3}(v-2)V^{1/3}(v-4)A(v-2)\Psi(v-4;\phi)\Big]\end{aligned} \tag{3.78}$$

In this case, $\hat{\mathcal{C}}^{(2)}_{\rm grav}$ annihilate the $\Psi(0;\phi)$ so this state does not evolve to the other states. At the other hand, the only states which can evolve to this state are $\Psi(\pm2;\phi)$ and $\Psi(\pm4;\phi)$ but in that case, their coefficient are zero. It means that $\Psi(0;\phi)$ is an isolated state which cannot evolve to other states and any of other states cannot evolve to this state. Therefore it seems that with this choice (and other similar choices) of operator ordering, is easy to see that the singularity is resolved in quantum level.

Although there are some differences between quantum theories with different choices of ordering, they have some similar properties. For example for all of them the non-separable Hilbert space $\mathcal{H}_{\rm kin}$ of the gravitational degrees of freedom is decomposed into an uncountable number, label by a parameter ϵ, of superselected sectors $\mathcal{H}_\epsilon$, each of which is by itself, separable.

$$\begin{aligned}\mathcal{H}_{kin} &= \overline{\bigoplus_\epsilon \mathcal{H}_\epsilon}\\
\mathcal{H}_\epsilon &= \mathrm{Span}\left(|2n+\epsilon\rangle : \quad n\in\mathbb{Z} \quad , \quad \epsilon\in[0,2)\right),\end{aligned} \tag{3.79}$$

Also, the space of solutions can be given a Hilbert space structure if one restricts attention to *positive frequency*, with respect to the internal time ϕ. Thus physical solutions Ψ satisfy the Schrodinger like equation,

$$-i\partial_\phi\,\Psi = \sqrt{\hat{\Theta}}\,\Psi \tag{3.80}$$

where $\hat{\Theta} = -\hat{\mathcal{C}}_{\rm grav}\left(\widehat{V^{-2}\hat{V}}\right)^{-1}$.

A physical inner product can be defined on the space of solutions from which the physical Hilbert space can be constructed. An interesting avenue would be to perform a detailed analysis of the solutions of this theory, along the lines of [25]. We shall leave that for future work. Let us now consider the effective description associated to the quantum theory described in this part.

3.3.2 Properties of Gravitational part of the Hamiltonian Constraint

As we mentioned in previous section, the kinematical Hilbert space is Cauchy completion of the vector space of formal finite linear combinations of the elements of the basis $\{|v\rangle : v \in \mathbb{R}\}$ in which the volume operator (and $\hat{p}$) is diagonalized. In general (for any operator symmetry ordering), the domain of the operators $\hat{\mathcal{C}}_{\rm grav}$ is

$$D = \{\psi \in \mathcal{H}^{kin} | \psi = \sum_{i=1}^{n} a_i |v_i\rangle,\ a_i \in \mathbb{C},\ v_i \in \mathbb{R},\ n \in \mathbb{N}\}. \tag{3.81}$$

The operator $\hat{\mathcal{C}}_{grav}$ can be written in a simpler form

$$\hat{\mathcal{C}}_{grav} = -\frac{3}{8\pi G\gamma^2\lambda^2}(C_0 + C_{+2}U_{+2} + C_{-2}U_{-2} + C_{+4}U_{+4} + C_{-4}U_{-4}), \tag{3.82}$$

where U_i, $i = \pm 2, \pm 4$, are shift operators defined as

$$U_i|v\rangle = |v + i\rangle$$

and C's are some functions of variable v. For example for $\hat{\mathcal{C}}^{(1)}_{\rm grav}$ and $\hat{\mathcal{C}}^{(2)}_{\rm grav}$

$$\begin{aligned}
C^{(1)}_0(v) &= V(v+2)A(v+2) + V(v-2)A(v-2) \\
&\quad +\lambda^2\vartheta^2(1+\gamma^2)A(v)V^{1/3}(v), && (3.83)\\
C^{(1)}_{-2}(v) &= \frac{\lambda\vartheta}{2i}[V^{2/3}(v)A(v) + V^{2/3}(v-2)A(v-2)], && (3.84)\\
C^{(1)}_{+2}(v) &= -\frac{\lambda\vartheta}{2i}[V^{2/3}(v)A(v) + V^{2/3}(v+2)A(v+2)], && (3.85)\\
C^{(1)}_{-4}(v) &= -V(v-2)A(v-2), && (3.86)\\
C^{(1)}_{+4}(v) &= -V(v+2)A(v+2). && (3.87)
\end{aligned}$$

and

$$\begin{aligned} C_0^{(2)}(v) &= V^{2/3}(v)[V^{1/3}(v-2)A(v-2)+V^{1/3}(v+2)A(v+2) \\ &\quad +\lambda^2\vartheta^2(1+\gamma^2)V^{1/3}(v)A(v)], \qquad (3.88) \\ C_{-2}(2)(v) &= -\frac{i\lambda\vartheta}{2}[\mathrm{sgn}(v)A(v)+\mathrm{sgn}(v-2)A(v-2)], \qquad (3.89) \\ C_{+2}(2)(v) &= \frac{i\lambda\vartheta}{2}[\mathrm{sgn}(v)A(v)+\mathrm{sgn}(v+2)A(v+2)], \qquad (3.90) \\ C_{-4}(2)(v) &= -V^{1/3}(v)V^{1/3}(v-2)V^{1/3}(v-4)A(v-2), \qquad (3.91) \\ C_{+4}(2)(v) &= -V^{1/3}(v)V^{1/3}(v+2)V^{1/3}(v+4)A(v+2). \qquad (3.92) \end{aligned}$$

In the rest, we shall prove the following properties for $\hat{\mathcal{C}}^{(1)}_{\rm grav}$ and $\hat{\mathcal{C}}^{(2)}_{\rm grav}$.

1. $\hat{\mathcal{C}}_{grav}$ is essentially self adjoint. This is a general result.

2. $\hat{\mathcal{C}}_{grav}$ is sharply negative. This does not hold true for $\hat{\mathcal{C}}^{(2)}_{\rm grav}$ and those ones similar to it.

3. For each of the subspaces $\mathcal{H}_\epsilon$, the restricted operator $\hat{\mathcal{C}}_{grav} : \mathcal{H}_\epsilon \to \mathcal{H}_\epsilon$ considered as an essentially self adjoint operator in the Hilbert space $\overline{\mathcal{H}_\epsilon}$ has a discrete spectrum.

4. The above restricted operator satisfies:

$$\dim\mathcal{H}_{\mathcal{C}_{grav}>-E} \leq \dim\mathcal{H}_{A'\geq -E}$$

for arbitrary $E > 0$ where

$$A' := -\frac{3\vartheta^2}{8\pi G}\hat{V}^{1/3}\hat{A} \ : \ \mathcal{H}_\epsilon \to \mathcal{H}_\epsilon \qquad (3.93)$$

Property 1. To prove this property we use the following theorem (theorem VIII.3 of [64])

Theorem Let T be a densely defined symmetric operator on a Hilbert space. Then the followings are equivalent:

a. T is essentially self-adjoint.

b. $\mathrm{Ker}(T^* + z)$ and $\mathrm{Ker}(T^* + \bar{z})$ are equal to $\{0\}$.

c. $\mathrm{Ran}(T + z)$ and $\mathrm{Ran}(T + \bar{z})$ are dense.

Therefore, it is sufficient to show that $\mathrm{Ker}(\hat{\mathcal{C}}^*_{\rm grav} \pm i)$ is equal to the set $\{0\}$.
Let $\phi \in D(\hat{\mathcal{C}}^*_{\rm grav})$ be such that

$$\hat{\mathcal{C}}^*_{\rm grav}\phi = \mp i\phi. \tag{3.94}$$

The matrix representation of the operator $\hat{\mathcal{C}}_{\rm grav}$ can be defined in the basis $\{|v\rangle | v \in \mathbb{R}\}$ as

$$A_{vw} = \langle v|\hat{\mathcal{C}}_{\rm grav}|w\rangle,$$

and since $\hat{\mathcal{C}}_{\rm grav}$ is symmetric, $A_{vw} = A^*_{wv}$. Note that each row and column of A has, at most, five nonzero elements.
Lemma Let T be an operator on the Hilbert space $\mathcal{H}^{\rm kin}$ with domain $\mathcal{D}$ equal to $D(\hat{\mathcal{C}}_{\rm grav})$ and $A = (a_{v,w})_{v,w\in\mathbb{R}}$ be its matrix representation. Then, for ϕ and ψ in $\mathcal{H}^{\rm kin}$, the following statements are equivalent [65]

i. $\langle v, \phi\rangle = \sum_w a^*_{v,w}\langle w, \psi\rangle$ is absolutely convergent for each $v \in \mathbb{R}$ and $\phi \in \mathcal{H}^{\rm kin}$.

ii. $\psi \in D(T^*)$ and $T^*\psi = \phi$.

By applying the above lemma, Eq.(3.94) can be written as

$$\sum_v \sum_w a_v A_{v,w}|v\rangle = \mp i \sum_v a_v|v\rangle. \tag{3.95}$$

After multiplying ϕ from the left on both sides, the above equation gets the form

$$\sum_v \sum_w a_w a^*_v A_{v,w} = \mp i \sum_v |a_v|^2. \tag{3.96}$$

Since the left hand side is a real number and the right hand side is an imaginary number, $|\phi|$ and therefore ϕ should be 0 and the proof is complete.

It is indeed possible to generalize the above proof so that it applies to those symmetric operators which are defined on a Hilbert space $\mathcal{H}$ isomorphic to $L^2(S, \mu)$, where S is some measure space with counting measure μ and with domain $\mathcal{D}$ a subset of $\mathcal{H}$ which contains all finite linear combinations of the elements of the orthogonal basis of $\mathcal{H}$. Furthermore, the index set can be countable or uncountable, and their matrix representation has the same properties as the matrix of $\hat{\mathcal{C}}_{\rm grav}$, which means that in each row and column they have a finite number of elements.

The gravitational part of the Hamiltonian operators for the flat FRW model, closed FRW with curvature based quantization, Bianchi I, II and IX which come from LQC are some examples of theories where the corresponding geometric constraint operators are similar to $\hat{\mathcal{C}}_{\rm grav}$, so that one can apply the general form of the above proof to show that they are essentially self adjoint in their domain.

Property 2.

The operator $\hat{\mathcal{C}}^{(1or2)}_{\rm grav}$ can be written as (For a general form of the operator with arbitrary ordering one cannot use this proof)

$$\begin{aligned}\hat{\mathcal{C}}^{(1)}_{\rm grav} &= -\frac{3}{8\pi G\gamma^2\lambda^2}\Big(\widehat{\sin(\lambda\beta)}\hat{V}^{1/3}-\lambda\vartheta\hat{\epsilon}\Big)\hat{A}\hat{V}^{1/3}\Big(\widehat{\sin(\lambda\beta)}\hat{V}^{1/3}-\lambda\vartheta\hat{\epsilon}\Big)^{\dagger}\\ &\quad -\frac{3\vartheta^2}{8\pi G}\hat{A}\hat{V}^{1/3},\end{aligned} \tag{3.97}$$

and

$$\begin{aligned}\hat{\mathcal{C}}^{(2)}_{\rm grav} &= -\frac{3}{8\pi G\gamma^2\lambda^2}\Big(\hat{V}^{1/3}\widehat{\sin(\lambda\beta)}-\lambda\vartheta\hat{\epsilon}\Big)\hat{A}\hat{V}^{1/3}\Big(\hat{V}^{1/3}\widehat{\sin(\lambda\beta)}-\lambda\vartheta\hat{\epsilon}\Big)^{\dagger}\\ &\quad -\frac{3\vartheta^2}{8\pi G}\hat{A}\hat{V}^{1/3}.\end{aligned} \tag{3.98}$$

From the following inequalities

$$\Big(\widehat{\sin(\lambda\beta)}\hat{V}^{1/3}-\lambda\vartheta\hat{\epsilon}\Big)\hat{A}\hat{V}^{1/3}\Big(\widehat{\sin(\lambda\beta)}\hat{V}^{1/3}-\lambda\vartheta\hat{\epsilon}\Big)^{\dagger}\geq 0, \tag{3.99}$$

$$\Big(\hat{V}^{1/3}\widehat{\sin(\lambda\beta)}-\lambda\vartheta\hat{\epsilon}\Big)\hat{A}\hat{V}^{1/3}\Big(\hat{V}^{1/3}\widehat{\sin(\lambda\beta)}-\lambda\vartheta\hat{\epsilon}\Big)^{\dagger}\geq 0, \tag{3.100}$$

and

$$\frac{3\vartheta^2}{8\pi G}\hat{A}\hat{V}^{1/3}\geq 0, \tag{3.101}$$

it is obvious that $\hat{\mathcal{C}}_{\rm grav}$ is negative and holds

$$\hat{\mathcal{C}}_{grav}\leq -\frac{3\vartheta^2}{8\pi G}\hat{A}\hat{V}^{1/3}\leq 0. \tag{3.102}$$

As a more strong result, we show that the equation $\hat{\mathcal{C}}^{(1)}_{grav}\phi=0$ has no nontrivial solution for ϕ and hence $\hat{\mathcal{C}}_{grav}<0$.
Assume some $\phi=\sum_{j=1}^{n}a_j|v_j\rangle$ as an element of D be a solution of equation $\hat{\mathcal{C}}^{(1)}_{\rm grav}\phi=0$, thus we have

$$\begin{aligned}0 &= \sum_{j=1}^{n}a_j\Big(C_0(v_j)|v_j\rangle+C_{-2}(v_j)|v_j-2\rangle+C_{+2}(v_j)|v_j+2\rangle\\ &\quad +C_{-4}(v_j)|v_j-4\rangle+C_{+4}(v_j)|v_j+4\rangle\Big).\end{aligned} \tag{3.103}$$

If there exists a non trivial ϕ that satisfies the above equation, the terms with the same $|v\rangle$ should cancel each other. Without losing the generality, one can write $\phi = \sum_{j=1}^{n} a_j |v_j\rangle$ in such a way that $v_1 \leq v_2 \leq ... \leq v_n$. Hence, it is easy to see that there are two terms $a_n C^{(1)}_{+4}(v_n)|v_n + 4\rangle$ and $a_1 C^{(1)}_{-4}(v_1)|v_1 - 4\rangle$ which cannot cancel with other terms and the only way to cancel them is to put $a_1 C^{(1)}_{-4}(v_1) = 0$ and $a_n C^{(1)}_{+4}(v_n) = 0$. According to definition of $C^{(1)}_{-4}$ and $C^{(1)}_{+4}$ and our assumption $v_1 \leq v_n$, $C^{(1)}_{-4}$ and $C^{(1)}_{+4}$ cannot be zero simultaneously and therefore at least one of a_1 or a_n should be zero which means there is no term with $|v_1\rangle$ or $|v_n\rangle$ in ϕ. We can repeat the same argument and show step by step that all a_j's in ϕ are zero and therefore $\phi = 0$.

However, this result does not hold for $\hat{\mathcal{C}}^{(2)}_{grav}$ because this operator gives zero when acts on $\phi = a|0\rangle$.

Properties 3 and 4 Here we use the same procedure as in [26]. Before proving these two properties, we should be precise about the meaning of discreteness.

Definition Let T be an essentially self-adjoint operator defined in some domain $\mathcal{D}$ in the Hilbert space $\mathcal{H}$, we say its spectrum is discrete whenever the following conditions are satisfied:

- there exists a basis of $\mathcal{H}$ consisting of the eigenvectors of T,
- for each eigenvalue the corresponding eigenvectors span a finite dimensional subspace,
- for every finite interval I of $\mathbb{R}$, the set of the eigenvalues of T contained in I is finite.

Also let T be a self-adjoint operator in a Hilbert space $\mathcal{H}$, α be a real number and ι be an inequality relation, we define $\mathcal{P}_{T\iota\alpha} : \mathcal{H} \to \mathcal{H}$ as the spectral projector of T onto the interval $\{t \in \mathbb{R} \ : \ t\iota\alpha\}$. We mean by $\mathcal{H}_{T\iota\alpha}$ as the image of $\mathcal{P}_{T\iota\alpha}$

$$\mathcal{H}_{T\iota\alpha} := \mathcal{P}_{T\iota\alpha}(\mathcal{H}). \tag{3.104}$$

To prove the properties 3 and 4, we use the following lemma (for the proof see [**?**]):

Lemma Let $(B,\mathcal{D}(B))$ and $(B',\mathcal{D}(B'))$ be operators in a Hilbert space $\mathcal{H}$ with their domains and $\mathcal{D} \subset \mathcal{D}(B) \cap \mathcal{D}(B')$ be a dense subspace of $\mathcal{H}$. Suppose the following conditions are satisfied:

- On the domain $\mathcal{D}$ the following inequality holds

$$0 \leq B \leq B',$$

- The operator B' is essentially self-adjoint in $\mathcal{D}$,
- B, as an operator defined in $\mathcal{D}(B)$, is self adjoint, positive and has discrete spectrum.

Then B is also positive and has discrete spectrum. Moreover, the following inequality holds for arbitrary $\lambda \geq 0$

$$\dim\mathcal{H}_{B'<\lambda} \;\leq\; \dim\mathcal{H}_{B\leq\lambda}.$$

By fixing $\epsilon \in \mathbb{R}$ and defining $\mathcal{H} = \overline{\mathcal{H}_\epsilon}$ and $\mathcal{D} = \mathcal{H}_\epsilon$ as the corresponding Hilbert space and the domain of the following operators

$$B = \hat{A}\hat{V}^{1/3} \;:\; \mathcal{H}_\epsilon \to \mathcal{H}_\epsilon, \tag{3.105}$$

$$B' = -\frac{8\pi G}{3\vartheta^2}\hat{\mathcal{C}}_{grav} \;:\; \mathcal{H}_\epsilon \to \mathcal{H}_\epsilon, \tag{3.106}$$

the above lemma implies the properties 3 and 4.

3.3.3 Effective Equations

It is straightforward to see that the effective Hamiltonian one obtains from the quantum theory of the previous part, when neglecting inverse scale factor effects (as was done in [25] and [60]), is

$$\mathcal{H}_{\text{eff}} = -\frac{3}{8\pi G\gamma^2\lambda^2}V\left[(\sin\lambda\beta - D)^2 + \gamma^2 D^2\right] + \rho V\,. \tag{3.107}$$

It is then straightforward to compute the corresponding effective equations of motion. In particular, by computing $\dot{V} = \{V, \mathcal{H}_{\text{eff}}\}$, we can find the expression for the expansion as

$$\theta = \frac{3}{\lambda\gamma}\cos\lambda\beta\,(\sin\lambda\beta - D)\;. \tag{3.108}$$

From which we can find the effective Friedman equation,

$$H^2 = \frac{1}{\lambda^2\gamma^2}\cos^2\lambda\beta\,(\sin\lambda\beta - D)^2 = \frac{8\pi G}{3}(\rho - \rho_1)(1 - \frac{\rho - \rho_2}{\rho_{\text{crit}}})\,, \tag{3.109}$$

where $\rho_1 = \rho_{\text{crit}}\gamma^2 D^2$ and $\rho_2 = \rho_{crit}D[(1+\gamma^2)D - 2\sin\lambda\beta]$. Let us now explore what is the difference in the behavior of the Universe as described by these equations, compared to the dynamics given by the holonomy-based quantization. The first obvious observation from Eq. (3.108) is that the universe undergoes a turnaround whenever the expansion vanishes. This can happen either when: a) $\sin\lambda\beta = D$, or

b) when $\cos\lambda\beta = 0$. The first condition can also be written, by using (3.109), as $\rho = \rho_1 = \rho_{\rm crit}\gamma^2 D^2$, and in the limit $D \ll 1$ –when the volume is large in Planck units– corresponds to the point of re-collapse. It is interesting to note that, in contrast to the other quantum theory, the expression for the point of re-collapse here coincides *exactly* with that of the classical theory (recall that in the previous case, we only recovered this value in the large volume/momentum limit).

Just as we had in the previous case, we expect that the nature of the turnaround points (whether they correspond to a bounce or a re-collapse) will be determined only after we consider the rate of change of the expansion (the Hubble). The second condition above, namely condition b) can be written as $\rho = \rho_{crit} + \rho_2$, or alternatively, as $\cos\lambda\beta = 0$. Now, for this condition "b)", there is a crucial difference with the previous case. While in the effective description of the holonomy based quantization all equations were invariant under the mapping $\beta \to \beta + \pi/\lambda$ (and therefore implementing an effective periodicity of β with period π/λ), this is no longer the case here. Even when the zeros of the term $\cos\lambda\beta$ have that periodicity, the term $\sin\lambda\beta - D$ does not. Therefore, there are two kind of roots for the equation $\cos\lambda\beta = 0$. The first root 'b.1' occurs when $\beta_n = \frac{(4n+1)\pi}{2\lambda}$, where $\sin\lambda\beta_n = 1$. The other root 'b.2' is when $\beta_m = \frac{(4m+3)\pi}{2\lambda}$, in which case $\sin\lambda\beta_m = -1$. The important thing here to notice is that the density (and therefore, volume) are different in these two cases, which implies that *there are two different kind of turnarounds of type 'b)'.*

In order to identify the nature of these turnaround point, let us use the rest of the equations of motion,

$$\dot\beta = 4\pi G\gamma P - \frac{1}{2\gamma\lambda^2}\left[3\sin^2\lambda\beta - 4D\sin\lambda\beta + (1+\gamma^2)D^2\right] , \tag{3.110}$$

and, from the continuity equation, we get

$$\dot\beta = -4\pi G\gamma(\rho - \rho_3 + P) \quad \text{where} \quad \rho_3 = \frac{2\rho_{\rm crit}D}{3}\left[(1+\gamma^2)D - \sin\lambda\beta\right] \tag{3.111}$$

Finally, we have the change of the expansion function given as

$$\dot\theta = \frac{3}{\gamma}\dot\beta\,(\cos 2\lambda\beta + D\sin\lambda\beta) + \frac{D\theta}{\lambda\gamma}\cos\lambda\beta \tag{3.112}$$

From this last equation we can then determine the identity of the turnaround points. For the different cases as defined above we have,
Case a): It is defined by $\sin\lambda\beta = D$, or alternatively by $\rho = \tilde\rho_1 = \rho_{\rm crit}\gamma^2 D^2$. In this case,

$$\dot\theta = \frac{3}{\gamma}\,\dot\beta(\cos^2\lambda\beta - \sin^2\lambda\beta + D\sin\lambda\beta) = \frac{3}{\gamma}\,\dot\beta\,\cos^2\lambda\beta \tag{3.113}$$

Thus, just as it happened in the holonomy-based quantization, when $\dot{\beta} < 0$ this point corresponds to a re-collapse, while in the case that $\dot{\beta} > 0$, this is a bounce.
Case b): It is defined by $\cos\lambda\beta = 0$, or equivalently by $\rho = \rho_{\rm crit}[1 + D((1+\gamma^2)D - 2\sin\lambda\beta)]$. In this case we have two subcases, corresponding to the two roots of the equation $\cos\lambda\beta = 0$.
Case b.1) This corresponds to the roots $\lambda\beta_n = \frac{(4n+1)\pi}{2\lambda}$, for n integer. In this case, $\sin\lambda\beta_n = 1$, so the change of the expansion in given by,

$$\dot{\theta}_1 = -\frac{3}{\gamma}\,\dot{\beta}\,(1 - D) \tag{3.114}$$

Thus, we see that the nature of the turnaround depends not only on the sign of $\dot{\beta}$ but also on the magnitude of D. In the large volume regime, where $D \ll 1$, we have the same situation as in the holonomy-based quantization, namely that in the $\dot{\beta} < 0$ case, the turnaround point corresponds to a *bounce* (and in the $\dot{\beta} > 0$ case, to a *re-collapse*). The density is given then by,

$$\rho_{\rm b}^1 = \rho_{\rm crit}\left[(1 - D)^2 + \gamma^2 D^2\right]\,, \tag{3.115}$$

Let us nos consider the other root.
Case b.2) This corresponds to the root $\lambda\beta_m = \frac{(4m+3)\pi}{2}$ for m integer. In this case, $\sin\lambda\beta_n = -1$, so the change of the expansion in given by,

$$\dot{\theta}_2 = -\frac{3}{\gamma}\,\dot{\beta}\,(1 + D)\,. \tag{3.116}$$

We have the same situation as in the holonomy-based quantization, namely that in the $\dot{\beta} < 0$ case, the turnaround point corresponds to a *bounce* (and in the $\dot{\beta} > 0$ case, to a *re-collapse*). The density is given then by,

$$\rho_{\rm b}^2 = \rho_{\rm crit}\left[(1 + D)^2 + \gamma^2 D^2\right]\,. \tag{3.117}$$

To summarize, instead of two turnaround points as in the holonomy-based quantization, this new quantization has the novel feature that there are three different turnaround points. In the case of large volume and for $\dot{\beta} < 0$, they correspond to *two bounces* and a re-collapse. For extreme situations near the Planck scale and for certain matter content one might have different scenarios [44].

3.3.3.1 An example: A massless scalar

Let us now consider as matter field a massless scalar field ϕ, for which $\dot{\beta} < 0$ and does not change sign during the dynamical evolution. Furthermore, we shall

assume $D < 1$, in which case, the case a) above corresponds to the point of re-collapse, while the points b.1) and b.2) correspond to the two distinct *bounces*. The maximum value of volume is exactly given by,

$$V_{\rm max} = \left(\frac{64\pi G}{3\vartheta^2}\right)^{3/4} p_\phi^{3/2} \tag{3.118}$$

which is equal to the classical value for maximum volume for the FRW model with k=1. The equations for minimum volumes which correspond to the two different bounces are

$$\frac{p_\phi^2}{2V_{\rm min}^2} = \rho_{\rm crit}\left[(1+\frac{\lambda\vartheta}{V_{\rm min}^{1/3}})^2 + \frac{\gamma^2\lambda^2\vartheta^2}{V_{\rm min}^{2/3}}\right] \tag{3.119}$$

and

$$\frac{p_\phi^2}{2V_{\rm min}^2} = \rho_{\rm crit}\left[(1-\frac{\lambda\vartheta}{V_{\rm min}^{1/3}})^2 + \frac{\gamma^2\lambda^2\vartheta^2}{V_{min}^{2/3}}\right] \tag{3.120}$$

In the limit of large field's momentum p_ϕ, since the volume is also large then we have $D \ll 1$. We can write the density at the two bounces as follows,

$$\rho_{\rm b}^1 = \rho_{\rm crit}\left[(1+D)^2+\gamma^2D^2\right] \quad \text{and} \quad \rho_{\rm b}^2 = \rho_{\rm crit}\left[(1-D)^2+\gamma^2D^2\right],$$

from which it follows that, in the limit $D \ll 1$ they both tend to $\rho_{\rm crit}$ from above. Therefore the density at the bounce for both approaches with different quantization in this limit approaches $\rho_{\rm crit}$ the critical density for the k=0 FRW model. Since both bounce densities have the same limit, then the minimum value of the volume for both cases goes to

$$V_{\rm min} \approx \sqrt{\frac{1}{2\rho_{\rm crit}}}\, p_\phi \tag{3.121}$$

therefore, when the field's momentum p_ϕ is very large, since we can ignore the negative powers of volume, the maximum absolute value of expansion for the second approach goes to $3/2\gamma$ which is the same as in first approach.

In Fig. (3.2) we have plotted the time evolution of the universe for different values of the minimum volume at the bounce. As we can see, as we increase this value, and therefore, the field's momentum p_ϕ, the two bounces tend to each other, both in terms of the value of the volume and in the maximum value of the densities. Note that the densities at the 'strongest' bounce are much higher, in this regime, than in the holonomy-based quantization, and that they decrease as one increases the value of p_ϕ. One can further compare both description by fixing the value of p_ϕ and comparing the time evolution of volume and density. We have plotted such comparison in Fig. (3.3) for $p_\phi = 10^5$. Note that the density at the

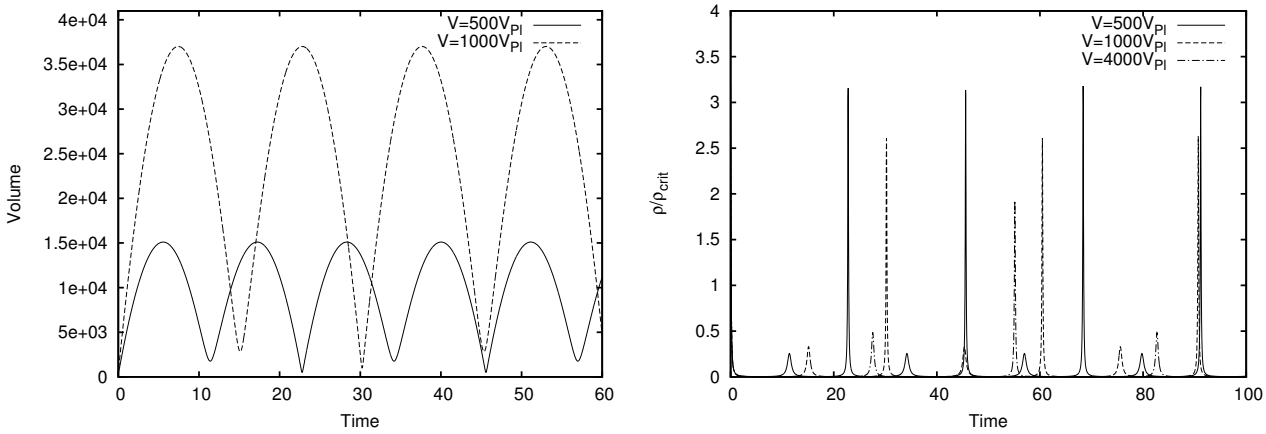

Figure 3.2: Time evolution of the volume V (left) and the density ρ (right) for three values of the volume at the bounce $V_{\rm b}$ correspond to the values $V_{\rm b} = 500\ell_{\rm Pl}$ (—- line), $V_{\rm b} = 1000\ell_{\rm Pl}$ ($- - - - -$ line), and $V_{\rm b} = 4000\ell_{\rm Pl}$ ($- \cdot - \cdot - \cdot -$ line).

bounce in the holonomy-based quantization is in between the two densities for the connection-based quantization. The period between the point of re-collapse is not the same for both schemes but, as one increases p_ϕ, they approach each other, just at the volume and density at the bounce converge.

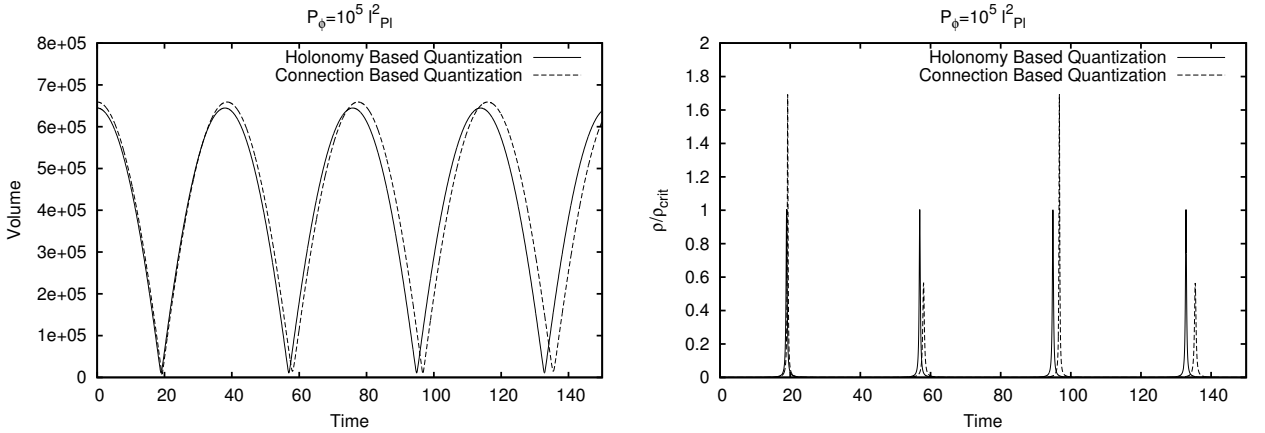

Figure 3.3: Time evolution of the volume V (left) and the density ρ (right), for the two quantization methods, for $p_\phi = 10^5$.

3.3.4 Effective Equations with Inverse Triad Corrections

Not ordering constraint operator for this case is

$$\hat{\mathcal{C}_H} = -\frac{3}{8\pi G\gamma^2\lambda^2}\hat{A}(\hat{|p|^{3/2}}\sin^2\bar{\mu}c - 2\lambda\vartheta\hat{|p|}\sin\bar{\mu}c + (1+\gamma^2)\lambda^2\vartheta^2\hat{|p|^{1/2}}) + \hat{\rho}\hat{|p|}^{3/2}$$

The modified effective hamiltonian with variables β and V is

$$\begin{aligned}\mathcal{H}_{eff} =& -\frac{3}{8\pi G\gamma^2\lambda^2}A(V)\left[V\sin^2\lambda\beta - 2\lambda\vartheta V^{2/3}\sin\lambda\beta + (1+\gamma^2)\lambda^2\vartheta^2V^{1/3}\right] \\ &+ \rho V\end{aligned} \tag{3.122}$$

The equations of motion for V and β are given by

$$\dot{V} = \frac{3}{\gamma\lambda}A(V)\cos\lambda\beta(V\sin\lambda\beta - \lambda\vartheta V^{2/3}) \tag{3.123}$$

and

$$\begin{aligned}\dot{\beta} =& -\frac{3}{2\gamma\lambda^2}\left[\left(VA_{,V} + A(V)\right)\sin^2\lambda\beta - 2\lambda\vartheta\sin\lambda\beta\left(\frac{2}{3}A(V)V^{-1/3} + A_{,V}V^{2/3}\right)\right. \\ &\left. + \lambda^2\vartheta^2(1+\gamma^2)\left(\frac{A(V)V^{-2/3}}{3} + A_{,V}V^{1/3}\right)\right] + 4\pi G\gamma\left(V\frac{\partial\rho}{\partial V} + \rho\right)\end{aligned} \tag{3.124}$$

The expansion is

$$\theta = \frac{3}{\gamma\lambda}A(V)\cos\lambda\beta(\sin\lambda\beta - \lambda\vartheta V^{-1/3}) \tag{3.125}$$

and its time derivative

$$\dot{\theta} = \frac{3}{\gamma}\dot{\beta}A(V)(\cos 2\lambda\beta + D\sin\lambda\beta) + \frac{3}{\gamma\lambda}D\cos\lambda\beta\left(\frac{A(V)\theta}{3} - \dot{V}A_{,V}\right) \tag{3.126}$$

Expansion θ is absolutely bounded because in Eq.3.125
1. The maximum and minimum values for $\cos\lambda\beta$ are 1 and -1,
2. The absolute value of $A(V)(\sin\lambda\beta - \vartheta\lambda V^{-1/3})$ is always less than $1 + 3^{1/6}\vartheta$,
Therefore, the absolute value of θ is less than $3/\gamma\lambda + 3^{7/6}\vartheta/\gamma\lambda$.

To study about matter density we have following expression

$$\rho = \frac{3}{8\pi G\gamma^2\lambda^2}A(V)\left[\sin^2\lambda\beta - 2\lambda\vartheta V^{-1/3}\sin\lambda\beta + (1+\gamma^2)\lambda^2\vartheta^2V^{-2/3}\right] \tag{3.127}$$

which has an upper limit

$$\rho \leq \frac{3}{8\pi G\gamma^2\lambda^2}\left[1+2\lambda\vartheta V_c^{-1/3}+(1+\gamma^2)\lambda^2\vartheta^2 V_c^{-2/3}\right] \tag{3.128}$$

In previous section with no inverse triad effects both density and expansion for this model are unbounded.

A common result for both quantization is according to Eqs.(3.50),(3.126) it can be seen that the nature of turnaround points is depend on the sign of $\dot{\beta}$.

One should note that these results are not exact because to achieve them we use the inverse triad corrections which are important effects for very small volumes that we do not expect to have a good effective equations to describe our system, classically.

Let us summarize the results of this section. First, we developed the quantum theory for k=1 loop quantum gravity coupled to a scalar field, employing a quantization method the uses open holonomies to regulate the field strength appearing in the constraint. In the second part we studied some properties of the gravitational part of the Hamiltonian constraint operator. In the third part we derived some of the consequences of such a quantum theory, by means of its effective description. We found that the most dramatic difference from the quantization previous explored is that the cyclic universe undergoes cycles of contraction and expansion, but alternating between two different quantum bounces (or alternating between two kinds of points of re-collapse and a bounce). Furthermore, we saw that for 'large universes', where the universe expands to a large volume (in Planck units), the densities (and volumes) of the two distinct bounces approach each other and converge to the values attained in the k=0 theory. At the end, we worked with the effective equations with more quantum corrections and we found in that case both density and expansion are bounded.

3.4 Discussion

In this chapter we have explored a quantization ambiguity that exists for certain models in loop quantum cosmology. This correspond to the freedom of using closed holonomies around loops to define curvature or open holonomies to define connections. Since it is only the latter choice that is available for anisotropic models with non-trivial spatial curvature, it is important to understand the particular features of this quantization, and compare it to the original holonomy-based loop quantization. In this regard, the isotropic k=1 FRW model is ideal since both quantizations exist and are not equivalent (while they are in the case of k=0 and Bianchi I). We have explored some of the differences between these two theories,

by means of their corresponding *effective* descriptions. The equation of motion for both theories are not the same, and therefore their underlying dynamics is different. The most dramatic difference is that, while the universe is cyclic in the holonomy-based quantization with a bounce followed by a re-collapse, in the new quantization the situation is more complicated, with three different turnaround points. In the semiclassical limit where the universe is a assumed to grow large, we have seen that there are *two* kinds of bounces with different densities that alternate with the re-collapse. The volume at which the expansion stops and the universe starts to contract is also different.

Interestingly, in the limit of large universes both theories converge and the two distinct bounces of the connection-based theory approach that of the holonomy-based quantization. In this limit both descriptions approximate general relativity during the small density epochs of the cyclic universes, making them almost indistinguishable. It would be interesting to explore further the similarities and differences of the two approaches regarding singularity resolution, as was done in [60] for the holonomy based description. Further numerical analysis with various matter fields might yield significant differences that could have potential observable consequences. This shall be reported elsewhere [44].

Also by adding the inverse corrections, they *do* play a role when considering the affective dynamics for both curvature and connection based quantizations. In particular, relevant geometrical and matter scalars become absolutely bounded when such effects are taken into account. One might wonder, for instance, what is the relevance of such results, given that, in any case, all effective trajectories do have a bounce and therefore the singularity is resolved. The answer to this questions comes when one is interested in asking questions that involve all possible trajectories. For instance, if one is interested in computing the probability of inflation for such models, one has to consider all possible trajectories and 'weight them' (along the lines of [38, 56]). If we ignore the inverse volume corrections, the energy density is unbounded on the phase space so the volume under which one has to integrate to compute the probability of inflation becomes infinite and there seems no natural way to regularize it [66]. However, when the energy density becomes absolutely bounded, then we have a natural cut-off and one can then hope to compute finite probabilities. Another possible consequence of the boundedness of the scalars pertains to generic singularity resolution, for generic matter content. It would be interesting to explore those issues along the lines of [60].

Matter doesn't matter.

John A. Wheeler

4

Bianchi type IX Model

According to the BKL conjuncture, in a generic gravitational collapse when the classical singularity is approached, the spatial geometry is made of infinite number of small independent patches which are very similar to Bianchi IX vacuum solutions (for a numerical result see [42]). One of the several formulations of Einstein field equations for Bianchi IX model is the Hamiltonian description by Misner [67]. In this formulation, the solutions can be expressed qualitatively in terms of a ball in a billiard with moving walls which have an oscillatory and chaotic behavior[68]. A general solution between two reflections (bounces) is a Kasner solution and during the transition between Kasner epochs, it can be approximated by a Taub vacuum Bianchi II solution. The chaotic nature of the solution arises from the fact that the billiard volume is finite [68]. One reason for that is the divergency of the spatial curvature near the classical singularity and since near to the singularity, quantum effects become important, this behavior cannot be trusted.

In LQC, due to the discreteness of the geometry, it is presumed that the solutions do not behave chaotically and they have at most some finite oscillations. Bojowald et.al. [69], in the context of early LQC have shown that the potential wall is suppressed before the classical singularity and thus Bianchi IX solutions do not have chaotic behavior but in that study, they used pre-$\bar{\mu}$ scheme which now it is recognized that it is not physically meaningful. In this chapter we will work with the $\bar{\mu}$ scheme and explore the effective equations to find out if the chaotic behavior of Bianchi IX model can be treated.

This chapter is organized as follows: In Sec. 4.1, we briefly review some classical

properties of Bianchi IX in terms of Ashtekar variables which are necessary for the quantization process. Then in Sec. 4.2, the quantization of the model in $\bar{\mu}$ scheme is described. This part has been done before in [30] but here since we choose a different lapse function, there are some additional operators containing in Hamiltonian constraint operator. The effective equations are studied in Sec. 4.3. These equations are similar to those ones in [30] (with different lapse function). In Sec. 4.4, we introduce the effective equations with more quantum corrections which make the equations more convenient for studying the behavior of the solutions near the classical singularity. In Sec. 4.5 we focus on the vacuum Bianchi IX and finally we end in Sec. 4.6 with a discussion.

4.1 Classical Theory

Bianchi models are spatially homogenous models such that the symmetry group $\mathcal{S}$ acts simply and transitively on space manifold $\Sigma \cong \mathcal{S}$. the symmetry group for Bianchi IX model is three spatial rotations on a 3-sphere. To define fiducial frames and co frames, we identify this group by SU(2) which carries Cartan connection

$$^o\omega = g^{-1}\mathrm{d}g = {}^o\omega^i\tau_i$$

This connection satisfies Maurer-Cartan structure equation

$$\mathrm{d}^o\omega^i + \frac{1}{2}{}^o\epsilon^i{}_{jk}\,{}^o\omega^j \wedge {}^o\omega^k = 0$$

Where ${}^o\epsilon_{ijk}$ is completely antisymmetric tensor and defined such that ${}^o\epsilon_{123} = 1$. We denot dual vectors ${}^oe_i$ correspond to ${}^o\omega^i$ such that ${}^oe_i^a\,{}^o\omega_a^j = \delta_i^j$ and ${}^oe_i^a\,{}^o\omega_b^i = \delta_b^a$. These vectors read the Lie bracket

$$[{}^oe_i, {}^oe_j] = {}^o\epsilon_{ij}{}^k\,{}^oe_k.$$

Therefore the fiducial metric on Σ is

$${}^oq_{ab} := {}^o\omega_a^i\,{}^o\omega_b^j\,k_{ij},$$

with k_{ij} the Killing-Cartan metric on su(2). This fiducial metric is the metric of a 3-sphere with radius $a_o = 2$. The volume of this 3-sphere is $V_o = 2\pi^2\,a_0^3$. It is useful to define $\ell_o = V_o^{1/3}$ and $\vartheta = \ell_o/a_o$.

In general relativity, the gravitational phase space consists of pairs (A_a^i, E_i^a) on Σ where A_a^i is a SU(2) connection and E_i^a is a densitized triad of weight 1. Since Bianchi IX model is homogeneous and, if we restrict ourselves to diagonal metrics,

one can fix the gauge in such a way that A_a^i has 3 independent components, c^i, and E_i^a has 3 independent components, p_i,

$$A_a^i = \frac{c^i}{\ell_o} {}^o\omega_a^i \quad \text{and} \quad E_i^a = \frac{p_i}{\ell_o^2}\sqrt{{}^oq}\ {}^oe_i^a \tag{4.1}$$

where p_i in terms of the scale factors a_i are $|p_i| = \ell_o^2 a_j a_k$ $(i \neq j \neq k)$. c_i are dimension-less and p_i have dimensions of length-squared. Using (c^i, p_i) the Poisson brackets can be expressed as

$$\{c^i, p_j\} = 8\pi G\gamma\delta_j^i$$

where γ is Barbero-Immirizi parameter. The physical frames and co-frames are

$$\omega^i = a^i {}^o\omega^i \quad \text{and} \quad a_i e_i = {}^oe_i. \tag{4.2}$$

Also the physical metric in diagonal manner can be written as

$$q_{ab} = a_i^2 {}^o\omega_a^i\, {}^o\omega_b^i. \tag{4.3}$$

and thus the physical volume of Σ is $V = 2\pi^2 a_1 a_2 a_3$ which is equal to $\sqrt{|p_1 p_2 p_3|}$.

Since the fiducial frames and co-frames are fixed and because of the way of parametrization of connections and triads, the only relevant constraint is the Hamiltonian constraint that has the form,

$$\mathcal{C}_H = N\Big(\mathcal{H}_{\text{grav}} + \mathcal{H}_{\text{matter}}\Big), \tag{4.4}$$

where N is lapse function, $\mathcal{H}_{\text{matter}}$ is ρV (ρ is matter density) and

$$\mathcal{H}_{\text{grav}} = \int_\Sigma \left[-\frac{\epsilon^{ij}{}_k E_i^a E_j^b}{16\pi G\gamma^2\sqrt{|q|}} \left(F_{ab}^k - (1+\gamma^2)\Omega_{ab}^k\right)\right], \tag{4.5}$$

where $e = \sqrt{|\det E|}$, F_{ab}^k and Ω_{ab}^k are respectively the curvature of connection A_a^i and the curvature of the spin-connection Γ_a^i compatible with the triad. F_{ab}^k in terms of phase space variables is

$$F_{ab}^k = \frac{2}{\ell_o^2}(\varepsilon c_i c_j - 2\vartheta c_k)\, {}^o\epsilon^{ijk}\, {}^o\omega_a^i\, {}^o\omega_b^j \tag{4.6}$$

where ε shows the orientation of physical frames (is 1 when $p_1 p_2 p_3 \geq 0$ and -1 when $p_1 p_2 p_3 < 0$).

For calculating the spin connection curvature it is good to first compute Γ^i.

$$\Gamma^i_a = \frac{\varepsilon}{a_o}\left(\frac{a_j}{a_k}+\frac{a_k}{a_j}-\frac{a_i^2}{a_j a_k}\right){}^o\omega^i_a = \frac{\varepsilon}{a_o}\left(\frac{p_j}{p_k}+\frac{p_k}{p_j}-\frac{p_j p_k}{p_i^2}\right){}^o\omega^i_a \quad i\neq j\neq k. \tag{4.7}$$

and then

$$\Omega^k_{ab} = -\frac{2\varepsilon}{a_o^2}\left(3\frac{p_i p_j}{p_k^2}+2\frac{p_k^2}{p_i p_j}-2\frac{p_i}{p_j}-2\frac{p_j}{p_i}-\frac{p_k^2 p_i}{p_j^3}-\frac{p_k^2 p_j}{p_j^3}\right){}^o\omega^k_a \quad i\neq j\neq k. \tag{4.8}$$

So the classical Hamiltonian constraint is given by

$$\begin{aligned}\mathcal{C}_H =& -\frac{N}{8\pi G\gamma^2\lambda^2}\Bigg(\operatorname{sgn}(p_1p_2)\sqrt{\left|\frac{p_1p_2}{p_3}\right|}c_1c_2+\operatorname{sgn}(p_2p_3)\sqrt{\left|\frac{p_2p_3}{p_1}\right|}c_2c_3+\operatorname{sgn}(p_1p_3)\sqrt{\left|\frac{p_1p_3}{p_2}\right|}c_1c_3\\
&-\vartheta\left[\operatorname{sgn}(p_1\sqrt{\left|\frac{p_2p_3}{p_1}\right|}c_1+\operatorname{sgn}(p_2)\sqrt{\left|\frac{p_1p_3}{p_2}\right|}c_2+\operatorname{sgn}(p_3)\sqrt{\left|\frac{p_1p_2}{p_3}\right|}c_3\right]\\
&+\vartheta^2(1+\gamma^2)\left[2|p_1|\sqrt{\left|\frac{p_1}{p_2p_3}\right|}+2|p_2|\sqrt{\left|\frac{p_1}{p_1p_3}\right|}+2|p_3|\sqrt{\left|\frac{p_3}{p_1p_2}\right|}\right.\\
&\left.-\frac{|p_1p_2|^{3/2}}{|p_3|^{5/2}}-\frac{|p_2p_3|^{3/2}}{|p_1|^{5/2}}-\frac{|p_1p_3|^{3/2}}{|p_2|^{5/2}}\right]\Bigg)\\
&+\rho\sqrt{|p_1p_2p_3|}\end{aligned} \tag{4.9}$$

In the rest of this chapter we choose lapse function N to be equal to 1.[1]

4.2 Quantum Theory

To construct the quantum kinematics, we have to select a set of elementary observables such that their associated operators are unambiguous. In loop quantum gravity they are the holonomies h_e defined by the connection A^i_a along edges e and the fluxes of the densitized triad E^a_i across surfaces. For our model we choose p_i and $e^{i\mu c_i}$ (because a holonomy along the edge e_i parallel to i-th vector basis with length μ is made by the combination of these operators). We take the gravitational part of the kinematical Hilbert space as a space of countable linear combinations of orthonormal basis $\{|l_1,l_2,l_3\rangle :\ l_1,l_2,l_3\in\mathbb{R}\}$ where in this basis the operators $\hat{p}_i$'s are diagonalized and they satisfy

$$\langle l_1,l_2,l_3|l_1',l_2',l_3'\rangle = \delta_{l_1,l_1'}\delta_{l_2,l_2'}\delta_{l_3,l_3'}. \tag{4.10}$$

[1]This choice will allow us to include more corrections to the effective Hamiltonian in Sec. 4.4.

. The elements of this space are square summable functions.

The action of the elementary operators on this basis are

$$\hat{p}_i|l_1,l_2,l_3\rangle = (2V_c)^{2/3}\mathrm{sgn}(l_i)l_i^2|l_1,l_2,l_3\rangle$$

and

$$e^{i\mu c_i}|l_1,l_2,l_3\rangle = |l_i - \frac{\mathrm{sgn}(\mu)\sqrt{\mu|}}{1v_c^{1/3}},l_j,l_k\rangle \quad , \quad i\neq j\neq k$$

where $V_c = 2\pi G\gamma\lambda$.

To have the corresponding constraint operator, one needs to express it in terms of the chosen phase space functions $e^{i\mu c_i}$ and p_i. The first term, $\epsilon^{ij}{}_k E_i^a E_j^b/\sqrt{|q|}$, as in loop quantum gravity, can be treated by using Thiemann's strategy [3].

$$\epsilon_{ijk}\frac{E^{ai}E^{bj}}{\sqrt{|q|}} = \sum_i \frac{1}{2\pi\gamma G\mu}\ {}^o\epsilon^{abc}\ {}^o\omega_c^i \mathrm{Tr}(h_i^{(\mu)}\{h_i^{(\mu)-1},V\}\tau_k) \tag{4.11}$$

where $h_i^{(\mu)}$ is the holonomy along the edge parallel to i-th vector basis with length μ and V is the volume, which is equal to $\sqrt{|p_1p_2p_3|}$. Note that μ is arbitrary. Now, to define an operator related to the first term of Eq.(4.5), we can use the right hand side of Eq.(4.11) and replace Poisson brackets with commutators. To find an operator related to the curvature F_{ab}^k, for isotropic models and Bianchi I, one can consider a square $\Box_{ij}$ in the $i-j$ plane which is spanned by two of the fiducial triads (for the closed isotropic model since triads do not commute, to define this plane we use a triad and a right invariant vector ${}^o\xi_i^a$), with each of its sides having length μ_i'. Therefore, F_{ab}^k is given by

$$F_{ab}^k = 2\lim_{Area_\Box\to 0}\epsilon_{ij}{}^k \mathrm{Tr}\left(\frac{h_{\Box_{ij}}^{\mu'}-\mathbb{I}}{\mu_i'\mu_j'}\tau^k\right){}^o\omega_a^i\,{}^o\omega_b^j\,. \tag{4.12}$$

Since in loop quantum gravity, the area operator does not have a zero eigenvalue, one can take the limit of Eq.(4.12) to the point where the area is equal to the smallest eigenvalue of the area operator, $\lambda^2 = 4\sqrt{3}\pi\gamma l_p^2$, instead of zero. Then, $\mu_i' a_i = \lambda$. We take $\mu_i' = \bar{\mu}_i\ell_o$ where $\bar{\mu}_i$ is a dimensionless parameter and, by previous considerations, is equal to $\bar{\mu}_i = \lambda\sqrt{|p_i|}/\sqrt{|p_jp_k|}$ $(i\neq j\neq k)$.

For Bianchi IX, we cannot use this method because the resulting operator is not almost periodic, therefore we express the connection A_a^i in terms of holonomies and then use the standard definition of curvature F_{ab}^k.

$$A_a^i = \lim_{\ell_i\to 0}\frac{1}{2\ell_i}(h^{(\ell_i)} - h^{(\ell_i)-1})$$

To be consistent with other models, we choose

$$\ell_i = 2\mu_i'$$

Thus the operators corresponding to the connection are given by [29]

$$\hat{c}_i = \frac{\widehat{\sin\bar{\mu}_i c_i}}{\bar{\mu}_i}\,. \tag{4.13}$$

Also, one can see that the terms related to the curvatures, F_{ab}^k and Ω_{ab}^k, contain some negative powers of p_i which are not well defined operators. To solve this problem we use the same idea as Thiemann's strategy.

$$|p_i|^{(\ell-1)/2} = -\frac{\sqrt{|p_i|}\ell_o}{2\pi G\gamma\tilde{\mu}_i\ell}\mathrm{Tr}(\tau_i h_i^{(\tilde{\mu}_i)}\{h_i^{(\tilde{\mu}_i)-1}, |p_i|^{\ell/2}\})\,, \tag{4.14}$$

where $\tilde{\mu}_i$ is the length of a curve and $\ell \in (0,1)$. Therefore, for these three different operators we have three different curve lengths $(\mu, \mu', \tilde{\mu})$ where μ and $\tilde{\mu}$ can be some arbitrary functions of p_i, so for simplicity we can choose all of them to be equal to μ'. On the other hand we have another free parameter in the definition of negative powers of p_i which is ℓ. Since the largest negative power of p_i which appears in the constraint is $-1/4$, we will take $\ell = 1/2$ and obtain it directly from Eq.(4.14), and after that we express the other negative powers by them.

By the above choices, the operators related to the Eqs.(4.11, 4.14) take the form

$$\begin{aligned}\widehat{\epsilon^{ij}_{\ k}\frac{E_i^a E_j^b}{\sqrt{|q|}}} &= \frac{\hat{\epsilon}\widehat{\sqrt{\left|\frac{p_i p_j}{p_k}\right|}}}{4\pi G\gamma\lambda}(\widehat{e^{i\bar{\mu}_k c_k}}\hat{V}\widehat{e^{-i\bar{\mu}_k c_k}} - \widehat{e^{-i\bar{\mu}_k c_k}}\hat{V}\widehat{e^{i\bar{\mu}_k c_k}})\ {}^o\epsilon^{abc}\ {}^o\omega_c^k \\ &= \widehat{\sqrt{\left|\frac{p_i p_j}{p_k}\right|}}\hat{A}_k\ {}^o\epsilon^{abc}\ {}^o\omega_c^k\,,\end{aligned} \tag{4.15}$$

and

$$\widehat{|p_i|^{-1/4}} = \frac{\sqrt{|p_j p_k|}}{2\pi G\gamma\lambda}(\widehat{e^{i\bar{\mu}_i c_i/2}}\widehat{|\hat{p}|^{1/2}}\widehat{e^{-i\bar{\mu}_i c_i/2}} - \widehat{e^{-i\bar{\mu}_i c_i/2}}\widehat{|\hat{p}|^{1/2}}\widehat{e^{i\bar{\mu}_i c_i/2}}). \tag{4.16}$$

where

$$\hat{A}_k = \frac{\hat{\epsilon}}{4\pi G\gamma\lambda}(\widehat{e^{i\bar{\mu}_k c_k/2}}\hat{V}\widehat{e^{-i\bar{\mu}_k c_k/2}} - \widehat{e^{-i\bar{\mu}_k c_k/2}}\hat{V}\widehat{e^{i\bar{\mu}_k c_k/2}}) \tag{4.17}$$

In the above equations instead of $e^{i\mu c_i}$ with arbitrary real number μ, the operators $e^{i\bar{\mu}_i c_i/2}$ and their powers appear. Therefore we choose $e^{i\bar{\mu}_i c_i/2}$ to be the elementary operators along with p_i. The action of these operators are given by

$$e^{i\bar{\mu}_i c_i}|l_1, l_2, l_3\rangle = |l_i - \frac{1}{|l_j l_k|}, l_j, l_k\rangle \quad , \quad i \neq j \neq k.$$

Also, since the operators $\hat{A}_k$ have the same action on elements of Hilbert space, in the rest we show them by $\hat{A}$.

By using these results the constraint operator without factor ordering is

$$\begin{aligned}
\widehat{\mathcal{C}_H} =& -\frac{1}{8\pi G\gamma^2\lambda^2}\hat{A}\widehat{p_1^{-1/2}}\widehat{p_2^{-1/2}}\widehat{p_3^{-1/2}}(\hat{p_1}\hat{p_2}\hat{|p_3|}\sin\bar{\mu}_1 c_1 \sin\bar{\mu}_2 c_2 \\
&+ \hat{p_1}\hat{|p_2|}\hat{p_3}\sin\bar{\mu}_1 c_1 \sin\bar{\mu}_3 c_3 + \hat{|p_1|}\hat{p_2}\hat{p_3}\sin\bar{\mu}_2 c_2 \sin\bar{\mu}_3 c_3) \\
&+ \frac{\vartheta}{4\pi G\gamma^2\lambda}\hat{\varepsilon}\hat{A}\Big(\hat{p_1}\hat{p_2}\widehat{p_3^{-1}}\sin\bar{\mu}_3 c_3 + \hat{p_2}\hat{p_3}\widehat{p_1^{-1}}\sin\bar{\mu}_1 c_1 + \hat{p_1}\hat{p_3}\widehat{p_2^{-1}}\sin\bar{\mu}_2 c_2\Big) \\
&- \frac{\vartheta^2(1+\gamma^2)}{8\pi G\gamma^2}\hat{A}\Big(2\widehat{p_1^{3/2}}\widehat{p_2^{-1/2}}\widehat{p_3^{-1/2}} + 2\widehat{p_2^{3/2}}\widehat{p_1^{-1/2}}\widehat{p_3^{-1/2}} + 2\widehat{p_3^{3/2}}\widehat{p_1^{-1/2}}\widehat{p_2^{-1/2}} \\
&- \widehat{p_1^{3/2}}\widehat{p_2^{3/2}}\widehat{p_3^{-5/2}} - \widehat{p_1^{3/2}}\widehat{p_3^{3/2}}\widehat{p_2^{-5/2}} - \widehat{p_2^{3/2}}\widehat{p_3^{3/2}}\widehat{p_1^{-5/2}}\Big) \\
&+ \hat{\rho}\,\widehat{p_1^{1/2}}\widehat{p_2^{1/2}}\widehat{p_3^{1/2}}
\end{aligned} \tag{4.18}$$

After choosing some factor ordering, we can construct the total constraint operator. Note that different choices of factor ordering will yield different operators, but the main results will remain almost the same. By solving the constraint equation $\hat{\mathcal{C}}_H \cdot \Psi = 0$, we can obtain the physical states and the physical Hilbert space $\mathcal{H}_{\text{phys}}$. As a final step, one would need to identify the physical observables, that in our case would correspond to relational observables as functions of the internal time ϕ. Here we choose the factor ordering which is similar to $\hat{\mathcal{C}}_H^{(2)}$ in the previous chapter and the ones in [28–30].

$$\hat{\mathcal{C}}_H = \hat{\mathcal{C}}^{(1)} + \hat{\mathcal{C}}^{(2)} + \hat{\mathcal{C}}^{(3)} + \hat{\mathcal{H}}_{\text{matt}} \tag{4.19}$$

where

$$\hat{\mathcal{C}}^{(1)} = \frac{1}{32\pi G\gamma^2\lambda^2}\sum_{i=1}^{3}\sum_{j\neq i}^{3}\hat{\mathcal{C}}_{ij}^{(1)++} + \hat{\mathcal{C}}_{ij}^{(1)+-} + \hat{\mathcal{C}}_{ij}^{(1)-+} + \hat{\mathcal{C}}_{ij}^{(1)--} \tag{4.20}$$

$$
\begin{aligned}
\hat{\mathcal{C}}^{(1)++}_{ij} &= \left(\frac{\hat{V}}{\sqrt{\hat{V}}}\right)^{2/3}(\mathrm{sgn}(l_i)e^{i\bar{\mu}_i c_i}+e^{i\bar{\mu}_i c_i}\mathrm{sgn}(l_i))\left(\frac{\hat{V}}{\sqrt{\hat{V}}}\right)^{2/3}\\
&\quad\times\hat{A}(\mathrm{sgn}(l_j)e^{i\bar{\mu}_j c_j}+e^{i\bar{\mu}_j c_j}\mathrm{sgn}(l_j))\left(\frac{\hat{V}}{\sqrt{\hat{V}}}\right)^{2/3}\\
\hat{\mathcal{C}}^{(1)+-}_{ij} &= -\left(\frac{\hat{V}}{\sqrt{\hat{V}}}\right)^{2/3}(\mathrm{sgn}(l_i)e^{-i\bar{\mu}_i c_i}+e^{-i\bar{\mu}_i c_i}\mathrm{sgn}(l_i))\left(\frac{\hat{V}}{\sqrt{\hat{V}}}\right)^{2/3}\\
&\quad\times\hat{A}(\mathrm{sgn}(l_j)e^{i\bar{\mu}_j c_j}+e^{i\bar{\mu}_j c_j}\mathrm{sgn}(l_j))\left(\frac{\hat{V}}{\sqrt{\hat{V}}}\right)^{2/3}\\
\hat{\mathcal{C}}^{(1)-+}_{ij} &= -\left(\frac{\hat{V}}{\sqrt{\hat{V}}}\right)^{2/3}(\mathrm{sgn}(l_i)e^{i\bar{\mu}_i c_i}+e^{i\bar{\mu}_i c_i}\mathrm{sgn}(l_i))\left(\frac{\hat{V}}{\sqrt{\hat{V}}}\right)^{2/3}\\
&\quad\times\hat{A}(\mathrm{sgn}(l_j)e^{-i\bar{\mu}_j c_j}+e^{-i\bar{\mu}_j c_j}\mathrm{sgn}(l_j))\left(\frac{\hat{V}}{\sqrt{\hat{V}}}\right)^{2/3}\\
\hat{\mathcal{C}}^{(1)--}_{ij} &= \left(\frac{\hat{V}}{\sqrt{\hat{V}}}\right)^{2/3}(\mathrm{sgn}(l_i)e^{-i\bar{\mu}_i c_i}+e^{-i\bar{\mu}_i c_i}\mathrm{sgn}(l_i))\left(\frac{\hat{V}}{\sqrt{\hat{V}}}\right)^{2/3}\\
&\quad\times\hat{A}(\mathrm{sgn}(l_j)e^{-i\bar{\mu}_j c_j}+e^{-i\bar{\mu}_j c_j}\mathrm{sgn}(l_j))\left(\frac{\hat{V}}{\sqrt{\hat{V}}}\right)^{2/3}
\end{aligned}
\tag{4.21}
$$

$$
\begin{aligned}
\hat{\mathcal{C}}^{(2)} = &- \frac{i\vartheta}{16\pi G\gamma^2\lambda}\Bigg[\hat{p}_2\hat{p}_3|\hat{p_1}|^{-1/2}\left(\hat{\epsilon}\hat{A}(e^{i\bar{\mu}_1 c_1}-e^{-i\bar{\mu}_1 c_1})+(e^{i\bar{\mu}_1 c_1}-e^{i\bar{\mu}_1 c_1})\hat{\epsilon}\hat{A}\right)|\hat{p_1}|^{-1/2}\\
&+ \hat{p}_1\hat{p}_3|\hat{p_2}|^{-1/2}\left(\hat{\epsilon}\hat{A}(e^{i\bar{\mu}_2 c_2}-e^{-i\bar{\mu}_2 c_2})+(e^{i\bar{\mu}_2 c_2}-e^{i\bar{\mu}_2 c_2})\hat{\epsilon}\hat{A}\right)|\hat{p_2}|^{-1/2}\\
&+ \hat{p}_1\hat{p}_2|\hat{p_3}|^{-1/2}\left(\hat{\epsilon}\hat{A}(e^{i\bar{\mu}_3 c_3}-e^{-i\bar{\mu}_3 c_3})+(e^{i\bar{\mu}_3 c_3}-e^{i\bar{\mu}_3 c_3})\hat{\epsilon}\hat{A}\right)|\hat{p_3}|^{-1/2}\Bigg]
\end{aligned}
\tag{4.22}
$$

$$
\begin{aligned}
\hat{\mathcal{C}}^{(3)} = &-\frac{\vartheta^2(1+\gamma^2)}{8\pi G\gamma^2}\hat{A}\Big(2\widehat{p_1^{3/2}}\widehat{p_2^{-1/2}}\widehat{p_3^{-1/2}}+2\widehat{p_2^{3/2}}\widehat{p_1^{-1/2}}\widehat{p_3^{-1/2}}+2\widehat{p_3^{3/2}}\widehat{p_1^{-1/2}}\widehat{p_2^{-1/2}}\\
&-\widehat{p_1^{3/2}}\widehat{p_2^{3/2}}\widehat{p_3^{-5/2}}-\widehat{p_1^{3/2}}\widehat{p_3^{3/2}}\widehat{p_2^{-5/2}}-\widehat{p_2^{3/2}}\widehat{p_3^{3/2}}\widehat{p_1^{-5/2}}\Big)
\end{aligned}
\tag{4.23}
$$

and by choosing massless scalar field (as internal time), the matter part is given by

$$\hat{\mathcal{H}}_{\rm matt} = \frac{1}{2}\widehat{p_\phi^2}\ \widehat{p_1^{-1}}\widehat{p_1^{1/2}}\widehat{p_2^{-1}}\widehat{p_2^{1/2}}\widehat{p_3^{-1}}\widehat{p_3^{1/2}} \tag{4.24}$$

To calculate the action of the constraint operator it is simpler to work with dimensionless variable v, which is related to the volume, and two variables of three l_1, l_2 and l_3. v is equal to $2l_1l_2l_3$ and $\hat{V} = V_c|v||l_1, l_2, l_3\rangle$. Because of the symmetry in the model, there is no preference to choose one of l_i's to replace with v. Here, we choose l_3. One should note that we cannot use variable v in a case that the state has zero volume. However, it is easy to see that the constraint operator annihilates the states with zero volume and also the other states cannot reach those states. Therefore, we can use variable v with no problem.

In those variables, the action of operators $e^{i\bar{\mu}_i c_i/2}$, $\hat{A}$ and $\widehat{|p|^{-1/4}}$ are given by

$$e^{i\bar{\mu}_1 c_1/2}|l_1, l_2, v\rangle = |l_1 - \frac{1}{|l_1 v|}, l_2, v - \mathrm{sgn}(l_1 v)\rangle \tag{4.25}$$

and

$$\hat{A}|l_1, l_2, v\rangle = A(v)|l_1, l_2, v\rangle, \tag{4.26}$$

and

$$\widehat{|p|^{-1/4}}|l_1, l_2, v\rangle = \frac{h(v)}{V_c}\prod_{j\neq i} p_j^{1/4}|l_1, l_2, v\rangle \tag{4.27}$$

where

$$A(v) = (||v|+1| - ||v|-1|) = \begin{cases} |v| & |v|<1 \\ 1 & |v|\geq 1 \end{cases}, \tag{4.28}$$

$$h(v) = \sqrt{V_c}\Big(\sqrt{||v|+1|} - \sqrt{||v|-1|}\Big). \tag{4.29}$$

In the previous chapter we showed that the operators similar to the constraint operator for closed FLRW model are essentially self adjoint and since, here, the constraint operator has a similar form as FLRW one, it is essentially self adjoint, too and we will work on its extended domain.

Also, since the constraint operator is invariant under parity, to see the full action of this operator on a state, one need just calculate its action on the positive octant (which means $l_1, l_2, v > 0$). The action of the constraint operator on state

$\Psi(l_1, l_2, v; \phi)$ is given by

$$\begin{aligned}
-\partial_\phi^2 \Psi(l_1, l_2, v; \phi) &= \frac{V_c v^{-5} h^{-12}(v)}{8\pi G\gamma}\Bigg[\frac{\chi_{v-4} V_c v^{4/3}}{2\lambda^2}(v-2)^{4/3}(v-4)^{4/3}A(v-2) \\
&\times h^{4/3}(v)h^{4/3}(v-2)h^{4/3}(v-4)\Psi_{-4}(l_1, l_2, v; \phi) \\
&+\frac{1}{2\lambda^2}V_c v^{4/3}(v+2)^{4/3}(v+4)^{4/3}A(v+2) \\
&\times h^{4/3}(v)h^{4/3}(v+2)h^{4/3}(v+4)\Psi_4(l_1, l_2, v; \phi) \\
&-\frac{1}{2\lambda^2}V_c v^{8/3}h^{8/3}(v)\Psi_0(l_1, l_2, v; \phi) \\
&-\frac{i\vartheta}{2\lambda}(16V_c)^{2/3}h^2(v)h^2(v-2)\Psi_{-2}(l_1, l_2, v; \phi) \\
&+\frac{i\vartheta}{2\lambda}(16V_c)^{2/3}h^2(v)h^2(v+2)\Psi_2(l_1, l_2, v; \phi) \\
&+2^{13/3}\vartheta^2(1+\gamma^2)V_c^{1/3}A(v)h^4(v)\Big(l_1^5 l_2 l_3 + l_2^5 l_1 l_3 + l_3^5 l_1 l_2 \\
&-2l_1^8 l_2^8 h^6(v) - 2l1^8 l_3^8 h^6(v) - 2l_2^8 l_3^8 h^6(v)\Big)\Psi(l_1, l_2, v; \phi)\Bigg]
\end{aligned} \tag{4.30}$$

where

$$\begin{aligned}
\Psi_{\pm 4}(l_1, l_2, v; \phi) &= \Psi(\frac{v\pm 2}{v}l_1, \frac{v\pm 4}{v\pm 2}l_2, v\pm 4; \phi) + \Psi(\frac{v\pm 4}{v\pm 2}l_1, \frac{v\pm 4}{v\pm 2}l_2, v\pm 4; \phi) \\
&+\Psi(\frac{v\pm 2}{v}l_1, l_2, v\pm 4; \phi) + \Psi(\frac{v\pm 4}{v\pm 2}l_1, l_2, v\pm 4; \phi) \\
&+\Psi(l_1, \frac{v\pm 2}{v}l_2, v\pm 4; \phi) + \Psi(l_1, \frac{v\pm 4}{v\pm 2}l_2, v\pm 4; \phi),
\end{aligned} \tag{4.31}$$

$$\begin{aligned}
\Psi_{\pm 2}(l_1, l_2, v; \phi) &= \mathrm{sgn}(v\pm 2)A(v\pm 2)\Big(l_1^4 l_2^4 \Psi(l_1, l_2, v\pm 2; \phi) \\
&+l_2^4 l_3^4 \Psi(\frac{v\pm 2}{v}l_1, l_2, v\pm 2; \phi) + \Psi(l_1, \frac{v\pm 2}{v}l_2, v\pm 2; \phi)\Big) \\
&+A(v)\Big(l_1^4 l_2^4 \Psi(l_1, l_2, v\pm 2; \phi) + l_2^4 l_3^4 \Psi(\frac{v\pm 2}{v}l_1, l_2, v\pm 2; \phi) \\
&+\Psi(l_1, \frac{v\pm 2}{v}l_2, v\pm 2; \phi)\Big),
\end{aligned} \tag{4.32}$$

$$\begin{aligned}\Psi_0(l_1,l_2,v;\phi) &= \chi_{v-2}A(v-2)(v-2)^{2/3}h^{2/3}(v-2)\Big(\Psi(\frac{v-2}{v}l_1,\frac{v}{v-2}l_2,v;\phi)\\
&+\Psi(\frac{v}{v-2}l_1,\frac{v-2}{v}l_2,v;\phi)+\Psi(\frac{v-2}{v}l_1,l_2,v;\phi)\\
&+\Psi(\frac{v}{v-2}l_1,l_2,v;\phi)+\Psi(l_1,\frac{v-2}{v}l_2,v;\phi)+\Psi(l_1,\frac{v}{v-2}l_2,v;\phi)\Big)\\
&+A(v+2)(v+2)^{2/3}h^{2/3}(v+2)\Big(\Psi(\frac{v+2}{v}l_1,\frac{v}{v+2}l_2,v;\phi)\\
&+\Psi(\frac{v}{v+2}l_1,\frac{v+2}{v}l_2,v;\phi)+\Psi(\frac{v+2}{v}l_1,l_2,v;\phi)\\
&+\Psi(\frac{v}{v+2}l_1,l_2,v;\phi)+\Psi(l_1,\frac{v+2}{v}l_2,v;\phi)+\Psi(l_1,\frac{v}{v+2}l_2,v;\phi)\Big),\end{aligned} \tag{4.33}$$

and χ_a is a step function, it is zero when $a \leq 0$ otherwise it is 1.

As an interesting (and somehow expected) result, because of the presence of negative powers of p_i in the Hamiltonian constraint and the fact that the operator $\hat{p}_i^a$ is not inverse of the operator $\widehat{p_i^{-a}}$ where a is a positive real number, the quantum theory of closed FLRW model (connection based quantization which was described in previous chapter) is not a reduced theory of the quantum Bianchi IX

4.3 Effective Equations

The effective Hamiltonian constraint which extracted from the Hamiltonian operator by neglecting the inverse triad effects is given by

$$\begin{aligned}\mathcal{H}_{eff} &= -\frac{V}{8\pi G\gamma^2\lambda^2}(\sin\bar{\mu}_1c_1\sin\bar{\mu}_2c_2+\sin\bar{\mu}_1c_1\sin\bar{\mu}_3c_3+\sin\bar{\mu}_2c_2\sin\bar{\mu}_3c_3)\\
&+\frac{\vartheta}{8\pi G\gamma^2\lambda}\Big(\frac{p_1p_2}{p_3}\sin\bar{\mu}_3c_3+\frac{p_2p_3}{p_1}\sin\bar{\mu}_1c_1+\frac{p_1p_3}{p_2}\sin\bar{\mu}_2c_2\Big)\\
&-\frac{\vartheta^2(1+\gamma^2)}{32\pi G\gamma^2}\Big(2\frac{p_1^{3/2}}{\sqrt{p_2p_3}}+2\frac{p_2^{3/2}}{\sqrt{p_1p_3}}+2\frac{p_3^{3/2}}{\sqrt{p_1p_2}}\\
&-\frac{(p_1p_2)^{3/2}}{p_3^{5/2}}-\frac{(p_1p_3)^{3/2}}{p_2^{5/2}}-\frac{(p_2p_3)^{3/2}}{p_1^{5/2}}\Big)+\rho V.\end{aligned} \tag{4.34}$$

By computing the poisson brackets between p_i and c_i with the effective Hamiltonian we get the equations of motion for p_i and c_i. The time evolution of p_1 and c_1

are as follows

$$\dot{p}_1 = \frac{1}{\gamma\lambda}\cos\bar{\mu}_1 c_1\left[p_1(\sin\bar{\mu}_2 c_2 + \sin\bar{\mu}_3 c_3) - \lambda\sigma\sqrt{\frac{p_2 p_3}{p_1}}\right], \tag{4.35}$$

and

$$\begin{aligned}
\dot{c}_1 \;=\; & -\frac{1}{\gamma\lambda^2}\sqrt{\frac{p_2p_3}{p_1}}\Big(\sin\bar{\mu}_1c_1\sin\bar{\mu}_2c_2 + \sin\bar{\mu}_1c_1\sin\bar{\mu}_3c_3 + \sin\bar{\mu}_2c_2\sin\bar{\mu}_3c_3\Big)\\
& -\frac{\vartheta}{\lambda\gamma}\Big(\frac{p_2p_3}{p_1^2}\sin\bar{\mu}_1c_1 - \frac{p_3}{p_2}\sin\bar{\mu}_2c_2 - \frac{p_2}{p_3}\sin\bar{\mu}_3c_3\Big)\\
& -\frac{c_1\cos\bar{\mu}_1c_1}{2\gamma\lambda}\Big(-\frac{\lambda\vartheta}{p_1}\sqrt{\frac{p_2p_3}{p_1}} + \sin\bar{\mu}_2c_2 + \sin\bar{\mu}_3c_3\Big)\\
& +\frac{c_2\cos\bar{\mu}_2c_2}{2\gamma\lambda\sqrt{p_1}}\Big(-\lambda\vartheta\sqrt{\frac{p_3}{p_2}} + \frac{p_2}{\sqrt{p_1}}\sin\bar{\mu}_1c_1 + \frac{p_2}{\sqrt{p_1}}\sin\bar{\mu}_3c_3\Big)\\
& +\frac{c_3\cos\bar{\mu}_3c_3}{2\gamma\lambda\sqrt{p_1}}\Big(-\lambda\vartheta\sqrt{\frac{p_2}{p_3}} + \frac{p_3}{\sqrt{p_1}}\sin\bar{\mu}_1c_1 + \frac{p_3}{\sqrt{p_1}}\sin\bar{\mu}_2c_2\Big)\\
& -\frac{\vartheta^2(1+\gamma^2)}{4\gamma}\Big(\frac{5}{2}\frac{p_2^{3/2}p_3^{3/2}}{p_1^{7/2}} - \frac{1}{p_1^{3/2}\sqrt{p_2p_3}}(p_2^2+p_3^2)\\
& -\frac{3\sqrt{p_1}}{2}(\frac{p_2^{3/2}}{p_3^{5/2}} + \frac{p_3^{3/2}}{p_2^{5/2}}) + 3\sqrt{\frac{p_1}{p_2p_3}}\Big) + 4\pi G\gamma\Big(V\frac{\partial\rho}{\partial p_1} + \rho\frac{1}{2}\sqrt{\frac{p_2p_3}{p_1}}\Big).
\end{aligned} \tag{4.36}$$

The equations of motion for other c_i and p_i can be obtain by proper permutations.

By having $\dot{p}_i$ it is straightforward to calculate the expansion θ

$$\begin{aligned}
\theta =& \frac{1}{2\gamma\lambda}A(V)(\cos\bar{\mu}_1c_1\left[(\sin\bar{\mu}_2c_2 + \sin\bar{\mu}_3c_3) - \lambda\sigma\frac{1}{p_1}\sqrt{\frac{p_2p_3}{p_1}}\right]\\
& + \cos\bar{\mu}_2c_2\left[(\sin\bar{\mu}_1c_1 + \sin\bar{\mu}_3c_3) - \lambda\sigma\frac{1}{p_2}\sqrt{\frac{p_1p_3}{p_2}}\right]\\
& + \cos\bar{\mu}_3c_3\left[(\sin\bar{\mu}_1c_1 + \sin\bar{\mu}_2c_2) - \lambda\sigma\frac{1}{p_3}\sqrt{\frac{p_1p_2}{p_3}}\right])
\end{aligned} \tag{4.37}$$

For large volume, the second term of $\dot{p}_1/p_1$ behaves like $\sqrt{p_2p_3}/p_1^{3/2}$ and in the limit of small volume behaves like p_2p_3/p_1. Since p_i's can be small or large numbers, there is no bound for $\dot{p}_1/p_1$ and with similar arguments about unboundedness of $\dot{p}_2/p_2$ and $\dot{p}_3/p_3$, it can be proved that expansion is not bounded.

Another interesting quantities are shear, matter density and Ricci scalar. The shear is given by

$$\sigma^2 = \frac{1}{3}[(H_1-H_2)^2 + (H_2-H_3)^2 + (H_1-H_3)^2] \tag{4.38}$$

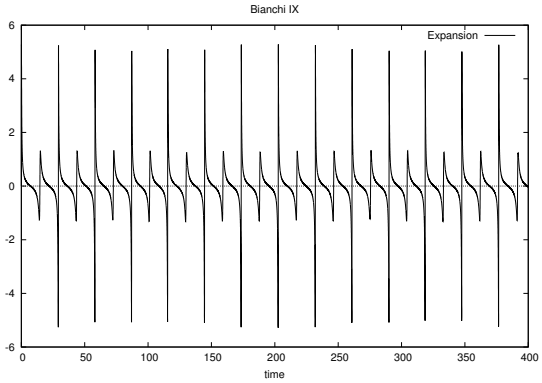

Figure 4.1: Evolution of expansion θ for Bianchi IX.

where $H_i = 1/2[\dot{p}_j/p_j + \dot{p}_k/p_k - \dot{p}_i/p_i]$ $(i \neq j \neq k)$ and $H_i - H_j = \dot{p}_j/p_j - \dot{p}_i/p_i$. For the matter density we have the following expression

$$\begin{aligned}\rho &= \frac{1}{8\pi G\gamma^2\lambda^2}(\sin\bar{\mu}_1c_1\sin\bar{\mu}_2c_2 + \sin\bar{\mu}_1c_1\sin\bar{\mu}_3c_3 + \sin\bar{\mu}_2c_2\sin\bar{\mu}_3c_3)\\ &-\frac{\vartheta}{8\pi G\gamma^2\lambda}\left(\frac{1}{p_3}\sqrt{\frac{p_1p_2}{p_3}}\sin\bar{\mu}_3c_3 + \frac{1}{p_1}\sqrt{\frac{p_2p_3}{p_1}}\sin\bar{\mu}_1c_1 + \frac{1}{p_2}\sqrt{\frac{p_1p_3}{p_2}}\sin\bar{\mu}_2c_2\right)\\ &-\frac{\vartheta^2(1+\gamma^2)}{32\pi G\gamma^2}\left(2\frac{p_1}{p_2p_3} + 2\frac{p_2}{p_1p_3} + 2\frac{p_3}{p_1p_2}\right.\\ &\left.-\frac{p_1p_2}{p_3^3} - \frac{p_1p_3}{p_2^3} - \frac{p_2p_3}{p_1^3}\right)\end{aligned} \tag{4.39}$$

In Fig. 4.2 the maximum allowed density is plotted which shows that the density does not have an upper bound.

And the Ricci scalar can be written as

$$R = 2\dot{\theta} + \sum_{i=1}^{3}(\frac{\dot{p}_i}{p_i})^2 \tag{4.40}$$

$\dot{\theta}$ is the time derivative of expansion and given by

$$\dot{\theta} = \frac{1}{2}\sum_i r_i \tag{4.41}$$

where r_i is time derivative of $\dot{p}_i/p_i$ then

$$\begin{aligned}r_1 =&\frac{\bar{\mu}_1}{\gamma\lambda}(H_1c_1 + \dot{c}_1)\sin\bar{\mu}_1c_1)\left(\sin\bar{\mu}_2c_2 + \sin\bar{\mu}_3c_3 - \vartheta\lambda^2\frac{1}{\bar{\mu}_1p_1}\right)\\ &+\frac{1}{\gamma\lambda}\cos\bar{\mu}_1c_1\left(\bar{\mu}_2(\dot{c}_2 - H_2c_2)\cos\bar{\mu}_2c_2 + \bar{\mu}_3(\dot{c}_3 - H_3c_3)\cos\bar{\mu}_3c_3 - \vartheta\lambda^2\frac{H_1}{\bar{\mu}_1}\right)\end{aligned} \tag{4.42}$$

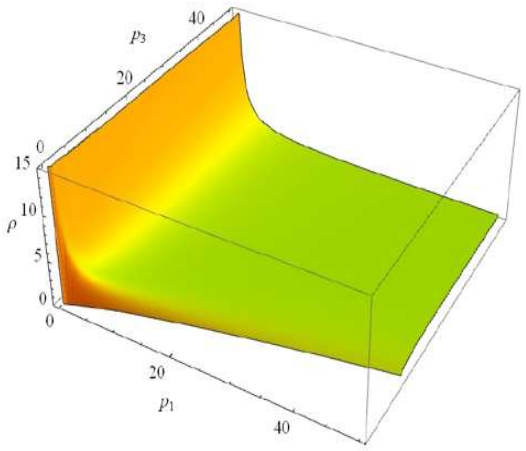

Figure 4.2: Maximum allowed density vs. p_1 and p_3 where $p_2 = p_1$, in Planck units.

By the same argument which we use to show that expansion is unbounded, it is easy to prove that the shear, matter density and Ricci scalar are unbounded, too or at least just by looking at their expression, one cannot find any upper bound for them.

The solutions of the effective equations similar to the closed FLRW model, have infinite number of bounces and recollapses. Some interesting behaviors of expansion, shear and curvature in the duration of some bounces and re-collapses can be seen in Figs. 4.1 and 4.3.

One should note that although the isotropic limit of the quantum equations of Bianchi IX model does not reduce to the quantum closed FLRW model, the effective Hamiltonian in Eq.(4.34) do reduce to the one for closed FLRW model.

4.4 Effective Equations With Inverse Triad Correction

By choosing the eigenvalues of the operators, negative powers of $|p_i|$ and $\hat{A}$ as corrections to the effective Hamiltonian, the modified effective Hamiltonian, with

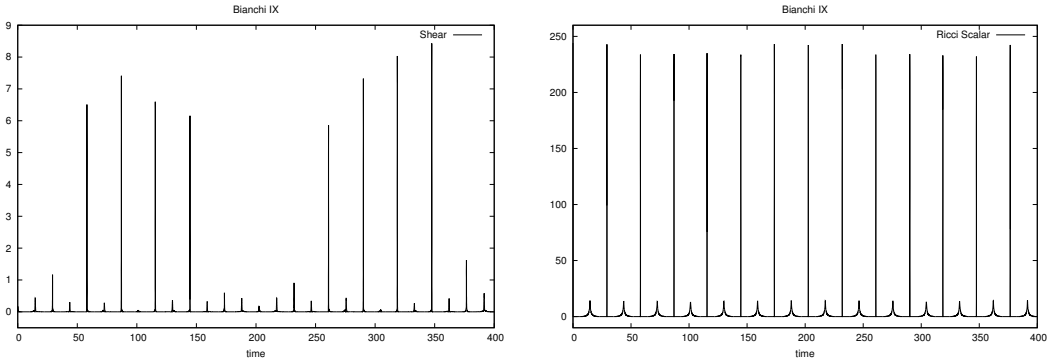

Figure 4.3: Evolution of shear σ^2 and Ricci scalar R for Bianchi IX. The initial conditions at $t = 0$ are: $\bar{\mu}_i c_i = \pi/2$, $p_1 = 90$, $p_2 = 80$ and $p_3 = 100$.

a nonspecific matter density, is given by

$$\begin{aligned}\mathcal{H}_{\rm BIX} &= -\frac{V^4 A(V) h^6(V)}{8\pi G V_c^6 \gamma^2 \lambda^2}\Big(\sin\bar{\mu}_1 c_1 \sin\bar{\mu}_2 c_2 + \sin\bar{\mu}_1 c_1 \sin\bar{\mu}_3 c_3 + \sin\bar{\mu}_2 c_2 \sin\bar{\mu}_3 c_3\Big) \\ &+\frac{\vartheta A(V) h^4(V)}{4\pi G V_c^4 \gamma^2 \lambda}\Big(p_1^2 p_2^2 \sin\bar{\mu}_3 c_3 + p_2^2 p_3^2 \sin\bar{\mu}_1 c_1 + p_1^2 p_3^2 \sin\bar{\mu}_2 c_2\Big) \\ &-\frac{\vartheta^2(1+\gamma^2) A(V) h^4(V)}{8\pi G V_c^4 \gamma^2}\Big(2V[p_1^2 + p_2^2 + p_3^2] \\ &-\Big[(p_1 p_2)^4 + (p_1 p_3)^4 + (p_2 p_3)^4\Big]\frac{h^6(V)}{V_c^6}\Big) + \rho V \approx 0 \end{aligned} \tag{4.43}$$

where $A(V)$ and $h(V)$ are the same as Eqs.(4.28),(4.29) but now as a function of volume instead of v.

$$A(V) = \frac{1}{V_c}(V + V_c - |V - V_c|) = \begin{cases} V/V_c & V < V_c \\ 1 & V \geq V_c \end{cases}, \tag{4.44}$$

and

$$h(V) = \sqrt{V + V_c} - \sqrt{|V - V_c|}. \tag{4.45}$$

The equation of motion for p_1 and c_1 are

$$\dot{p}_1 = \frac{1}{V_c^4 \gamma} A(V) V h^4(V) \cos\bar{\mu}_1 c_1 \left[\frac{V^2 h^2(V) p_1}{V_c^2 \lambda}(\sin\bar{\mu}_2 c_2 + \sin\bar{\mu}_3 c_3) - 2\vartheta p_2 p_3\right], \tag{4.46}$$

and

$$
\begin{aligned}
\dot{c}_1 =& -\frac{h^5(V)}{V_c^6\gamma\lambda^2}\Big(2p_2^2p_3^2p_1A(V)h(V)+V^4A_{,p_1}h(V)+6V^4A(V)h_{,p_1}\Big)\\
&\times\Big(\sin\bar{\mu}_1c_1\sin\bar{\mu}_2c_2+\sin\bar{\mu}_1c_1\sin\bar{\mu}_3c_3+\sin\bar{\mu}_2c_2\sin\bar{\mu}_3c_3\Big)\\
&+\frac{2\vartheta}{V_c^4\gamma\lambda}h^3(V)\Bigg[\Big(2p_1p_2^2A(V)h(V)+p_1^2p_2^2A_{,p_1}h(V)+4p_1^2p_2^2A(V)h_{,p_1}\Big)\sin\bar{\mu}_3c_3\\
&+\Big(2p_1p_3^2A(V)h(V)+p_1^2p_3^2A_{,p_1}h(V)+4p_1^2p_3^2A(V)h_{,p_1}\Big)\sin\bar{\mu}_2c_2\\
&+\Big(p_2^2p_3^2A_{,p_1}h(V)+4p_2^2p_3^2A(V)h_{,p_1}\Big)\sin\bar{\mu}_1c_1\Bigg]\\
&-A(V)h^4(V)\frac{c_1\cos\bar{\mu}_1c_1}{2V_c^4\gamma}\left(\frac{V^3h^2(V)}{V_c^2\lambda}(\sin\bar{\mu}_2c_2+\sin\bar{\mu}_3c_3)-2\frac{p_2^{3/2}p_3^{3/2}}{p_1^{1/2}}\vartheta\right)\\
&+A(V)h^4(V)\frac{c_2\cos\bar{\mu}_2c_2}{2V_c^4\gamma}\left(\frac{p_2^{5/2}p_3^{3/2}p_1^{1/2}h^2(V)}{V_c^2\lambda}(\sin\bar{\mu}_1c_1+\sin\bar{\mu}_3c_3)-2\vartheta p_3V\right)\\
&+A(V)h^4(V)\frac{c_3\cos\bar{\mu}_3c_3}{2V_c^4\gamma}\left(\frac{p_3^{5/2}p_2^{3/2}p_1^{1/2}h^2(V)}{V_c^2\lambda}(\sin\bar{\mu}_1c_1+\sin\bar{\mu}_2c_2)-2\vartheta p_2V\right)\\
&-\frac{\vartheta^2(1+\gamma^2)}{V_c^4\gamma}h^3(V)\Bigg[4p_1A(V)Vh(V)\\
&+(p_1^2+p_2^2+p_3^2)\left(\sqrt{\frac{p_2p_3}{p_1}}A(V)h(V)+8A(V)Vh_{,p_1}+2A_{,p_1}Vh(V)\right)\\
&-\frac{4}{V_c^6}p_1^3h^7(V)A(V)(p_2^4+p_3^4)\\
&-\frac{1}{V_c^6}\Big(10h^6(V)h_{,p_1}A(V)+h^7(V)A_{,p_1}\Big)\Big(p_1^4p_2^4+p_1^4p_3^4+p_2^4p_3^4\Big)\Bigg]\\
&+4\pi G\gamma\left(V\frac{\partial\rho}{\partial p_1}+\rho\frac{1}{2}\sqrt{\frac{p_2p_3}{p_1}}\right)
\end{aligned}
\tag{4.47}
$$

where the partial derivatives of $A(V)$ and $h(V)$ respect to p_i are

$$
A_{,p_i}=\begin{cases}\frac{1}{V_c}\sqrt{\frac{p_jp_k}{p_i}} & V<V_c\\ 0 & V>V_c\end{cases},\ i\neq j\neq k\neq i \tag{4.48}
$$

and

$$\widehat{h}_{,p_i} = \frac{\sqrt{p_j p_k}}{4\sqrt{p_i}} \left[(V+V_c)^{-1/2} - \frac{\sqrt{|V-V_c|}}{V-V_c} \right] \ , \ i \neq j \neq k \neq i \tag{4.49}$$

The equations for $\dot{p}_2$,$\dot{c}_2$,$\dot{p}_3$ and $\dot{c}_3$ can be attain by appropriate permutations. One of the quantity which we want to know if it is bounded or not is the expansion

$$\begin{aligned}\theta =& \frac{1}{2}\sum_i \frac{\dot{p}_i}{p_i} = \frac{1}{2V_c^4\gamma} A(V) V h^4(V) \Bigg(\cos\bar{\mu}_1 c_1 \left[\frac{V^2 h^2(V)}{V_c^2\lambda} (\sin\bar{\mu}_2 c_2 + \sin\bar{\mu}_3 c_3) - 2\vartheta \frac{p_2 p_3}{p_1} \right] \\ &+ \cos\bar{\mu}_2 c_2 \left[\frac{V^2 h^2(V)}{V_c^2\lambda} (\sin\bar{\mu}_1 c_1 + \sin\bar{\mu}_3 c_3) - 2\vartheta \frac{p_1 p_3}{p_2} \right] \\ &+ \cos\bar{\mu}_3 c_3 \left[\frac{V^2 h^2(V)}{V_c^2\lambda} (\sin\bar{\mu}_1 c_1 + \sin\bar{\mu}_2 c_2) - 2\vartheta \frac{p_1 p_2}{p_3} \right] \Bigg)\end{aligned} \tag{4.50}$$

At the limit of large volumes, the first term of $\dot{p}_1/p_1$ behaves like a combination of some trigonometric functions and the second $\sqrt{p_2 p_3}/p_1^{3/2}$ and in the limit of small volume the first term behaves like V^{10} and the second $V^4 p_2^2 p_3^2$. For any amount of volume, p_1 or p_2 or p_3 can be small or large numbers; therefore $\dot{p}_1/p_1$ is not bounded. Since there are similar statements for $\dot{p}_2/p_2$ and $\dot{p}_3/p_3$, the expansion is unbounded.

The other interesting quantities are shear and matter density. The expression for matter density in this modified theory is given by

$$\begin{aligned}\rho =& \frac{V^3 A(V) h^6(V)}{8\pi G V_c^6 \gamma^2 \lambda^2} \left(\sin\bar{\mu}_1 c_1 \sin\bar{\mu}_2 c_2 + \sin\bar{\mu}_1 c_1 \sin\bar{\mu}_3 c_3 + \sin\bar{\mu}_2 c_2 \sin\bar{\mu}_3 c_3 \right) \\ &- \frac{\vartheta A(V)}{4\pi G V_c^4 \gamma^2 \lambda} \left(\frac{p_1^{3/2} p_2^{3/2}}{p 3^{1/2}} \sin\bar{\mu}_3 c_3 + \frac{p_2^{3/2} p_3^{3/2}}{p_1^{1/2}} \sin\bar{\mu}_1 c_1 + \frac{p_1^{3/2} p_3^{3/2}}{p_2^{1/2}} \sin\bar{\mu}_2 c_2 \right) h^4(V) \\ &+ \frac{\vartheta^2 (1+\gamma^2) A(V) h^4(V)}{8\pi G V_c^4 \gamma^2} \Bigg(2\left[p_1^2 + p_2^2 + p_3^2 \right] - \left[\frac{(p_1 p_2)^{7/2}}{p_3^{1/2}} + \frac{(p_1 p_3)^{7/2}}{p 2^{1/2}} \right. \\ &\left. + \frac{(p_2 p_3)^{7/2}}{p_1^{1/2}} \right] \frac{h^5(V)}{V_c^5} \Bigg)\end{aligned} \tag{4.51}$$

With the same arguments which we used to prove unboundedness of the expansion, we can show that the shear and the density are unbounded, too. It is easy to see that because of the function $A(V)$, when volume goes to zero, expansion, shear and density go to zero, too.

In the general case, as it can be seen in Fig.4.4, the maximum allowed density which arises from the modified Hamiltonian, has two distinct disconnected regions with positive values unlike the maximum allowed density in previous section which is always positive. If we impose the weak energy condition and start the evolution within one region, the universe cannot reach the other region. These two regions have different dynamics. To study the vacuum Bianchi IX, we start from large volumes which lie in region B of Fig.4.4 and, as we go to smaller volumes we cannot reach zero volume because 'crossing' to region A is not allowed. Therefore, there is a smallest reachable volume in region B and, since very large anisotropies are not allowed near this smallest volume, and the modified potential is not too large there, then we have, at most, finite oscillations before reaching the bounce. On the other hand, in the internal region A, the anisotropies are very large when some of the p_i are very small, and then the volume of the universe cannot be large enough to start the evolution from there.

In [40] the authors used a modified effective equation and calculated the matter density with almost similar behavior. The differences between their work and ours are

i) They neglected the effect of operator $\hat{A}$.

ii) In their work, the matter density is the eigenvalue of a density operator which they defined it as

$$\hat{\rho} := -\widehat{V^{-1}}\hat{\mathcal{H}}_{grav}.$$

but we use the usual definition of matter density which is [2]

$$\rho := -\mathcal{H}_{grav}/V. \tag{4.52}$$

As we mentioned before, the operator $\hat{V}$ is not the inverse of the operator $\widehat{V^{-1}}$ and from the constraint operator we know that $\hat{\rho} = -(\hat{V})^{-1}\hat{\mathcal{H}}_{grav}$ which is different from their choice. Also they showed that if one calculates the matter density as in Eq.(4.52), the maximum allowed density in their modified theory behaves more similar to the density in Eq.(4.39) than the matter density in Eq.(4.51).

More numerical results for the effective equations with and without inverse triad corrections can be found in [70].

In previous section we mentioned that the effective Hamiltonian Eq.(4.34) reduces to the effective Hamiltonian for closed FLRW model with less correction. This property does not longer hold for the modified Hamiltonian Eq.(4.43) and the closed FLRW model effective Hamiltonian with inverse triad correction is not a reduction of this modified Hamiltonian.

[2] Since $\mathcal{C} = \mathcal{H}_{grav} + \rho V \approx 0$ therefore as a natural choice ρ should be equal to $-\mathcal{H}_{grav}/V$.

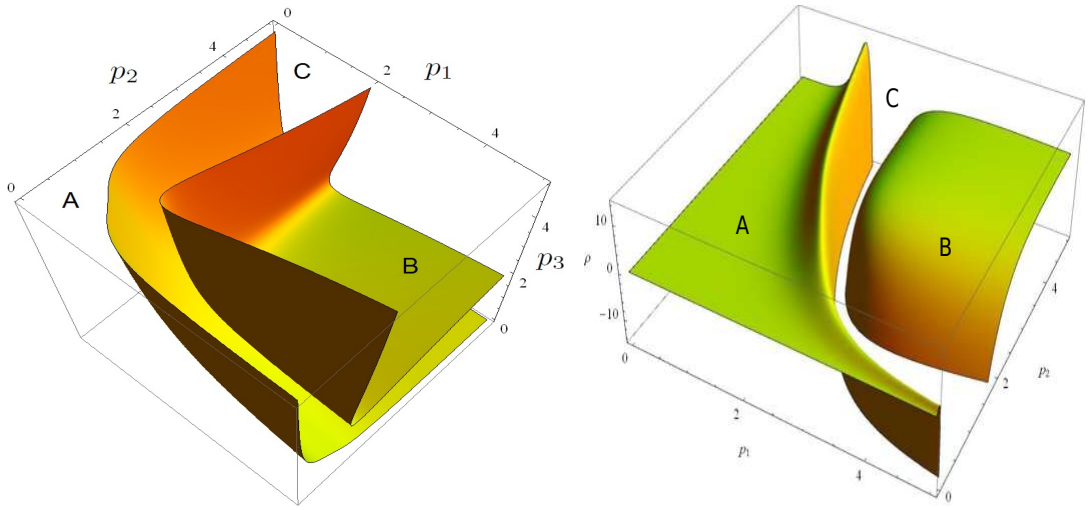

Figure 4.4: Left, zero surfaces of the maximum allowed density. Right, maximum allowed density vs. p_1 and p_2 where $p_3 = p_1$. Both in Planck units.

4.5 Effective Vacuum Bianchi IX

In this section we study the vaccum Bianchi IX due to its non trivial classical behavior, in the sense that near to the classical singularity it presents a chaotic behavior described by the Belinski, Khalatnikov and Lifshitz (BKL) scenario. To study the BKL scenario within the effective theory we use the same idea given by Misner [67, 69], i.e., we study the potential term in the Hamiltonian constraint. Due to the new features introduced by the effective theory, to study the potential term is not enough. Therefore, we analyze also the density in order to determine how the BKL scenario changes.

4.5.1 The Effective Potential

It is helpful to use the potential term of the constraint to study the solutions. The classical potential which comes from the spin connection's curvature in the classical constraint, in terms of Misner variables is [67]

$$W = \frac{1}{2}e^{-4\Omega}\left(e^{-4\beta_+} - 4e^{-\beta_+}\cosh\sqrt{3}\beta_- + 2e^{-2\beta_+}[\cosh 2\sqrt{3}\beta_- - 1]\right), \qquad (4.53)$$

where $\Omega = -\frac{1}{3}\log V$ and the anisotropies $\beta_\pm$ are defined via

$$a_1 = e^{-\Omega+(\beta_+ + \sqrt{3}\beta_-)/2}, \quad a_2 = e^{-\Omega+(\beta_+ - \sqrt{3}\beta_-)/2}, \quad a_3 = e^{-\Omega-\beta_+}. \qquad (4.54)$$

Since the Ω dependence factorizes, one can obtain an anisotropy potential $\mathcal{V}(\beta_+, \beta_-)$ which exhibits exponential walls for large anisotropies. The universe can be seen as a particle moving in such a potential (W) that presents reflections at the walls. An infinite number of these reflections implies that the system behaves chaotically. When the volume becomes small, the quantum effects become important and one should work with the full quantum theory, but one can use the effective equations to have a qualitative view of what happens near the classical singularity. In Eq.(4.34), the only difference from the classical Hamiltonian is in the kinetic part and the potential part (the curvature of spin connection) remains the same as the classical one, therefore, we need to work with the effective Hamiltonian with more corrections.

From the effective Hamiltonian Eq.(4.43), the modified potential can be derived as a function of p_i

$$W_{\text{eff}} = -\frac{V^2 A(V) h^4(V)}{V_c^4}\left(p_1^2+p_2^2+p_3^2-\left[(p_1p_2)^4+(p_1p_3)^4+(p_2p_3)^4\right]\frac{h^6(V)}{2VV_c^6}\right). \quad (4.55)$$

For a simple case, when $\beta_- = 0$ and $\beta_+ \to -\infty$, the classical potential is $W(\beta_+, \Omega) \sim \frac{1}{2}e^{-4\Omega-4\beta_+}$. If we rewrite the modified potential in terms of Misner variables, we can see that in this limit, the modified potential behaves as $W_{\text{eff}} \sim \frac{1}{2V_c^9}e^{-52\Omega-4\beta_+}$, where the β_+-dependency of both classical and modified potential are the same. Thus, we have an infinite wall for the modified potential, too (See Fig.4.5.1). However, for small volumes, the modified potential can be negative at some points.

One should note that the kinetic term is also modified. However, this modification does not change the qualitative behavior, because the kinetic term is always finite and different form zero for a finite time.

4.5.2 Chaotic Behavior

As we showed in section 4.5.1, the potential wall does not disappear even when quantum effects become important and we have potential chaotic behavior near the classical singularity. However, as we discussed in Sec. 4.4, if the weak energy condition holds and if we start from large volumes and evolve the equations into small volumes, as it can be seen in Fig.4.4, there will be a lower bound for volume within region B, and one does not reach region A (connected to zero volume). Since there are no large anisotropies near the smallest allowed volume, the solutions will not exhibit chaotic behavior.

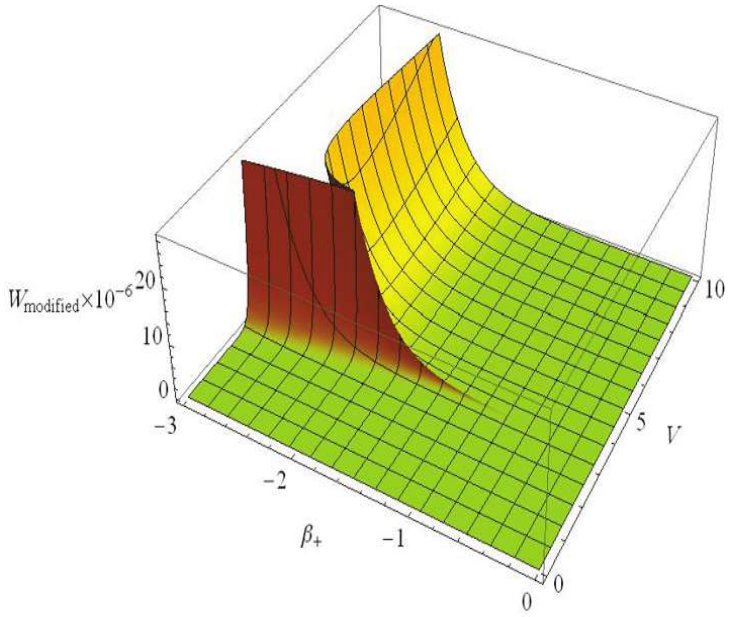

Figure 4.5: Modified potential when $\beta_- = 0$ in Plank unit.

4.6 Discussion

In this chapter we have studied Bianchi IX model within the improved LQC dynamic. We have shown that similarly to the works on [28–30] with an appropriate choice of factor ordering, at quantum level the singularity is resolved.

We have also derived the effective equations with and without inverse triad corrections. We have proved that in both effective theories, the expansion, shear, matter density and curvature are not bounded. Although in both theories those scalars are unbounded, they behave differently. For example if we consider the inverse triad corrections, when volume goes to zero all of those scalars goes to zero too while in the absence of those corrections, the scalars diverge near zero volume. As an interesting result we have shown that the plot of the matter density in the presence of inverse triad corrections (Fig. 4.4), consists of 2 or more disconnected regions. Within those regions, the matter density can be positive or zero but between them is negative definite which means that if weak energy condition holds, the solutions at the effective level cannot have support in both regions and always remain in the same region.

To study the Mixmaster behavior, we have calculated the potential term of vacuum Bianchi IX Hamiltonian in terms of Misner variables. This potential term can be seen as a billiard [68]. We have shown that in both effective theories, this potential acts as an infinite wall (or equivalently the billiard has finite volume)

which can cause the chaotic behavior in the solutions. However, in the theory with inverse triad corrections, by considering weak energy condition, if a solution starts from a large volume and evolves backward, it cannot reach the region around classical singularity. As it can be seen in Fig. 4.4, a solution with support in large volumes lies in region B. In this region there is a lower bound for volume which can suppress the potential wall and therefore at most we will have some finite oscillations near to the bounce and the system will not acts chaotically. However, this argument is not complete and more analytical and numerical investigations are needed for a stronger proof.

Finally, since Bianchi IX vacuum solutions have an important role in BKL scenario, it is worth exploring the Bianchi IX quantum and effective solutions and find out their properties analytically and numerically.

If we knew what it was we were doing, it would not be called research, would it?

Anonymous

5 Conclusion

In this thesis, we have considered several system within LQC. One common theme is the different types of ambiguities which arise from quantization methods in LQC.

In chapter 2, we studied the consequence of the ambiguity which arises from the nature of the polymer quantization, in the effective level. In polymer quantization one can take different curve lengths for calculating the holonomy to have different theories. In fact, having different curve lengths leads to different constraint operators and then to different semi-classical equations. We took the length scale for calculating the holonomy not to be fixed constant, which is common in LQC, but as a fparameter and then studied the limit when it goes to zero and the classical theory is recovered. We found that by choosing different length scales at effective level, the probabilities of occurring sufficient inflation in flat FLRW model are different but they converge when one goes to the classical limit.

In chapter 3, the ambiguity in the definition of the curvature operator in closed FLRW model was considered. It is important to mention that this ambiguity only exists for this model in LQC.
We used two different definitions of the curvature operator to construct two nonequivalent theories. We showed that although we have different constraint operators, in the big volume limit, the effective theories approach each other and both recover the classical equations.
The other ambiguity in the loop quantization of cosmological models which was considered in this chapter, pertains to the factor ordering of the operators contained in the Hamiltonian operator. We showed that the different operator order-

ing leads to different Hamiltonian operators with different properties. However, the semi-classical equations of these different theories are the same.
There is another type of ambiguity which appears in all the models in LQC. As it can be seen in chapter 3 and 4, in the definition of the inverse triad operators there are some free parameters. By fixing those parameters in different ways, the resulting operators are inequivalent. Although these operators are not the same, their qualitative behaviour are similar. In our study, to have a qualitative view of how those operators affect the theory at the semi-classical level, we chose the parameters in such a way that the operator has a simple form and showed that the corrections from these operators can cure the unboundedness of some scalars in the effective phase space.

In chapter 4, we chose a different lapse function compared to previous works in Bianchi IX model. We showed that with this new lapse we get a different constraint operator which has more inverse triad operators, and therefore more corrections could be added to the effective theory. By considering these corrections the scalars behave differently in the semi-classical phase space compared to previous works. However in the classical limit the effective theories become the same.

Except for the ambiguity in the length scale which can be resolved by choosing the square root of the smallest non-zero eigenvalue of the area operator as a natural choice for it, for the other ambiguities there is no natural way to find a preferred constraint operator.

Since these ambiguities appear in LQC, we do not expect the same to happen in the full theory (LQG). However, these results show that there should be some ambiguities of a similar nature to the above ones in the full theory and a proper understanding of their consequence and how to deal with them become important. Therefore, we hope that this work which explores the ambiguities in a simpler theory (LQC), in detail, could provide us with some insight towards the full theory.

Bibliography

[1] A. Ashtekar and J. Lewandowski "Background independent quantum gravity: A status report," *Class. Quant. Grav.* **21**, R53 (2004).

[2] C. Rovelli, "*Quantum Gravity*", Cambridge University Press, Cambridge, 2004.

[3] T. Thiemann, *Modern Canonical Quantum General Relativity*, Cambridge University Press, Cambridge, 2007.

[4] A. Ashtekar, A. Corichi and J. A. Zapata, "Quantum theory of geometry: III. Non-commutativity of Riemannian structures," *Class. Quant. Grav.* **15**, 2955 (1998).

[5] C. Fleischhack, "Representations of the Weyl Algebra in Quantum Geometry," *Commun. Math. Phys.* **285**, 67 (2009).

[6] J. Lewandowski, A. Okołów, H. Sahlmann, and T. Thiemann, "Uniqueness of diffeomorphism invariant states on holonomyflux algebras", *Commu. Math. Phys.* **267**, 730 (2006).

[7] K. Giesel and T. Thiemann, "Algebraic quantum gravity (AQG). IV. Reduced phase space quantisation of loop quantum gravity," *Class. Quant. Grav.* **27**, 175009 (2010).

[8] M. Domagala, K. Giesel, W. Kamiński and J. Lewandowski, "Gravity quantized: Loop quantum gravity with a scalar field," *Phys. Rev. D* **82**, 104038 (2010).

[9] A. Ashtekar, M. Bojowald and L. Lewandowski, "Mathematical structure of loop quantum cosmology" *Adv. Theor. Math. Phys.* **7**, 233 (2003).

[10] M. Bojowald, "Loop quantum cosmology", *Living Rev. Rel.* **8**, 11 (2005).

[11] A. Ashtekar, "Loop Quantum Cosmology: An Overview," *Gen. Rel. Grav.* **41**, 707 (2009).

[12] A. Ashtekar and P. Singh, "Loop quantum cosmology: a status report," *Class. Quant. Grav.* **28**, 213001 (2011).

[13] I. Agullo and A. Corichi, "Loop Quantum Cosmology," arXiv:1302.3833 [gr-qc].

[14] A. Ashtekar, T. Pawlowski and P. Singh, "Quantum Nature of the Big Bang: Improved dynamics", *Phys. Rev. D*, **74**, 084003, (2006).

[15] A. Ashtekar, T. Pawlowski and P. Singh, "Quantum Nature of the Big Bang," *Phys. Rev. Lett.* **96**, 141301 (2006).

[16] A. Ashtekar, T. Pawlowski and P. Singh, "Quantum Nature of the Big Bang: An Analytical and Numerical Investigation," *Phys. Rev. D* **73**, 124038 (2006).

[17] W. Kamiński and J. Lewandowski, The flat FRW model in LQC: the self-adjointness, em Class. Quant. Grav. **25**, 035001 (2008).

[18] A. Ashtekar, A. Corichi and P. Singh, "Robustness of key features of loop quantum cosmology," *Phys. Rev. D* **77**, 024046 (2008).

[19] A. Corichi and P. Singh, "Quantum bounce and cosmic recall", *Phys. Rev. Lett.*, **100**, 161302, (2008).

[20] W. Kaminski and T. Pawlowski, "Cosmic recall and the scattering picture of Loop Quantum Cosmology", *Phys.Rev.*, **D81**, 084027, (2010).

[21] A. Corichi and E. Montoya, "On the Semiclassical Limit of Loop Quantum Cosmology," em Int. J. Mod. Phys. D **21**, 1250076 (2012).

[22] A. Corichi and E. Montoya,"Coherent semiclassical states for loop quantum cosmology," *Phys. Rev. D* **84**, 044021 (2011).

[23] A. Corichi and P. Singh, "Is loop quantization in cosmology unique?," *Phys. Rev. D* **78**, 024034 (2008).

[24] A. Corichi and P. Singh, "A geometric perspective on singularity resolution and uniqueness in loop quantum cosmology," *Phys. Rev. D* **80**, 044024 (2009).

[25] A. Ashtekar, T. Pawlowski, P. Singh, K. Vandersloot, "Loop quantum cosmology of k=1 FRW models," *Phys.Rev. D* **75**, 024035 (2007).

[26] L. Szulc, W. Kamiński, J. Lewandowski, "Closed FRW model in Loop Quantum Cosmology," *Class. Quant. Grav.* **24**, 2621 (2007).

[27] K. Vandersloot, "Loop quantum cosmology and the k = - 1 RW model," *Phys. Rev. D* **75**, 023523 (2007).

[28] A. Ashtekar and E. Wilson-Ewing, "Loop quantum cosmology of Bianchi I models", *Phys. Rev. D*, **79**, 083535, (2009).

[29] A. Ashteka and E. Wilson-Ewing, "Loop quantum cosmology of Bianchi type II models", *Phys. Rev. D*, **80**, 123532, (2009).

[30] E. Wilson-Ewing, "Loop quantum cosmology of Bianchi type IX models", *Phys. Rev. D*, **82**, 043508, (2010).

[31] A. Ashtekar and P. Singh, "Loop quantum cosmology: a status report", *Class. Quant. Grav.*, **28**, 213001, (2011).

[32] A. Ashtekar and T. Schilling, "Geometrical formulation of quantum mechanics," *On Einstein's Path*, Springer New York, 23-65 (1999), arXiv:9706069 [gr-qc].

[33] J. Willis, *ON The Low-Energy Ramifications and a Mathematical Extension of Loop Quantum Gravity*, PhD Thesis, Pennsylvania State University, 2004.

[34] D. Sloan, *Loop Quantum Cosmology and the Early Universe*, PhD Thesis, The Pennsylvania State University, 2010.

[35] V. Taveras, "Corrections to the Friedman equations from LQG for a Universe with a free scalar field", *Phys. Rev. D* **78**, 064072 (2008).

[36] A. Ashtekar and D. Sloan, "Loop quantum cosmology and slow roll inflation," *Phys. Lett. B* **694**, 108 (2010).

[37] G. W. Gibbons and N. Turok, "The measure problem in cosmology," *Phys. Rev. D* **77**, 063516 (2008).

[38] A. Corichi and A. Karami, "On the measure problem in slow roll inflation and loop quantum cosmology," *Phys. Rev. D* **83**, 104006 (2011).

[39] A. Corichi and A. Karami, "Loop quantum cosmology of k=1 FRW: A tale of two bounces", *Phys. Rev. D*, **84**, 044003, (2011).

[40] B. Gupt and P. Singh, "Contrasting features of anisotropic loop quantum cosmologies: The Role of spatial curvature," *Phys. Rev. D* **85**, 044011 (2012).

[41] A. Corichi, and A. Karami, "Loop quantum cosmology of k= 1 FLRW: Effects of inverse volume corrections", *Class. Quant. Grav.*, **31**, 035008, (2014).

[42] D. Garfinkle, "Numerical simulations of generic singularities," arXive:0312117 [gr-qc].

[43] M. Bojowald, G. Date and G. M. Hossain, "The Bianchi IX model in Loop Quantum Cosmology," Class. Quant. Grav. **21**, 3541 (2004); `arXiv:qr-qc/0404039`.

[44] A. Corichi, A. Karami and E. Montoya, "Loop Quantum Cosmology: Anisotropy and singularity resolution," arXiv:1210.7248 [gr-qc].

[45] G. W. Gibbons, S. W. Hawking and J. M. Stewart, "A natural measure on the set of all universes," *Nucl. Phys. B* **281**, 736 (1987).

[46] S. W. Hawking and D. N. Page, "How probable is inflation?," *Nucl. Phys. B* **298**, 789 (1988).

[47] V. A. Belinsky, I. M. Khalatnikov, L. P. Grishchuk and Y. B. Zeldovich, "Inflationary Stages In Cosmological Models With A Scalar Field," *Phys. Lett. B* **155**, 232 (1985).

[48] P. Singh, K. Vandersloot and G. V. Vereshchagin, "Non-singular bouncing universes in loop quantum cosmology," *Phys. Rev. D* **74**, 043510 (2006).

[49] L. Kofman, A. D. Linde and V. F. Mukhanov, "Inflationary theory and alternative cosmology," *JHEP* **0210**, 057 (2002).

[50] A. D. Linde, "Inflationary Cosmology," *Lect. Notes Phys.* **738**, 1 (2008).

[51] A. Corichi, T. Vukasinac and J.A. Zapata, "Polymer quantum mechanics and its continuum limit", *Phys. Rev. D* **76**, 044016 (2007).

[52] A. Corichi, T. Vukasinac and J.A. Zapata, "On a Continuum Limit for Loop Quantum Cosmology," *AIP Conf. Proc.* **977**, 64 (2008).

[53] C. Germani, W. Nelson and M. Sakellariadou, "On the onset of inflation in loop quantum cosmology," *Phys. Rev. D* **76**, 043529 (2007).

[54] J. Mielczarek, "Possible observational effects of loop quantum cosmology," *Phys. Rev. D* **81**, 063503 (2010).

[55] A. Corichi, "Black holes and entropy in loop quantum gravity: An overview," arXiv:0901.1302 [gr-qc].

[56] A. Ashtekar and D. Sloan, "Probability of Inflation in Loop Quantum Cosmology," *Gen. Rel. Grav.* **43**, 3619 (2011).

[57] A. Ashtekar, T. Pawlowski, P. Singh, (In preparation).

[58] J. B. Hartle, S. W. Hawking and T. Hertog, "The No-Boundary Measure of the Universe," em Phys. Rev. Lett. **100**, 201301 (2008).

[59] J. Hartle and T. Hertog, "Replication Regulates Volume Weighting in Quantum Cosmology," em Phys. Rev. D **80**, 063531 (2009).

[60] P. Singh and F. Vidotto, "Exotic singularities and spatially curved Loop Quantum Cosmology," *Phys. Rev. D* **83**, 064027 (2011).

[61] P. Singh, "Are loop quantum cosmos never singular?," *Class. Quant. Grav.* **26**, 125005 (2009).

[62] E. Bentivegna and T. Pawlowski, "Anti-de Sitter universe dynamics in loop quantum cosmology," *Phys. Rev. D* **77**, 124025 (2008).

[63] J. Yang, Y. Ding, Y. Ma, "Alternative quantization of the Hamiltonian in isotropic loop quantum cosmology," arXiv:0902.1913 [gr-qc].

[64] M. Reed and B. Simon, *Methods of Modern Mathematical Physics Vol. I*, Academic Press, London 1980.

[65] P. E. T. Jorgensen, E. P. J. Pearse, "Spectral Reciprocity and Matrix Representations of Unbounded Operators", *J. Funct. Anal.*, **261(3)**, 749, (2011).

[66] D. Sloan, private communication.

[67] C.W. Misner, "Mixmaster Universe", *Phys. Rev. Lett.*, **22**, 1071, (1969).

[68] T. Damour, M. Henneaux, and H. Nicolai, "Cosmological Billiards," *Class. Quant. Grav.* **20**, R145 (2003).

[69] M. Bojowald and G. Date, "Quantum Suppression of the Generic Chaotic Behavior Close to Cosmological Singularities", *Phys. Rev. Lett.*, **92**, 071302, (2004).

[70] E. A. Montoya, *Cosmología Numérica en Gravedad Cuántica de Lazos*, PhD Thesis, Universidad Michoacana de San Nicolás de Hidalgo, 2013.